On low-dimensional stochastic models

Inaugural-Dissertation
zur
Erlangung des Doktorgrades
der Mathematisch-Naturwissenschaftlichen Fakultät
der Universität zu Köln

vorgelegt von
Kai-Oliver Klauck
aus Köln

KÖLN 2000

Contents

Abstract

Several extensions of existing approaches to low-dimensional stochastic models are proposed. It is shown that the stationary state of a wide class of one-dimensional stochastic processes can be written as a matrix product state. Next, the exact solution of a staggered hopping model with reflective boundaries is presented. The connection between such boundaries and the occurrence of optimum ground states is clarified. In the fourth chapter the Gibbs probability measure of a two-dimensional classical vertex model is used for the description of traffic flow. The phase diagram of this traffic flow model is outlined. For comparison a cellular automaton with similar properties is suggested. The stationary state of this automaton is calculated exactly, both, for forward sequential and fully parallel update. Thereafter, the dynamics of the asymmetric simple exclusion process (ASEP) with open boundaries and parallel update is examined. For large portions of the parameter space of this model the time and space dependent generalization of the $(2, 1)$-cluster approximation is shown be in good agreement with our Monte-Carlo simulations. The remaining information on the dynamics is extracted from a domain wall description. Finally, stochastic hopping models on two-leg ladders are studied. These models can be used for the description of traffic flow on a two-lane highway. Exact solutions are given for open and periodic boundary conditions.

PACS: 02.50.Ey; 02.50.Ga; 02.60.Cb; 05.20.-y; 05.40.Fb; 05.70.Ln;
            45.70.Vn; 89.40.+k

Key Words: Cellular automata; Markov processes; optimum ground
                states; matrix product ansatz; reaction-diffusion models;
                traffic flow; vertex models

1. Introduction

1.1. Motivation

[1] Our understanding of nonequilibrium physics is far behind that for the equilibrium theory. One usually encounters systems that can be described neither by Newtonian mechanics nor by quantum mechanics. Moreover, on a phenomenological level, such systems behave stochastically and other approaches to their description have to be used. Unfortunately, a general framework which exists for equilibrium theory is still lacking. Nevertheless, many interesting phenomena fall into the class of nonequilibrium stochastic processes [3, 4]. Physical examples include driven lattice gases, reaction-diffusion systems, and the critical dynamics of classical spin systems [5, 6, 7, 2]. In addition to that, the latter models very often describe problems beyond physics, e.g., traffic flow phenomena [8, 9], biological mechanisms of growth and of protein synthesis [10, 11], the spreading of diseases [12], the formation of opinions in human groups [13], and the description of financial markets [14, 15, 16].

The past few years have seen exciting new developments in the field, which has led to a series of remarkable exact solutions for such stochastic systems and to a better understanding of the underlying mathematical structure. At the heart of this development is the close relationship between the Markov generator of the stochastic time evolution for the probability distribution in the master equation approach on the one hand and the Hamiltonians for quantum spin systems (or the transfer matrices of statistical models respectively) on the other hand. The new insight is the somewhat surprising observation that for a few of the most interesting interacting particle systems the time-translation operators T or H respectively turn out to be the transfer matrix or quantum Hamiltonian respectively of well-known equilibrium statistical mechanics models. Sometimes, these models are even found to be so-called integrable models [17], i.e., the complete spectrum of T or H can be found using free-fermion techniques or the Bethe ansatz [18, 19]. This, in turn, leads to the complete information on the stationary and dynamic properties of the associated stochastic nonequilibrium system.

1.2. Quantum Hamiltonian formalism for the master equation

Throughout this work the following coarse grained point of view will be adopted: Rather than a continuum of possible states (defined by positions and momenta) the particles are assumed to be located on some *discrete* lattice on which they can move and interact with each other. At any instant of time one thinks of the system as being in a random configuration $\eta \in X$, defined by the positions of the particles. X is the set of all possible states in which the system may be found. A complete description of the system is provided by the probability $P_\eta(t)$ of finding the system in the state η at time t.

---

[1]Sec. 1.1 and Sec. 1.2 follow very closely [1, 2], since both works offer a concise introduction to the topic and have influenced this thesis in a very strong way.

The time evolution of the system is assumed to proceed according to certain stochastic rules. These rules are encoded in transition probabilities $p_{\eta \to \eta'}$ for elementary moves from a state η to another state η'. An elementary move is a transition that takes place instantaneously after some time interval $\triangle t$. These probabilities do not depend on how the system got into state η in a previous move: The dynamics has no explicit memory of its own history. Thus, the type of processes examined in this work are so-called *Markov processes*. Of course, not all random processes in nature are Markovian. However, the lack of memory seems to be a reasonable approximation in many situations.

No matter if the dynamics is assumed to take place in discrete time steps or continuous time, the heuristic description of the time evolution is governed by the *master equation*:

$$P_\eta(t + \triangle t) = \sum_{\eta' \in X} p_{\eta' \to \eta} P_{\eta'}(t). \tag{1.1}$$

Thus, the evolution of the probability distribution is given by the action of a linear operator, the generator of the Markov process, on the probability distribution. One passes to a continuous-time description by defining the process in terms of rates $\omega_{\eta \to \eta'} \equiv p_{\eta \to \eta'}/\triangle t$ (for $\eta \neq \eta'$) which are the transition probabilities per time unit. Taking the limit $\triangle t \to 0$ Eq. (1.1) turns into the continuous-time master equation

$$\partial_t P_\eta(t) = \sum_{\substack{\eta' \neq \eta \\ \eta' \in X}} \left[\omega_{\eta' \to \eta} P_{\eta'}(t) - \omega_{\eta \to \eta'} P_\eta(t) \right], \tag{1.2}$$

where the rates satisfy

$$0 \leq \omega_{\eta \to \eta'} < \infty \qquad \text{for} \qquad \eta \neq \eta'. \tag{1.3}$$

Consider now a stochastic process on a chain of length L, where every site can be in one of m states leading to local variables $\beta_i \in \{1, 2, \ldots, m\}$. A configuration of the system will be denoted by $\{\beta\} = \{\beta_1, \beta_2, \ldots, \beta_L\}$ and its probability by $P_{\{\beta\}}(t)$. In many cases of practical interest one has only local, homogeneous transition rates $\omega_{\alpha_k, \alpha_{k+1} \to \beta_k, \beta_{k+1}}$, which do not depend on time. Hence, the master equation has the following form:

$$\begin{aligned}
\partial_t P_{\{\beta\}}(t) = \sum_{k=1}^{L-1} \Bigg\{ &\omega_{\beta_k, \beta_{k+1} \to \beta_k, \beta_{k+1}} P_{\{\beta\}}(t) \\
&+ \sum_{\substack{\alpha_k, \alpha_{k+1}=1 \\ \alpha_k, \alpha_{k+1} \neq \beta_k, \beta_{k+1}}}^{m} \omega_{\alpha_k, \alpha_{k+1} \to \beta_k, \beta_{k+1}} P_{\{\beta_1, \ldots, \beta_{k-1}, \alpha_k, \alpha_{k+1}, \ldots, \beta_L\}}(t) \Bigg\}
\end{aligned} \tag{1.4}$$

with

$$\omega_{\beta_k, \beta_{k+1} \to \beta_k, \beta_{k+1}} = - \sum_{\substack{\alpha_k, \alpha_{k+1}=1 \\ \alpha_k, \alpha_{k+1} \neq \beta_k, \beta_{k+1}}}^{m} \omega_{\alpha_k, \alpha_{k+1} \to \beta_k, \beta_{k+1}}. \tag{1.5}$$

The physical realization of this equation (in form of Monte-Carlo simulations) is the random sequential update, where in the course of each update a bond is chosen at random and the local update rule (given by the ω) is applied.

Next, one defines a ket state $|P\rangle$, the so-called *probability vector*, in the following way. One starts with an orthonormal basis in the configuration space $\{\beta\}$,

$$|\{\beta\}\rangle = |\beta_1, \ldots, \beta_L\rangle \tag{1.6}$$

with

$$\langle\{\beta'\}|\{\beta\}\rangle = \delta_{\{\beta'\},\{\beta\}} \tag{1.7}$$

and defines

$$|P(t)\rangle = \sum_{\{\beta\}} P_{\{\beta\}}(t)|\{\beta\}\rangle. \tag{1.8}$$

Then (1.4) turns into

$$\partial_t|P(t)\rangle = -H|P(t)\rangle \tag{1.9}$$

with the so-called *stochastic Hamiltonian*

$$H = \sum_{k=1}^{L-1} h_k. \tag{1.10}$$

The local stochastic Hamiltonian h_k acts non-trivially on the sites i and $i+1$ and its elements are defined by

$$h_k(\beta_k\beta_{k+1}, \alpha_k\alpha_{k+1}) = -\omega_{\alpha_k,\alpha_{k+1}\to\beta_k,\beta_{k+1}}. \tag{1.11}$$

Note that – in contrast to operators in quantum mechanics – stochastic Hamiltonians are generically *non-hermitian*.
Without adding a suitable constant, stochastic Hamiltonians have the following property.

Property 1. *The stationary state of the stochastic process with Markov generator $-H$ corresponds to the zero-energy ground state[2] of the quantum spin chain defined by H.*

For the calculation of expectation values one furthermore defines the *left complete state*:

$$\langle 0| = \sum_{\{\beta\}} \langle\{\beta\}|. \tag{1.12}$$

Since the total probability equals one,

$$\langle 0|P(t)\rangle = \sum_{\{\beta\}} P_{\{\beta\}}(t) = 1 \tag{1.13}$$

holds. Using (1.9) one directly infers that

$$\langle 0|H = 0. \tag{1.14}$$

Thus, one knows that H has a left eigenvector with eigenvalue zero. From this follows that H must have a right eigenvector with eigenvalue zero, too. This *guarantees* the existence of a stationary state.
The expectation value of an observable $F(\{\beta\})$ at time t is given by

$$\begin{aligned}
\langle F\rangle(t) &= \sum_{\{\beta\}} F(\{\beta\})P_{\{\beta\}}(t) \\
&= \langle 0|F|P(t)\rangle = \langle 0|Fe^{-Ht}|P(t=0)\rangle.
\end{aligned} \tag{1.15}$$

---

[2]From the mathematical properties of the Markov generator it can be shown exactly that the real parts of all eigenvalues are greater or equal zero [20, 21]. Eigenvalues with zero real part can be shown to have zero imaginary part, too. Thus, no undamped oscillations are possible.

If $|P(t=0)\rangle$ can be expanded in eigenkets $|\psi_\lambda\rangle$ of H with eigenvalues E_λ

$$|P(t=0)\rangle = \sum_\lambda a_\lambda |\psi_\lambda\rangle, \tag{1.16}$$

then

$$\langle F \rangle(t) = \sum_\lambda a_\lambda e^{-E_\lambda t} \langle 0|F|\psi_\lambda\rangle. \tag{1.17}$$

As a consequence one has another important property.

Property 2. *The low lying excitations of H determine the behaviour of the stochastic process at late stages of the dynamics.*

Performing all steps from above, but without taking the continuous-time limit, yields a master equation with a Markov generator which looks similar to the transfer matrix T of a statistical equilibrium model. In this case one often chooses the time scale such that $\triangle t = 1$. Hence, the master equation can be brought into the form

$$|P(t+1)\rangle = T|P(t)\rangle. \tag{1.18}$$

In practice one usually encounters one of the following three cases:

- Forward/backward sequential update:
  In this case the transfer matrix factorizes in the following way

$$T_\rightarrow = \tau_L \tau_{L-1} \cdots \tau_2 \tau_1 \tag{1.19}$$

  in case of forward sequential update, and

$$T_\leftarrow = \tau_1 \tau_2 \cdots \tau_{L-1} \tau_L \tag{1.20}$$

  in the backward sequential update.

  The τ_i are Markov generators acting on the sites i and $i+1$.

- Sublattice-parallel update:
  Here the transfer matrix is the product of two factorizing transfer matrices

$$T_{\underset{\sim}{}} = T_A T_B, \tag{1.21}$$

  with

$$T_A = \prod_{k=1}^{L/2} \tau_{2k-1}, \tag{1.22}$$

  and

$$T_B = \prod_{k=1}^{L/2} \tau_{2k}, \tag{1.23}$$

- Fully parallel update:
  All bonds are updated at once according to a local Markov generator. Such systems are called *cellular automata* [22]. The connection between cellular automata and statistical mechanical models has been elucidated in [23]. One usually distinguishes between *deterministic* and *probabilistic* cellular automata. A cellular automaton is deterministic if and only if all entries of the transfer matrix (the global Markov generator) are equal to one.

1.3. Matrix product ansatz and optimum ground states

The so-called matrix product ansatz (MPA) and the related optimum ground state (OGS) approach have by now become an important tool for the investigation of quantum spin chains (see e.g. [24, 25, 26, 27, 28, 29, 30] and references therein). However, these methods are not restricted to quantum systems, but can be applied to one-dimensional stochastic processes, too. The most prominent example in this area is the solution of the asymmetric simple exclusion process (ASEP) with open boundaries [31] [3], which has reached a paradigmatic status in the field of low-dimensional nonequilibrium processes.

Therefore, in this section the MPA for stochastic processes and the concept of optimum ground states will be introduced. A detailed introduction will be given with respect to processes in continuous time (random sequential update). For processes in discrete time the MPA has to be modified. The necessary modifications will be summarized at the end of this section.

Consider first the following *hermitian* Hamiltonian of a quantum spin chain (with periodic boundary conditions) of the form

$$H = \sum_{k=1}^{L} h_k. \tag{1.24}$$

h_k is a local hermitian Hamiltonian, which is independent of k and acts only on the spins at k and $k+1$. Without restriction one can assume that the lowest eigenvalue of h_k is equal to zero, since this can always be achieved by adding a suitable constant. Hence, zero becomes a lower bound for the ground state energy E_0 of H. Usually, E_0 is greater than zero and the global ground state involves also excited states of h_k. However, if E_0 equals zero,

$$H|\psi\rangle = 0, \tag{1.25}$$

then one has that for all k

$$h_k|\psi\rangle = 0. \tag{1.26}$$

This is due to the positive semi-definiteness of the local Hamiltonians. Therefore, a state $|\psi\rangle$ is called *optimum ground state* if and only if condition (1.26) holds. Of course, for local hermitian Hamiltonians Eq. (1.25) and Eq. (1.26) are equivalent. For stochastic Hamiltonians this equivalence is generically lost. Although E_0 is always zero in the stochastic case, $|\psi\rangle$ is only very seldom in the kernel of *all* the local Hamiltonians. Hence the structure of zero-energy ground states is of a different nature. This nature becomes transparent upon the introduction of matrix product states (MPS).

Suppose that one is given again a Hamiltonian of the form (1.24), where the h_k (and thus H) are not any longer hermitian but Markov generators. Hence, the ground state energy of H is zero. Assume further that the local Hilbert space at a site has $\{0,1\}$ as basis, i.e., a site can be occupied or empty.

In the MPA one makes the following ansatz for the stationary state of H: The (unnormalized) probability for any configuration on a chain of length L is the trace of an L-fold product of matrices

$$P(\tau_1, \tau_2, \dots, \tau_L) = \text{Tr}\left[\prod_{i=1}^{L} ((1 - \tau_i)E + \tau_i D)\right]. \tag{1.27}$$

---

[3]At the same time a solution using a different approach has been presented in [32].

E and D are matrices acting on some (unspecified) vector space A. For a ring of length 3 one has e.g.

$$
\begin{aligned}
P(0,0,0) &= \frac{1}{Z}\operatorname{Tr}(EEE), \\
P(0,0,1) &= P(0,1,0) = P(1,0,0) = \frac{1}{Z}\operatorname{Tr}(DEE), \\
P(0,1,1) &= P(1,1,0) = P(1,0,1) = \frac{1}{Z}\operatorname{Tr}(DED), \\
P(1,1,1) &= \frac{1}{Z}\operatorname{Tr}(DDD).
\end{aligned}
\tag{1.28}
$$

The constant Z is needed for normalization (all probabilities add up to one). By direct computation one can see that in this case the stationary probability vector can be written in a very compact way as

$$
|P\rangle = \operatorname{Tr}\left[\begin{pmatrix} E \\ D \end{pmatrix}^{\otimes L}\right].
\tag{1.29}
$$

The tensor product in the last formula is the usual tensor product of vectors, where the scalar multiplication of the scalar components is replaced by matrix multiplication of the matrix-valued entries. The trace is taken of every component of the resulting high-dimensional vector. The dimension of the local Hilbert space in our example was two and therefore two matrices E and D occurred in the ansatz (1.29). If the local Hilbert space has the dimension m, then the vector $(E, D)^t$ has to be replaced by a vector $\mathcal{D} = (D_1, D_2, \ldots, D_m)$ with matrix-valued entries. This leads to the general form of the MPA:

$$
|P\rangle = \operatorname{Tr}\left[\mathcal{D}^{\otimes L}\right].
\tag{1.30}
$$

Hinrichsen *et al.* [33] could recognize a general mechanism – the so-called *cancelling-mechanism* – which gives a local criterion that has to be fulfilled by the MPA vector in order to be a ground state. If one can find another vector $\mathcal{X} = (X_1, X_2, \ldots, X_m)$ with matrix-valued entries acting on A such that the following equation holds

$$
h(\mathcal{D} \otimes \mathcal{D}) = \mathcal{X} \otimes \mathcal{D} - \mathcal{D} \otimes \mathcal{X},
\tag{1.31}
$$

then $|P\rangle$ given by Eq. (1.30) is a ground state of H: Acting with H on $|P\rangle$ one sees that every h_k gives two contributions

$$
h_k|\psi\rangle = |k\rangle - |k+1\rangle,
\tag{1.32}
$$

where

$$
|k\rangle = \operatorname{Tr}\left[\mathcal{D}^{\otimes k-1}\mathcal{X} \otimes \mathcal{D}^{\otimes L-k}\right].
\tag{1.33}
$$

Thus

$$
H|P\rangle = \sum_{k=1}^{L} h_k|\psi\rangle = \sum_{k=1}^{L}[|k\rangle - |k+1\rangle] = 0.
\tag{1.34}
$$

How systems with other boundary conditions have to be treated will be the topic of the next chapter.

In case of discrete time updates the MPA and the cancelling-mechanism have to be slightly modified.

- Forward/backward sequential update:
  In this case the first site of the chain plays a special rôle. Hence, the MPA reads

$$|P\rangle = \mathrm{Tr}\left[\mathcal{X} \otimes \mathcal{D}^{\otimes L-1}\right]. \tag{1.35}$$

In the forward sequential update the cancelling-mechanism takes the form

$$\tau(\mathcal{X} \otimes \mathcal{D}) = \mathcal{D} \otimes \mathcal{X}, \tag{1.36}$$

and in the backward sequential case one finds

$$\tau(\mathcal{D} \otimes \mathcal{X}) = \mathcal{X} \otimes \mathcal{D}. \tag{1.37}$$

The vector $\mathcal{X}$ can be interpreted as a defect located at site one, which is transported through the complete chain during each update.

- Sublattice-parallel update:
  Here the MPA consists of the alternating ansatz

$$|P\rangle = \mathrm{Tr}\left[\mathcal{D} \otimes \mathcal{X} \otimes \cdots \otimes \mathcal{D} \otimes \mathcal{X}\right]. \tag{1.38}$$

The cancelling-mechanism reads

$$\tau(\mathcal{X} \otimes \mathcal{D}) = \mathcal{D} \otimes \mathcal{X}. \tag{1.39}$$

1.4. Outline of this work

In most of the existing approaches to low-dimensional stochastic nonequilibrium systems the properties of one-dimensional reaction-diffusion systems with a spatial homogeneous nearest neighbour interaction have been examined. Since a general framework for the description of nonequilibrium systems is still lacking, these approaches play a very important rôle for the understanding of such systems. Nevertheless, it is still unclear to what extent these results are universal. Therefore, the purpose of this thesis is to examine how far the existing approaches to particular nonequilibrium systems can be generalized. Since in our working group at the University of Cologne the investigation of traffic flow phenomena has a good tradition by now, most of the examples will be of relevance for the description of traffic flow. However, the restriction to traffic flow phenomena just reflects our personal scientific interest and has no influence on the fact that the methods are quite general.

In the second chapter of this thesis, as a generalization of a proposition of Krebs and Sandow [34], it will be shown that the stationary state of stochastic processes with finite but arbitrary interaction range in the bulk and some suitably defined boundary interactions can always be written as a matrix product state. Two applications to hopping models with next-nearest neighbour interaction will be given.

In the next chapter the stationary state of a staggered hopping model will be calculated. The connection between optimum ground states for stochastic processes and reflective boundaries will be clarified.

Then, in the fourth chapter, the Gibbsian statistics of a vertex model will be used for the description of traffic flow. A rich phase diagram with five distinct phases of traffic will be derived. In addition a cellular automaton will be presented that exhibits very similar features to the vertex model. The stationary state of this cellular automaton will be calculated exactly for two types of update. This clarifies the fundamental diagram, i.e.,

the relation between density and flow. The properties of the cellular automaton and the vertex model will be compared.

In chapter five the dynamics of the asymmetric simple exclusion process with parallel update will be studied. For large portions of the phase diagram the time and space dependent version of the $(2,1)$-cluster approximation will be shown to give acceptable results. This method completely fails on a submanifold of the parameter space, the so-called shock profile line. On this submanifold a domain wall picture will be proposed that allows a good description of the dynamics.

In the sixth chapter stochastic models on two-leg ladders will be treated. The chapter consists of two parts. In the first part a model with periodic boundary conditions is treated, the stationary state of which can be calculated due to the fact that the two legs of the ladder decouple. In the second part a two-leg ladder model with deterministic bulk dynamics and open, stochastic boundaries will be examined. The stationary state and the phase diagram will be calculated exactly.

Finally, the results will be summarized and an outlook to further applications will be given. It should be mentioned that the point of view adopted in this work is that of a physicist with a background in the field of exactly solvable low-dimensional models. Therefore, the measure theoretic flavour of probability theory has been totally neglected. The Markov generators presented in this work are constructed in such a way that their well-definedness is granted. Another point that has not been treated exhaustively on mathematical grounds is the question of unique stationary states. As can be seen from the caveat in chapter three, where a $\mathbb{Z}_3$-symmetric reaction-diffusion model is considered, uniqueness of the stationary state must not hold. Therefore, uniqueness of all exact solutions has been checked by the use of Monte-Carlo simulations. This explains why in this work exact solutions are compared with Monte-Carlo data so often. Of course, this would normally be superfluous – unless one would like to check the correctness of the Monte-Carlo simulations!

2. The ubiquity of matrix product states for stochastic processes

2.1. Introduction

For stochastic processes in one dimension with nearest-neighbour interaction in the bulk and boundary fields Krebs and Sandow (KS) [34] could prove that the stationary state is generically a matrix product state (MPS). The key of their proof is the identification of an appropriate cancelling-mechanism.

Such considerations are not restricted to systems with random sequential dynamics. In fact, the KS result has been generalized to discrete-time dynamics in [35].

Many stochastic systems arising in the context of such fields as traffic flow, granular matter, chemical reactions, and biological motion naturally have an interaction, which is not restricted to nearest neighbours. Therefore it is desirable to find an extension of the KS result to such systems.

The only example of an application of the MPA to stochastic models with an interaction range $r \geq 2$ seems to be the work of Eßler and Rittenberg [36]. They introduced a three-site ($r = 3$) version of the cancelling-mechanism used implicitly in [31]. Preliminary studies have indicated, however, that this mechanism is not general enough and allows only the solution of some special models. On this account, it was natural to look for a generalization of the proposition of KS in order to identify the correct mechanism for arbitrary interaction range $r \geq 2$.

Indeed, this generalization is possible. In the next section it will be shown how the mechanism of KS has to be extended to systems with interaction range $r \geq 2$. The usefulness of the method will be presented by solving two different particle hopping models with three-site interaction in the bulk for periodic boundary conditions and some suitably chosen boundary interactions. Both models are interesting on their own, since they can be interpreted as stochastic processes describing traffic flow on a highway. On the other hand, the mechanism is not only useful for a systematic search for exact solutions. Since it helps to identify the general structure of the stationary state of one-dimensional stochastic models, it allows to study general properties of such systems. One example for such an application is the work [35], where general relations between sublattice-parallel and sequential dynamics have been derived.

2.2. The generalized Krebs-Sandow proposition

It turned out to be useful to split the original proposition of Krebs and Sandow in two independent propositions A and B. The main reason is that proposition A gives a sufficient local criterion for the existence of MPS and covers stochastic processes both with boundary interactions and periodic boundary conditions. Proposition B deals with boundary interactions only, where it is possible to show explicitly that the criterion of proposition A can always be fulfilled.

Consider a stochastic process in continuous time on a chain consisting of L sites, where each site can be in one of m states. The Markov generator of the temporal evolution of the probability vector is given by the stochastic Hamiltonian H_L of the form

$$H_L(r) = h_{\text{left}}(r) + \sum_{k=1}^{L-r+1} h_{k,k+1,\ldots,k+r-1} + h_{\text{right}}(r) \tag{2.1}$$

in the case of boundary interactions and

$$H_L^{(p)}(r) = \sum_{k=1}^{L} h_{k,k+1,\ldots,k+r-1} \tag{2.2}$$

for periodic boundary conditions (p.b.c.). The integer r denotes the range of the interaction in the bulk, i.e., $h_{k,k+1,\ldots,k+r-1}$ acts (non-trivially) on r sites beginning with site k; $h_{\text{left}}(r)$ and $h_{\text{right}}(r)$ are boundary interactions acting on the first, respectively last, $r-1$ sites of the chain. Note that the stochastic Hamiltonians (2.1) and (2.2) are in general non-hermitian. From now on only the steady state solution of (1.9) will be examined, which is the eigenvector $|P_L\rangle_0$ of H_L with eigenvalue 0. $|P_L\rangle_0$ will be referred to as zero-energy eigenvector. In the following it will be clarified under which conditions $|P_L\rangle_0$ can be written as a matrix product state

$$|P_L\rangle_0 = \frac{1}{Z_L} \langle W|\mathcal{D}^{\otimes L}|V\rangle \tag{2.3}$$

in the presence of boundary interactions. For periodic boundary conditions one has to modify the ansatz to guarantee translational invariance

$$|P_L\rangle_0 = \frac{1}{Z_L} \text{Tr}[\mathcal{D}^{\otimes L}]. \tag{2.4}$$

In both cases $\mathcal{D}$ is a vector of dimension m with components D_i, where the D_i are matrices acting on some auxiliary vector space A. $|V\rangle$ and $\langle W|$ are vectors in A and its dual A^*, respectively. Z_L is a normalization constant.

Before in proposition A the cancelling mechanism will be given, the following definition has to be made:

Definition 1. $\mathcal{X}(r)$ *is a column-vector with m^{r-1} entries $X_{i_1,\ldots,i_{r-1}}$, $i_\gamma \in \{1,\ldots,m\}$. The $X_{i_1,\ldots,i_{r-1}}$ are matrices acting on the vector space A defined above. The position of $X_{i_1,\ldots,i_{r-1}}$ in the vector $\mathcal{X}(r)$ is given by $1 + (i_{r-1}-1) + m(i_{r-2}-1) + \ldots + m^{r-2}(i_1-1)$.*

Now, the first part of the generalized KS-proposition can be formulated:

Proposition 1 (A). *(i) If one can find m matrices D_i and m^{r-1} matrices $X_{i_1,i_2,\ldots,i_{r-1}}$ such that they fulfill*

$$h_{k,k+1,\ldots,k+r-1}(\overbrace{\mathcal{D}\otimes\mathcal{D}\otimes\cdots\otimes\mathcal{D}}^{r\ times}) = \mathcal{X}(r)\otimes\mathcal{D} - \mathcal{D}\otimes\mathcal{X}(r), \tag{2.5}$$

then $|P_L\rangle_0 = \text{Tr}[\mathcal{D}^{\otimes L}]$ is a zero-energy eigenvector of $H_L^{(p)}(r)$ (see (2.2)), i.e., a stationary state of the underlying stochastic process with periodic boundary conditions.
(ii) If in addition to (2.5) one can find vectors $|V\rangle \in A$ and $\langle W| \in A^*$ such that

$$\langle W|h_l(r)(\overbrace{\mathcal{D}\otimes\mathcal{D}\otimes\cdots\otimes\mathcal{D}}^{r-1\ times}) = -\langle W|\mathcal{X}(r), \tag{2.6}$$

and

$$h_r(r)(\underbrace{\mathcal{D} \otimes \mathcal{D} \otimes \cdots \otimes \mathcal{D}}_{r-1 \ times})|V\rangle = \mathcal{X}(r)|V\rangle, \tag{2.7}$$

then $|P_L\rangle_0 = \langle W|\mathcal{D}^{\otimes L}|V\rangle$ *is a zero-energy eigenvector of* $H_L(r)$ *(see (2.1)) with boundary interactions* $h_{\text{left}}(r)$ *and* $h_{\text{right}}(r)$.

Proof. The proof is given in Appendix A. □

In the case of boundary interactions another proposition can be derived. Here, the matrix product state is not an ansatz, but merely a reformulation of the fact that the stationary state is a zero-energy eigenvector of $H_L(r)$ for all system lengths.

Proposition 2 (B). *Given a stochastic process described by a stochastic Hamiltonian of the form (2.1) which has a unique stationary state for any system length L. Then the eigenstate* $|P_L\rangle_0$ *with eigenvalue 0 corresponding to this stationary state can be written as a matrix product state* $\langle W|\mathcal{D}^{\otimes L}|V\rangle$ *with* $\mathcal{D} = (D_1, D_2, \dots, D_m)^t$ *and vectors* $\langle W|, |V\rangle$. *Moreover one finds* m^{r-1} *matrices* $X_{i_1,\dots,i_{r-1}}$, *such that the cancelling-mechanism (2.5)-(2.7) is satisfied.*

Proof. See Appendix A where an explicit construction of the operators involved is given. □

In the case $r = 2$ the propositions from above reduce to the one given in [34]. In the case of $m = 2$ and $r = 3$ it is easy to see that the cancelling-mechanism proposed in [36] is a special case of (2.5)–(2.7). In [36]

$$\begin{aligned} h_{k,k+1,k+2}(\mathcal{D} \otimes \mathcal{D} \otimes \mathcal{D}) &= x \otimes \mathcal{D} \otimes \mathcal{D} - \mathcal{D} \otimes x \otimes \mathcal{D} \\ &+ y \otimes \mathcal{D} \otimes \mathcal{D} - \mathcal{D} \otimes \mathcal{D} \otimes y \\ &+ \mathcal{D} \otimes z \otimes \mathcal{D} - \mathcal{D} \otimes \mathcal{D} \otimes z \\ &+ t \otimes \mathcal{D} - \mathcal{D} \otimes t \end{aligned} \tag{2.8}$$

is used instead of (2.5). In this case $\mathcal{X}$ is given by

$$\mathcal{X} = (x + y) \otimes \mathcal{D} + \mathcal{D} \otimes (y + z) + t. \tag{2.9}$$

Note that the structure of the vectors $\mathcal{X}$ in this case is rather different, since the entries of the vectors x, y, z and the matrix t are c-numbers, not matrices. An $\mathcal{X}$ of the form (2.9) implies the existence of recursion relations which relate the weights $P_L(\tau_1, \dots, \tau_L)$ for a system of size L with those of smaller systems of size $L - 1$ and $L - 2$.
Using the mechanism (2.8) a proposition similar to proposition A could be formulated. However, an $\mathcal{X}$ of the form (2.9) does not necessarily lead to an algebra which is manifestly non-trivial [1]. This is different for the general cancelling-mechanism (2.5)–(2.7), since in the course of the proof of proposition B (see App. A) an explicit non-trivial representation of this algebra is constructed.

---

[1]By a trivial algebra we mean an algebra which is equal to 0.

2.3.   Applications

In order to illustrate the cancelling-mechanism, two applications which are generalizations of the ASEP will be studied.

In the first model (*model A*) particles hop exclusively in one direction, say to the right, along a one-dimensional chain of length L with periodic boundary conditions. Particles hop one site to the right at rate p_1, if this site is not occupied. If a particle has two empty sites in front of it, it may also move two sites to the right with rate p_2. The stochastic Hamiltonian of model A has the form (2.2) with $r = 3$. The local operator $h_{k,k+1,k+2}$ acts on sites k, $k + 1$ and $k + 2$ and its explicit form is given by the dynamics of the model.

Model A is of obvious relevance for the modeling of traffic flow. It can be interpreted as a model for cars which have a maximum velocity $v_{\max} = 2$ moving on a single-lane highway. The model is considerably simpler than the Nagel-Schreckenberg model [37] with $v_{\max} = 2$, since the particles do not have an internal degree of freedom ("velocity"). On the other hand, it keeps some of the basic properties.

For the stationary state an ansatz of the form (2.4) with $\mathcal{D} = (E, D)^t$ and matrices E, D is made. Note that this corresponds to a grand canonical description, since (2.4) is a superposition of states with different particle numbers. However, in our case it is not difficult to obtain results for fixed particle densities.

Using Proposition A from above, $|P_L\rangle_0$ is a stationary state if one can find 6 operators E, D, X_{11}, X_{12}, X_{21} and X_{22} such that they fulfill the following relations, which are given by the use of the cancelling-mechanism:

$$
\begin{aligned}
0 &= X_{11}E - EX_{11}, & p_2DEE &= X_{11}D - EX_{12}, \\
p_1DEE &= X_{12}E - EX_{21}, & p_1DED &= X_{12}D - EX_{22}, \\
-(p_1 + p_2)DEE &= X_{21}E - DX_{11}, & -p_1DED &= X_{21}D - DX_{12}, \\
0 &= X_{22}E - DX_{21}, & 0 &= X_{22}D - DX_{22}.
\end{aligned}
\tag{2.10}
$$

The algebra (2.10) has the following one-dimensional representation with $D, E \in \mathbb{R}$:

$$
\begin{aligned}
D &= 1 - E, \\
X_{11} &= xE/D + p_2E^2, & X_{12} &= x \in \mathbb{R} \qquad \text{(free parameter)}, \\
X_{21} &= x - p_1ED, & X_{22} &= xD/E - p_1D^2.
\end{aligned}
\tag{2.11}
$$

Hence, the stationary probability distribution is the mean-field measure. The particle density ρ is equal to D and the flow j is given by

$$
j(\rho, p_1, p_2) = \rho(1 - \rho)[p_1 + 2p_2(1 - \rho)],
\tag{2.12}
$$

which gives the *fundamental diagram*[2], i.e., the functional relation between flow and density, at hand (see Fig. 2.1). Since model A does not exhibit a particle-hole symmetry, the fundamental diagrams are not symmetric with respect to $\rho = 1/2$.

Model A has also been studied with parallel dynamics, which is more appropriate for traffic models [37]. Here a solution can be obtained by using the so-called car-oriented mean-field theory (COMF) [38]. This theory will be introduced in Chap. 4 in detail.

Note that the model can also be solved without matrix product ansatz by using the fact that the dynamics satisfies the so-called pairwise balance condition [39, 40].

Although model A is trivial for periodic boundary conditions since there are no correlations, the situation for open boundaries can be quite different. Open boundaries are

---

[2]The fundamental diagram is one of the most important observable quantities in traffic flow theory.
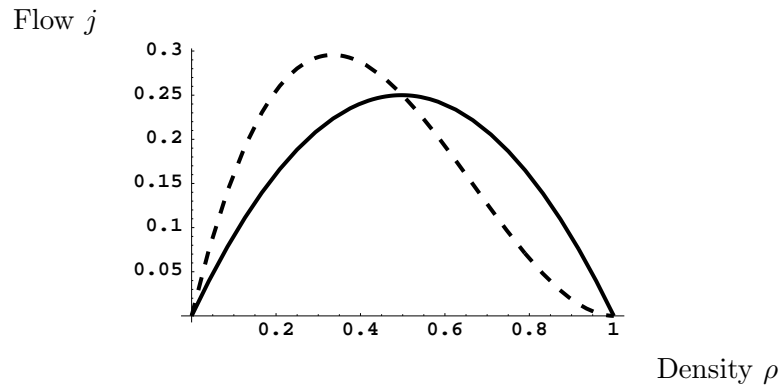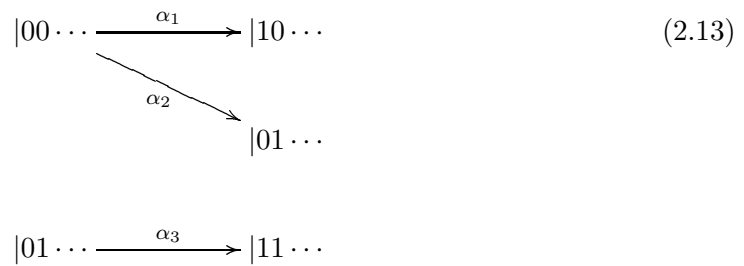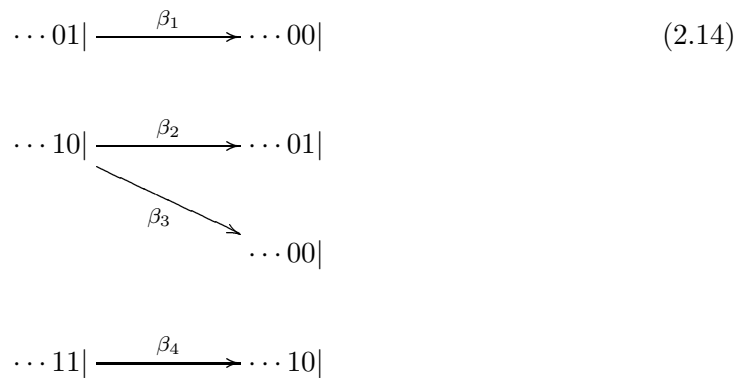
Figure 2.1.: Fundamental diagram for model A with $p_2 = 1$: The dashed line corresponds
to $p_1 = 0.01$ and the solid line to $p_1 = 0.99$.

introduced by allowing injection of particles at the left end of the chain and removal of
particles at the right end. For the left end one fixes the following input rates

$$|00 \cdots \xrightarrow{\alpha_1} |10 \cdots \tag{2.13}$$

$$\xrightarrow{\alpha_2}$$

$$|01 \cdots$$

$$|01 \cdots \xrightarrow{\alpha_3} |11 \cdots$$

Here '0' denotes an empty site and '1' an occupied one.
For the right end the output rates

$$\cdots 01| \xrightarrow{\beta_1} \cdots 00| \tag{2.14}$$

$$\cdots 10| \xrightarrow{\beta_2} \cdots 01|$$

$$\xrightarrow{\beta_3}$$

$$\cdots 00|$$

$$\cdots 11| \xrightarrow{\beta_4} \cdots 10|$$

were chosen.
Using the cancelling-mechanism one gets the following relations, which have to be fulfilled
in addition to (2.10)

$$
\begin{aligned}
-(\alpha_1 + \alpha_2)EE &= -X_{11}, & \beta_1 ED + \beta_3 ED &= X_{11}, \\
\alpha_2 EE - \alpha_3 ED &= -X_{12}, & (\beta_2 - \beta_1)ED &= X_{12}, \\
\alpha_1 EE &= -X_{21}, & -(\beta_3 + \beta_2)ED + \beta_4 DD &= X_{21}, \\
\alpha_3 ED &= -X_{22}, & -\beta_4 DD &= X_{22}.
\end{aligned}
\tag{2.15}
$$

The one-dimensional solution (2.11) still serves as a solution of (2.15), if the boundary rates are given by

$$
\begin{aligned}
\alpha_1 &= p_1 D + p_2 DE, & \beta_1 &= -\beta_3 + p_1 E + p_2 E(1 + E), \\
\alpha_2 &= p_2 D, & \beta_2 &= -\beta_3 + p_1 + p_2 E, \\
\alpha_3 &= \alpha_1, & \beta_4 &= p_1 E + p_2 E^2,
\end{aligned}
\tag{2.16}
$$

where $\beta_3 \in \mathbb{R}$ is a free parameter, and

$$
x = p_1 D^2 E - p_2 DE^3.
\tag{2.17}
$$

This solution corresponds to a flat density profile. Up to now it was not possible to determine solutions of the algebra for the case of arbitrary boundary rates. However, in [41] it has been argued that the form of the phase diagram is determined by the fundamental diagram of the periodic system. In the ASEP the line with a flat density profiles touches all phases. In this case the knowledge of the special line allows to conjecture e.g. the values of currents and the bulk densities as function of the boundary rates in the different phases. The second model – *model B* – shows again three-site interactions in the bulk. The same model has been studied independently in [42], where equivalent results for periodic and open systems have been found. Similar to model A, particles move along a chain of length L exclusively in one direction. If a particle has two empty sites in front of it, it moves one site with rate 1; if only the next site is empty, the particle performs the same move with rate λ. For $\lambda < 1$ this model may be considered as a traffic flow model with a so-called *slow-to-start rule* (see [43] and references therein).

The stochastic process obtained from model B after a particle-hole transformation [3] is also very interesting [44]. Here the hopping probability depends on the occupation number of the site directly behind the particle. If the site to the left is occupied a particle moves to the right with rate p_2, if it is empty it moves with rate p_1. For $p_1 > p_2$ the particles prefer to stick together, which can lead to interesting clustering properties. This model might have applications for granular matter and flocking behaviour, where similar interactions have been studied (see e.g. [45]).

The matrix product ansatz is the same as for model A and leads to the bulk-algebra:

$$
\begin{aligned}
X_{11} E &= E X_{11}, & X_{11} D &= E X_{12}, \\
DEE &= X_{12} E - E X_{21}, & \lambda DED &= X_{12} D - E X_{22}, \\
-DEE &= X_{21} E - D X_{11}, & -\lambda DED &= X_{21} D - D X_{12}, \\
X_{22} E &= D X_{21}, & X_{22} D &= D X_{22}.
\end{aligned}
\tag{2.18}
$$

For this algebra a two-dimensional representation was found, which has a structure generic for a two-cluster approximation [37] (see also App. B)

$$
E = \begin{pmatrix} e & 1 \\ 0 & 0 \end{pmatrix}, \qquad D = \begin{pmatrix} d & 0 \\ 1 & 0 \end{pmatrix}, \qquad ed = \frac{\lambda}{1 - \lambda},
\tag{2.19}
$$

$$
\begin{aligned}
X_{11} &= \frac{e}{d}(d + x)E, & X_{12} &= eD + \frac{x}{d}ED, \\
X_{21} &= \frac{x}{d}DE, & X_{22} &= xD,
\end{aligned}
\tag{2.20}
$$

where $x \in \mathbb{R}$ is a free parameter.

---

[3] And a parity transformation so that the particles again move from left to right.

Remark 1. *(i) It is not hard to prove that any two operators E and D, which fulfill*

$$E^2 = eE,$$
$$D^2 = dD, \tag{2.21}$$
$$\lambda DED = edD,$$

with e, d being c-numbers and the X_{ij} defined in terms of E, D as in (2.20), yield a representation of the algebra (2.18).
(ii) As a consequence of this, any representation of the Temperley–Lieb algebra gives a representation of (2.18).
The Temperley-Lieb algebra $T_n(Q)$ is an associative algebra with generators e_i $(i = 1, \ldots, n)$ satisfying the relations:

$$e_i \, e_{i\pm1} \, e_i = e_i, \tag{2.22}$$
$$e_i \, e_{i+j} = e_{i+j} \, e_i, \qquad (j \neq 1), \tag{2.23}$$
$$e_i^2 = \sqrt{Q} \, e_i. \tag{2.24}$$

If one uses $T_2(\lambda)$ and defines

$$E := \frac{e}{\sqrt{Q}} \, e_1, \tag{2.25}$$

$$D := \frac{d}{\sqrt{Q}} \, e_2, \tag{2.26}$$

then E and D fulfill (2.18).

With the use of the two-dimensional representation (2.19) it is possible to calculate the expectation value of any observable in the stationary state (see e.g. [31]). The fundamental diagram is given by

$$j(\rho) = \rho \left[1 - \frac{1 - \sqrt{1 - 4(1-\lambda)\rho(1-\rho)}}{2(1-\lambda)(1-\rho)} \right]. \tag{2.27}$$

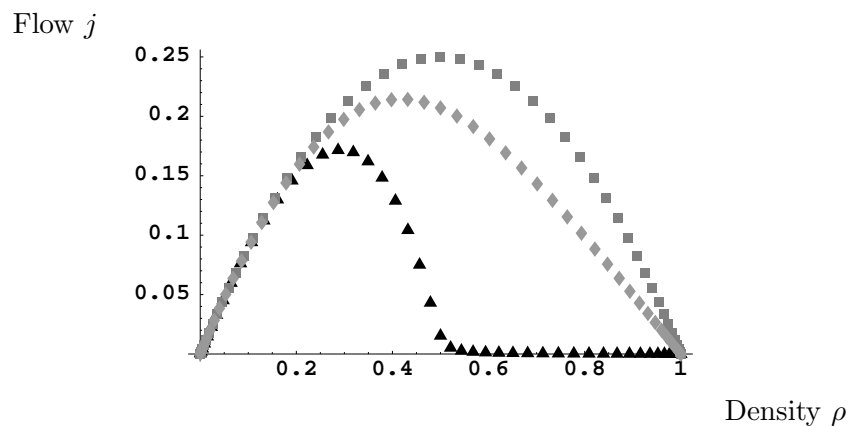For illustrational purposes some fundamental diagrams are shown in Fig. 2.2. Again, these

Figure 2.2.: Fundamental diagram of model B: squares correspond to $\lambda = 0.999$, triangles to $\lambda = 0.001$ and diamonds to $\lambda = 0.5$.

diagrams are non-symmetric due to the lack of a particle-hole symmetry.

Model B belongs to the class of zero-range processes [46] (see also [47]). Therefore one knows that the stationary state is described by a product-measure. The MPA offers a convenient way of determining this measure. However, the MPA approach is self-contained and does not use any a priori knowledge about special properties of the stochastic process under investigation.

As for model A, model B is now studied with open boundaries, having input rates

$$|00\cdots \xrightarrow{\ \alpha_1\ } |10\cdots \tag{2.28}$$

$$|01\cdots \xrightarrow{\ \alpha_2\ } |11\cdots$$

and output rates

$$\cdots 10| \xrightarrow{\ \beta_1\ } \cdots 01| \tag{2.29}$$

$$\cdots 01| \xrightarrow{\ \beta_2\ } \cdots 00|$$

$$\cdots 11| \xrightarrow{\ \beta_3\ } \cdots 10|$$

According to the cancelling-mechanism this gives the following relations, which supplement the algebra (2.18):

$$\langle W| \begin{pmatrix} -\alpha_1 EE \\ -\alpha_2 ED \\ \alpha_1 EE \\ \alpha_2 ED \end{pmatrix} = -\langle W| \begin{pmatrix} X_{11} \\ X_{12} \\ X_{21} \\ X_{22} \end{pmatrix} \tag{2.30}$$

$$\begin{pmatrix} \beta_2 ED \\ \beta_1 DE - \beta_2 ED \\ \beta_3 DD - \beta_1 DE \\ -\beta_3 DD \end{pmatrix} |V\rangle = \begin{pmatrix} X_{11} \\ X_{12} \\ X_{21} \\ X_{22} \end{pmatrix} |V\rangle. \tag{2.31}$$

Again, it is found that the two-dimensional representation (2.19), (2.20) is also a representation for (2.30), (2.31) if x is given by

$$x_\pm = \frac{\lambda}{1-\lambda} \left[e + d \pm \sqrt{(e-d)^2 + \frac{4}{\lambda} ed} \right], \tag{2.32}$$

where x_+ and x_- correspond to $\lambda > 1$ and $\lambda < 1$, respectively, and the boundary rates satisfy

$$\begin{aligned} \alpha_1 &= 1 + \frac{x}{d}, & \alpha_2 &= \lambda \alpha_1, \\ \beta_2 &= \beta_3 = -\frac{x}{d}, & \beta_1 &= \frac{-xe}{d(e+x)}, \\ \langle W| &= \left(-\frac{ed}{x}, 1 \right), & |V\rangle &= \left(1, -\frac{de}{x} - d - e \right)^t. \end{aligned} \tag{2.33}$$

That means that there is a two-dimensional submanifold of the parameter space on which the stationary state can be written as a matrix product state with two-dimensional matrices. The density profiles calculated on this submanifold are flat.

3. Exact solution of a staggered hopping model

3.1. Introduction

In this chapter, the N-particle stationary states of a staggered hopping model with reflective boundaries[1] will be calculated. The calculations rely on the fact that the stationary states are optimum ground states. Recursion relations in the particle number for any l-point density correlation function will be derived.

Furthermore, the connection between reflective boundaries and the occurrence of optimum ground states will be examined. Using a counterexample it will be shown that reflective boundaries do not enforce the stationary state to be an optimum ground state.

3.2. Definition of the model

Consider the following stochastic process: Particles with exclusion statistics occupy the sites of a chain of length L. The odd sites of the chain belong to sublattice A and the even sites to sublattice B (see Fig. 3.1).
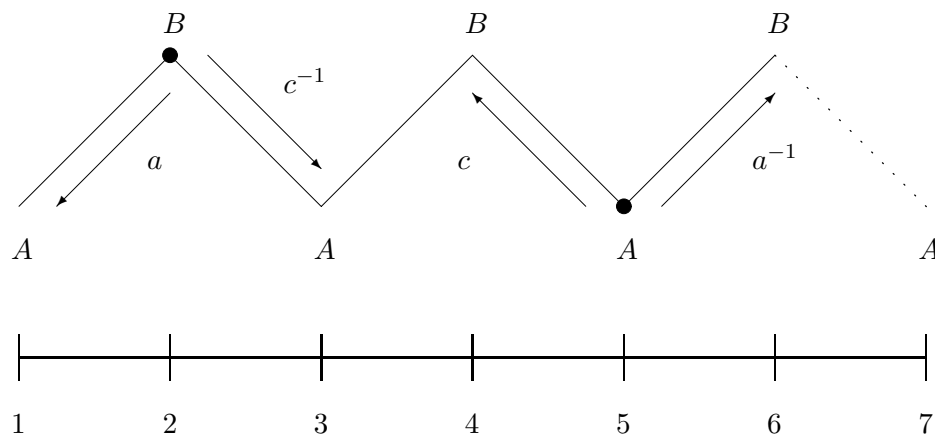

Figure 3.1.: Hopping model on a zig-zag chain. For illustrational purposes $\mu_i = 1$ for all bonds has been chosen.

---

[1]In the language of quantum spin chains such boundaries are usually denoted open boundaries.

The global stochastic Hamiltonian is an alternating sum of local two-site Hamiltonians

$$H_{a:c} = \sum_{i \in A} \mu_i h_i^A + \sum_{i \in B} \mu_i h_i^B, \tag{3.1}$$

where h_i^A and h_i^B act non-trivially only on sites i and $i+1$ according to

$$h_i^A = \begin{pmatrix} 0 & 0 & 0 & 0 \\ 0 & a & -\frac{1}{a} & 0 \\ 0 & -a & \frac{1}{a} & 0 \\ 0 & 0 & 0 & 0 \end{pmatrix}_{i,i+1}, \qquad h_i^B = \begin{pmatrix} 0 & 0 & 0 & 0 \\ 0 & c & -\frac{1}{c} & 0 \\ 0 & -c & \frac{1}{c} & 0 \\ 0 & 0 & 0 & 0 \end{pmatrix}_{i,i+1}. \tag{3.2}$$

The local two-site basis is ordered as follows: $\{\uparrow\uparrow, \uparrow\downarrow, \downarrow\uparrow, \downarrow\downarrow\}$. $\uparrow$ corresponds to an empty site, $\downarrow$ to an occupied site.

The $\mu_i \in \mathbb{R}^+$ are arbitrary constants, which may differ from site to site. They control the activities of the bonds and influence dynamical properties only.

3.3. Motivation

The model defined above can be regarded as the merger of two other problems. The first problem is that of hopping in the presence of quenched disorder and the second is that of a heuristic hopping model for the (effective) description of a flashing ratchet.

In [48] Sandow and Schütz examined the Hamiltonian $H_{q:q}$. There, the crucial point was the symmetry of $H_{q:q}$ under the action of the quantum algebra $U_q[SU(2)]$ [49, 50]. The generators $S^{\pm,z}$ of $U_q[SU(2)]$ satisfy

$$[S^+, S^-] = [2S^z]_q \qquad \text{and} \qquad [S^z, S^\pm] = \pm S^\pm, \tag{3.3}$$

where the expression $[x]_q$ is defined by $[x]_q = (q^x - q^{-x})/(q - q^{-1})$.

A representation in terms of Pauli matrices can be given by

$$S^+ = \sum_{k=1}^{L} s_k^+(q), \qquad S^- = \sum_{k=1}^{L} s_k^-(q), \qquad S^z = \sum_{k=1}^{L} (-n_k + \frac{1}{2}) \tag{3.4}$$

with

$$\begin{aligned} s_k^-(q) &= q^{\sum_{j=1}^{k-1}(n_j-1)} s_k^- q^{\sum_{j=k+1}^{L}(n_j-1)}, \\ s_k^+(q) &= q^{\sum_{j=1}^{k-1} n_j} s_k^+ q^{\sum_{j=k+1}^{L} n_j - 1}, \end{aligned} \tag{3.5}$$

and $n_k = s_k^- s_k^+ = (1 - \sigma_k^z)/2$.

By direct calculation it can be shown that every local Hamiltonian of $H_{q:q}$ commutes with all generators of $U_q[SU(2)]$. Hence,

$$[H, S^\pm] = [H, S^z] = 0. \tag{3.6}$$

From Eq. (3.6) all unnormalized N-particle stationary states can be constructed out of the zero particle state $|\text{vac}\rangle$ by

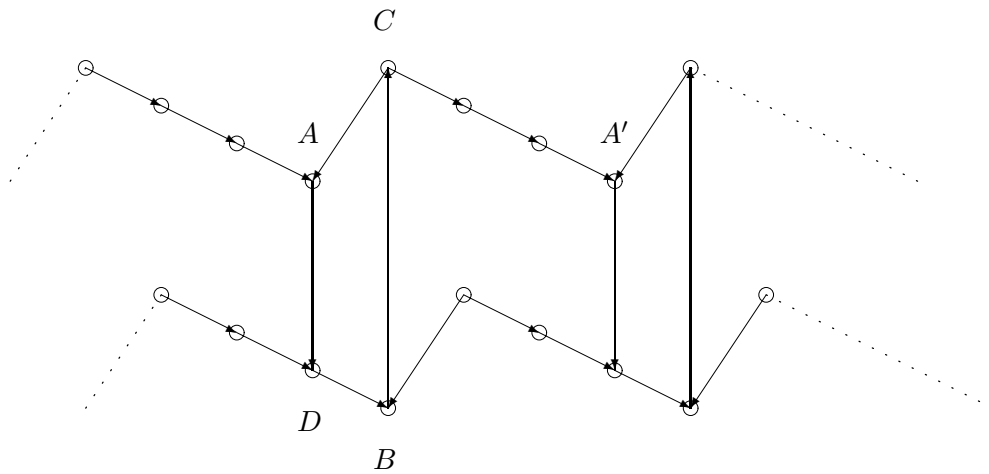$$|N\rangle = \frac{1}{[N]_q!} (S^-)^N |\text{vac}\rangle \tag{3.7}$$

Figure 3.2.: The two alternating potentials, at discrete positions marked by circles. Within each potential downward transitions occur instantly and irreversibly, while transitions between the potentials occur at finite rates. A and A' are minima of the upper potential, B is a minimum of the lower potential and C and D are examples of states from which downward transitions occur instantly.

with $[N]_q! = [1]_q[2]_q \cdots [N]_q$. Using the algebraic properties of $S^{\pm}$, S^z, Sandow and Schütz derived recursion relations for arbitrary l-point density correlation functions. In addition, they calculated some dynamical quantities from a generalized selection rule.

The second problem was introduced in [51]. In this work Kolomeisky and Widom proposed a hopping model as an effective model for the description of the motion of a motor protein on a micro-tubule. For this motion Ajdari, Prost *et al.* [52, 53, 54] and others [55, 56, 57] have proposed several "ratchet" models. Common to these models is that the motor protein on the micro-tubule, in either of its two states (bound to ATP or its hydrolysis products, or free of them), is represented by a particle on a line. This particle is confined to two potential energies, each potential being a periodic function in space but asymmetric within a period. The change in the protein's state is then modeled as a switching off of one of the potentials and a simultaneous switching on of the other. Thus, at a time, only one of the potentials is active. The particle is assumed to undergo a Brownian motion within each active potential. Due to this behaviour such ratchet models are called *flashing ratchets*.

In [51] a simplified version – an extreme limiting case – of such ratchet models has been examined. It is schematically pictured in Fig. 3.2. Both potentials are periodic in spatial direction.

Within each potential downward transitions are taken to occur instantly and irreversibly, so that a particle will always be in the potential minima. Transitions between the potentials take place with a finite rate, but only between states with the same position in spatial direction. Examples are the transitions $A \to D$ and $B \to C$ in the figure.

A particle that is found in position A at some time can only undergo a transition to D, but then it will move instantly to B. The next (possible) transition will be to C, from
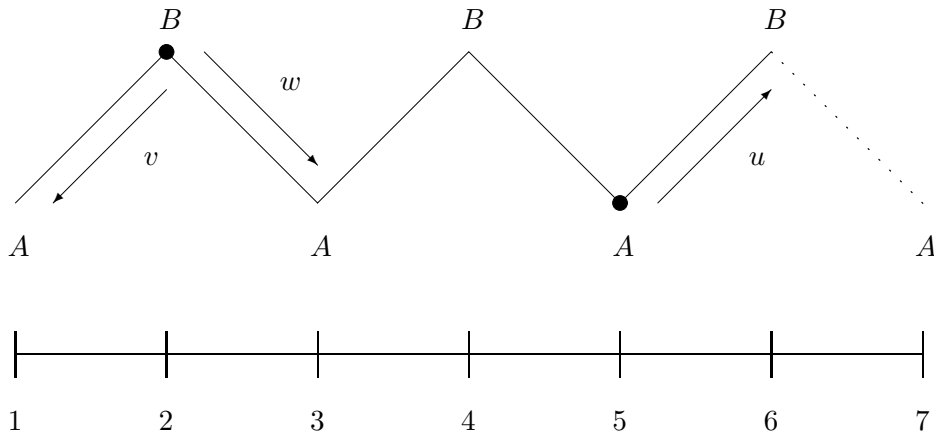
Figure 3.3.: Effective hopping model on a zig-zag chain for the description of a special
            flashing ratchet.

which the particle will directly move to A or A'. In the first case the particle has simply
undergone a cycle of changes. In the second case it has advanced by one spatial period.
Hence, a particle has a steady drift to the right.

Effectively the observable transitions are of three types: from A to B (via D), from B to
A (via C), and from B to A' (via C). If the respective transition rates are u, v and w,
then this ratchet can effectively be described by a hopping model like $H_{a:c}$ (see Fig. 3.3).
For this model Kolomeisky and Widom solved the one-particle problem, i.e., they calcu-
lated $P_x(t)$, which denotes the probability to find the particle at x at time t given initially
$P_x(0)$.

3.4. Construction of the stationary state

After the connection of $H_{a:c}$ to two existing models has been elucidated, in this section
the stationary state of $H_{a:c}$ will be derived.

As no particles enter or leave the chain from the outside, the total particle number N is
a conserved quantity. Thus, the stationary states of a chain of length L can be classified
according to the particle number $N \leq L$.

Exact solutions of small systems with $L \leq 4$ indicate that the stationary state for any
given particle number is unique and, more interestingly, that this stationary state is an
optimum ground state [24, 28, 29]. As a consequence of that, a ground state $|\psi\rangle$ which has
a component

$$|\alpha_1, \dots, \alpha_{i-1}, \downarrow, \uparrow, \beta_{i+2}, \dots, \beta_L\rangle$$

must also have a component

$$|\alpha_1, \dots, \alpha_{i-1}, \uparrow, \downarrow, \beta_{i+2}, \dots, \beta_L\rangle$$

with a relative weight given by

$$\left\{ \begin{matrix} a^{-2} \\ c^{-2} \end{matrix} \right\}_i := \begin{cases} a^{-2} \text{ if } i \text{ odd,} \\ c^{-2} \text{ if } i \text{ even.} \end{cases} \tag{3.8}$$

Hence, each stationary state with particle number N can be constructed in the following way. A reference state is given by the state where all particles occupy the first N sites of the chain. From this state all other states are built by moving particles exclusively to the right, respecting the exclusion principle, and only moving one particle at a time. According to the site i on which this particle has been sitting before its move, the weight of the new state is the one of the old state multiplied by $\left\{ \begin{smallmatrix} a^{-2} \\ c^{-2} \end{smallmatrix} \right\}_i$. In the end, one has reached all N-particle states, which can now be normalized. This construction is shown in Fig. 3.4 for a system of length $L = 4$ and particle number $N = 2$.
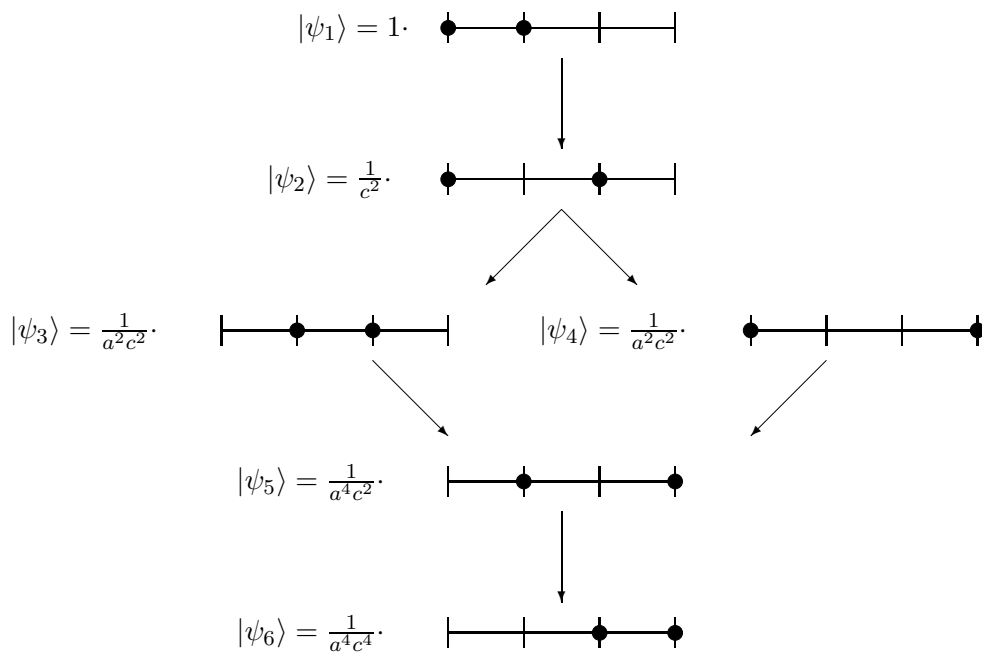

$|\psi_1\rangle = 1\cdot$

$|\psi_2\rangle = \frac{1}{c^2}\cdot$

$|\psi_3\rangle = \frac{1}{a^2c^2}\cdot$ $|\psi_4\rangle = \frac{1}{a^2c^2}\cdot$

$|\psi_5\rangle = \frac{1}{a^4c^2}\cdot$

$|\psi_6\rangle = \frac{1}{a^4c^4}\cdot$

Figure 3.4.: Construction of stationary state $|\psi\rangle = \sum_{i=1}^{6} |\psi_i\rangle$ for $L = 4$ and $N = 2$.

Although this procedure is fairly simple, it is very complicated to extract physical quantities like density profiles or any correlation function.

At this point, the connection between optimum ground states for stochastic processes, matrix product ansatz and the cancelling-mechanism will be discussed.

A closer inspection of the proof of the proposition by Krebs and Sandow [34] and the generalization thereof in this work (see Chap. 2) shows that no use has been made of the explicit form of the boundary operators. Thus, in the setting of the propositions, zero boundary operators, i.e., reflective boundaries are allowed as well!

A suitable ansatz for the stationary state in the presence of staggering has the form

$$|P_L\rangle = \langle W| \underbrace{\mathcal{D} \otimes \bar{\mathcal{D}} \otimes \cdots \otimes \begin{Bmatrix} \mathcal{D} \\ \bar{\mathcal{D}} \end{Bmatrix}_L}_{L\text{-fold product}} |V\rangle, \tag{3.9}$$

where

$$\mathcal{D} = \begin{pmatrix} E \\ D \end{pmatrix}, \qquad \bar{\mathcal{D}} = \begin{pmatrix} \bar{E} \\ \bar{D} \end{pmatrix}. \tag{3.10}$$

E, D, $\bar{E}$ and $\bar{D}$ are matrices acting on some auxiliary vector space A, $|V\rangle \in A$ and $\langle W| \in A^*$. By direct computation one verifies that this vector is a ground state of H, if one can find matrices X_1, X_2 and $\bar{X}_1$, $\bar{X}_2$, which are the components of the vectors $\mathcal{X}$ and $\bar{\mathcal{X}}$, respectively, such that the following relations are fulfilled

$$\begin{aligned} h^A(\mathcal{D} \otimes \bar{\mathcal{D}}) &= \mathcal{X} \otimes \bar{\mathcal{D}} - \mathcal{D} \otimes \bar{\mathcal{X}}, \\ h^B(\bar{\mathcal{D}} \otimes \mathcal{D}) &= \bar{\mathcal{X}} \otimes \mathcal{D} - \bar{\mathcal{D}} \otimes \mathcal{X}, \\ \langle W|\mathcal{X} &= 0, \\ \begin{Bmatrix} \mathcal{X} \\ \bar{\mathcal{X}} \end{Bmatrix}_L |V\rangle &= 0. \end{aligned} \tag{3.11}$$

The most simple way to satisfy this algebra is given by the choice $X_1 = X_2 = \bar{X}_1 = \bar{X}_2 = 0$. Then, the only remaining equations are

$$\begin{aligned} h^A(\mathcal{D} \otimes \bar{\mathcal{D}}) &= 0, \\ h^B(\bar{\mathcal{D}} \otimes \mathcal{D}) &= 0 \end{aligned} \tag{3.12}$$

turning $|P_L\rangle_0$ into an optimum ground state!

More explicitly, the problem of finding the ground state of $H_{a:c}$ becomes the problem of finding a representation of the quadratic algebra

$$\begin{aligned} E\bar{D} &= \frac{1}{a^2} D\bar{E}, \\ \bar{E}D &= \frac{1}{c^2} \bar{D}E. \end{aligned} \tag{3.13}$$

The algebra (3.13) fixes the relative weight of two configurations in $|P_L\rangle_0$ that differ only by the interchange of a particle and a hole at the sites i and $i + 1$. This relative weight is exactly the one that has been been proposed above by means of the optimum ground state property given by (3.8). Thus, in case of reflective boundaries the appearance of optimum ground states can be connected with the fact that the algebra, necessary for the construction of the ground state in form of a matrix product state, takes its most simple form. Nevertheless, it should be noticed that reflective boundaries do not enforce optimum ground states, as will be shown in the caveat at the end of this chapter.

Up to this point, two ways for the construction of the stationary state of $H_{a:c}$ have been presented. The first way gives a recipe for the construction of the relative probabilities of all states that are present in the stationary state. The second way is connected with the matrix product approach: The ground state problem is transformed into the purely algebraic problem of finding the representation of the quadratic algebra (3.13).

In the following, no use of these two possibilities will be made. Instead, a third way will be given that closely resembles the construction in [48]. The starting point will be the vacuum vector

$$|\text{vac}\rangle := \prod_{i=1}^{L}{}^{\otimes} |\uparrow\rangle \qquad (3.14)$$

describing a completely empty chain.

Out of this vacuum all N-particle stationary states will be constructed, using powers of suitable creation[2] operators.

With

$$q := \begin{pmatrix} 1 & 0 \\ 0 & ac \end{pmatrix} \qquad (3.15)$$

the particle creation operators can be defined.

Definition 2. *For every $j \in \{1, 2, \ldots, L\}$ a "local" particle creation operator b_j^- is given by*

$$b_j^- = \left(\frac{1}{a^2}\right)^{\lfloor \frac{j}{2} \rfloor} \left(\frac{1}{c^2}\right)^{\lfloor \frac{j-1}{2} \rfloor} \prod_{i=1}^{j-1} q_i \cdot s_j^- . \qquad (3.16)$$

The global creation operator B^- is the sum of all local creation operators

$$B^- = \sum_{j=1}^{L} b_j^- . \qquad (3.17)$$

In order to shorten the notation one furthermore defines

$$\{k\}_{a:c} := \left(\frac{1}{a^2}\right)^{\lfloor \frac{k}{2} \rfloor} \left(\frac{1}{c^2}\right)^{\lfloor \frac{k-1}{2} \rfloor} , \qquad (3.18)$$

and

$$[k]_{a:c} := \frac{1 - (ac)^k}{1 - ac}, \qquad (3.19)$$

as well as

$$[k]_{a:c}! := [1]_{a:c}[2]_{a:c} \cdots [k]_{a:c}. \qquad (3.20)$$

Note that the symbol $\{k\}_{a:c}$ looks similar to $\left\{ \begin{smallmatrix} a^{-2} \\ c^{-2} \end{smallmatrix} \right\}_i$ defined in (3.8), but has a different meaning.

Finally, the most important quantities will be introduced.

Definition 3. *The unnormalized N-particle stationary state $|N\rangle$ is built out of the vacuum by*

$$|N\rangle := \frac{1}{[N]_{a:c}!}(B^-)^N |vac\rangle. \qquad (3.21)$$

In addition, one has the left complete N-particle state, defined as

$$\langle N| := \langle vac| \frac{1}{N!}(S^+)^N. \qquad (3.22)$$

---

[2]Note that creation of particles corresponds to lowering a spin in the language of spin-operators.

For the left complete state it is straightforward to show that

$$\langle N|s_k^- = \langle N - 1|(1 - n_k). \tag{3.23}$$

From exact solutions of systems with $L < 4$ a similar relation has been guessed for the unnormalized N-particle state $|N\rangle$.

Property 3. *For all $k \in \{1, 2, \dots, L\}$ the following identity holds*

$$s_k^+|N\rangle = \{k\}_{a:c}(1 - n_k)|N - 1\rangle. \tag{3.24}$$

This property can be proven by direct calculation. As a consequence one finds another valuable property.

Property 4. *The l-point density correlation functions obey the recursion relation*

$$\langle N|n_{x_1} \dots n_{x_l}|N\rangle = \{x_l\}_{a:c}\langle N - 1|n_{x_1} \dots (1 - n_{x_l})|N - 1\rangle. \tag{3.25}$$

Next the proof will be given that $|N\rangle$ is indeed an optimum ground state and hence a stationary state.

Proof. It suffices to show that

$$\frac{P(\alpha_1, \dots, \alpha_{k-1}, \uparrow, \downarrow, \beta_{k+2}, \dots, \beta_L)}{P(\alpha_1, \dots, \alpha_{k-1}, \downarrow, \uparrow, \beta_{k+2}, \dots, \beta_L)} = \left\{ \begin{matrix} a^{-2} \\ c^{-2} \end{matrix} \right\}_k. \tag{3.26}$$

With the definition

$$\tau_{\alpha_i} = \begin{cases} (1 - n_i) & \text{for } \alpha_i = \uparrow, \\ n_i & \text{for } \alpha_i = \downarrow \end{cases} \tag{3.27}$$

one has

$$P(\alpha_1, \dots, \alpha_{k-1}, \gamma_k, \gamma_{k+1}, \beta_{k+2}, \dots, \beta_L) =$$
$$\frac{1}{Z(L)}\langle N|\tau_{\alpha_1} \cdots \tau_{\alpha_{k-1}}\tau_{\gamma_k}\tau_{\gamma_{k+1}}\tau_{\beta_{k+2}} \cdots \tau_{\beta_L}|N\rangle. \tag{3.28}$$

Thus,

$$\frac{P(\alpha_1, \dots, \alpha_{k-1}, \uparrow, \downarrow, \beta_{k+2}, \dots, \beta_L)}{P(\alpha_1, \dots, \alpha_{k-1}, \downarrow, \uparrow, \beta_{k+2}, \dots, \beta_L)}$$
$$= \frac{\langle N|\tau_{\alpha_1} \cdots \tau_{\alpha_{k-1}}(1 - n_k)n_{k+1}\tau_{\beta_{k+2}} \cdots \tau_{\beta_L}|N\rangle}{\langle N|\tau_{\alpha_1} \cdots \tau_{\alpha_{k-1}}n_k(1 - n_{k+1})\tau_{\beta_{k+2}} \cdots \tau_{\beta_L}|N\rangle}$$
$$\overset{(3.25)}{=} \frac{\{k + 1\}_{a:c}}{\{k\}_{a:c}} \frac{\langle N + 1|\tau_{\alpha_1} \cdots \tau_{\alpha_{k-1}}n_k n_{k+1}\tau_{\beta_{k+2}} \cdots \tau_{\beta_L}|N + 1\rangle}{\langle N + 1|\tau_{\alpha_1} \cdots \tau_{\alpha_{k-1}}n_k n_{k+1}\tau_{\beta_{k+2}} \cdots \tau_{\beta_L}|N + 1\rangle}$$
$$= \left\{ \begin{matrix} a^{-2} \\ c^{-2} \end{matrix} \right\}_k. \tag{3.29}$$

$\square$

Note that it has been checked that B^- does not commute with $H_{a:c}$ and so does *not* reflect a global symmetry. Both operators commute only, if they are restricted to the kernel of $H_{a:c}$. Therefore, the integrability found for $a = c = q$ is most presumably lost if $a \neq c$.

3.5. Density profiles from recursion relations

For the calculation of density profiles, in principle, the normalization of $|N\rangle$ has to be computed. Unfortunately, a direct computation of this quantity is very involved and tedious. Therefore a step-by-step method has been chosen. Assume that $Z(N-1)$ is the normalization of $|N-1\rangle$. Assume further that z_N is such that the normalization $Z(N)$ of $|N\rangle$ is given by

$$Z(N) = z_N Z(N-1). \tag{3.30}$$

This gives

$$\rho_k(N) = \frac{\langle N|n_k|N\rangle}{Z(N)} = \frac{\{k\}_{a:c}}{z_N}(1 - \rho_k(N-1)). \tag{3.31}$$
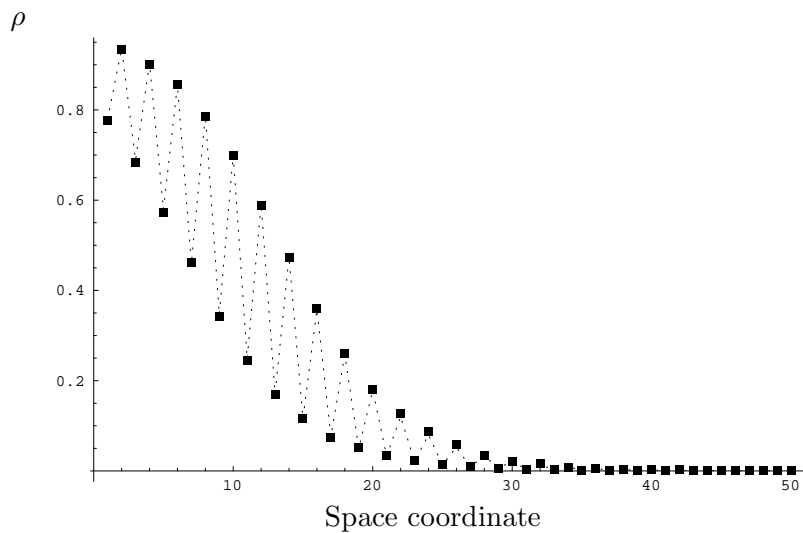

Figure 3.5.: Density profile of staggered hopping-model. $a = 0.5$, $c = 2.5$, $L = 50$ and $N = 10$. The dashed line corresponds to analytical data from (3.34). The boxes represent Monte-Carlo data.

In the N-particle state naturally the identity

$$\sum_{k=1}^{L} \rho_k(N) = N \tag{3.32}$$

holds. Thus,

$$z_N = \frac{1}{N}\sum_{k=1}^{L}\{k\}_{a:c}(1 - \rho_k(N-1)). \tag{3.33}$$

Finally, one finds a recursion relation for the local density of an N-particle stationary state

$$\rho_k(N) = N\frac{\{k\}_{a:c}(1 - \rho_k(N-1))}{\sum_{k=1}^{L}\{k\}_{a:c}(1 - \rho_k(N-1))}. \tag{3.34}$$
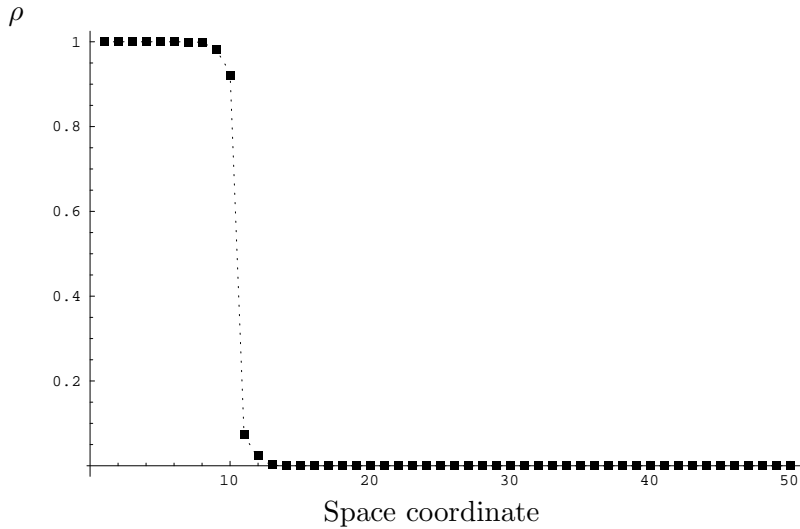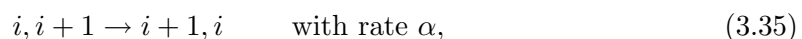
Figure 3.6.: Density profile of staggered hopping-model. $a = 2.0$, $c = 4.0$, $L = 50$ and $N = 10$. The dashed line corresponds to analytical data from (3.34). The boxes represent Monte-Carlo data.

Starting from the normalized stationary state $|\text{vac}\rangle$, which belongs to $N = 0$ and has $\rho_k(0) = 0$, the density profiles for all N can be computed. The results have been compared with Monte-Carlo data (see Fig. 3.5 and Fig. 3.6) showing perfect agreement. If one of the paramters is larger than one, whereas the other parameter is smaller than one, the density profiles clearly reflect the sublattice structure of the Hamiltonian, since the slope of the profile is alternatingly positve and negative along the bonds (see Fig. 3.5). In contrast to that, if both parameters are larger or smaller than one, the density profiles become monotonous functions of ρ and the sublattice structure is hidden (see Fig. 3.6).
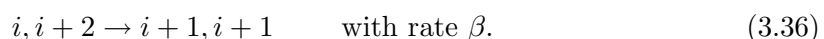
3.6. A caveat

As presented above, optimum ground states come into play naturally, if one encounters stochastic processes with reflective boundaries. Therefore one might conjecture that the stationary state of such processes is always of this special type. However, this is not true. In the following a $\mathbb{Z}_3$-symmetric reaction-diffusion model will be presented, which has zero-energy ground states that are not (always) optimum ground states.

The sites of a chain of length L are coloured with the elements of $\mathbb{Z}_3$, i.e., one has three types of particles on a completely filled chain. Two particles on neighbouring sites react according to the following rules (algebraic manipulations are done according to $\mathbb{Z}_3$)

$$i, i+1 \rightarrow i+1, i \qquad \text{with rate } \alpha, \tag{3.35}$$

and

$$i, i+2 \rightarrow i+1, i+1 \qquad \text{with rate } \beta. \tag{3.36}$$

Thus, the local Hamiltonian is given by

$$
h = \begin{pmatrix}
0 & 0 & 0 & 0 & 0 & 0 & 0 & -\beta & 0 \\
0 & \alpha & 0 & 0 & 0 & 0 & 0 & 0 & 0 \\
0 & 0 & \beta & 0 & 0 & 0 & -\alpha & 0 & 0 \\
0 & -\alpha & 0 & \beta & 0 & 0 & 0 & 0 & 0 \\
0 & 0 & -\beta & 0 & 0 & 0 & 0 & 0 & 0 \\
0 & 0 & 0 & 0 & 0 & \alpha & 0 & 0 & 0 \\
0 & 0 & 0 & 0 & 0 & 0 & \alpha & 0 & 0 \\
0 & 0 & 0 & 0 & 0 & -\alpha & 0 & \beta & 0 \\
0 & 0 & 0 & -\beta & 0 & 0 & 0 & 0 & 0
\end{pmatrix}. \tag{3.37}
$$

The operators h_i act as h on sites $i, i+1$ and as identity on the remaining sites of the chain, and hence the global stochastic Hamiltonian reads

$$
H = \sum_{i=1}^{L-1} h_i. \tag{3.38}
$$

The exact solution for $L = 2$ shows a threefold degenerate ground state

$$
|\psi\rangle_2 = |i, i\rangle \text{ with } i \in \mathbb{Z}_3. \tag{3.39}
$$

These states are optimum ground states.
Looking at $L = 3$ a new situation arises. One has again a threefold optimum ground state

$$
|\psi\rangle_3 = |i, i, i\rangle \text{ with } i \in \mathbb{Z}_3. \tag{3.40}
$$

In addition, one finds two qualitatively different ground states

$$
\begin{aligned}
|\varphi_1\rangle_3 &= \sum_{i\in\mathbb{Z}_3} \left[|i, i, i+2\rangle + \frac{\beta}{\alpha}|i, i+1, i+1\rangle + \frac{\beta}{\alpha+\beta}|i, i+2, i\rangle \right], \\
|\varphi_2\rangle_3 &= \sum_{i\in\mathbb{Z}_3} \left[|i, i+2, i+2\rangle + \frac{\beta}{\alpha}|i, i, i+1\rangle + \frac{\beta}{\alpha+\beta}|i, i+1, i\rangle \right].
\end{aligned} \tag{3.41}
$$

These states are not optimum ground states. Moreover

$$
h_1|\varphi_i\rangle_3 = -h_2|\varphi_i\rangle_3 \text{ with } i = 1, 2. \tag{3.42}
$$

The occurrence of such states is most presumably connected with the existence of a $\mathbb{Z}_2$-symmetry.
This result can be understood in the context of MPA as well. As the two states are not optimum ground states, the cancelling vector $\mathcal{X}$ has to be nontrivial. Therefore,

$$
|\varphi_i\rangle_3 = \langle W|\mathcal{D} \otimes \mathcal{D} \otimes \mathcal{D}|V\rangle. \tag{3.43}
$$

Using the fact that $\langle W|$ and $|V\rangle$ must be in the kernel of $\mathcal{X}$ one finds

$$
\begin{aligned}
h_1\langle W|\mathcal{D} \otimes \mathcal{D} \otimes \mathcal{D}|V\rangle &= -\langle W|\mathcal{D} \otimes \mathcal{X} \otimes \mathcal{D}|V\rangle, \\
h_2 W|\mathcal{D} \otimes \mathcal{D} \otimes \mathcal{D}|V\rangle &= \langle W|\mathcal{D} \otimes \mathcal{X} \otimes \mathcal{D}|V\rangle,
\end{aligned} \tag{3.44}
$$

and thus (3.42) holds.
Most interestingly systems of length $L = 4$ and $L = 5$ – like the two-site system – possess only threefold degenerate optimum ground states. But then, for $L = 6$, two additional ground states, presumably connected with a $\mathbb{Z}_2$-symmetry, show up again. This gives rise to the conjecture that a global $\mathbb{Z}_2$-symmetry shows up for system sizes which are an integer multiple of three.

4. Vertex models for traffic flow

4.1. Introduction

In [58] a dimer model has been proposed, the configurations of which have been mapped
onto the trajectories of a discrete stochastic one-dimensional traffic problem on a ring [59].
This dimer model corresponds to the free fermion case of an integrable five vertex model
studied in [60]. The interpretation as a traffic problem is not restricted to the free fermion
point, however, it can be extended to a whole submanifold of the integrable vertex model
in a natural way. This submanifold will be examined using the Bethe ansatz results of
[60]. This yields the existence of five different phases, four of which are frozen in the sense
of the six-vertex model [17], and one exceptional disordered critical phase. In this phase
it is – at least in principle – possible to compute a fundamental diagram, i.e., the relation
between flow and density.
Due to mathematical difficulties this program can only be carried out for some portions
of the fundamental diagram, using expansions of the free energy as given in [60]. The rest
of the information is approximately given by a suitably defined cellular automaton model,
the stationary state of which can be computed exactly. The quality of this approximation
is discussed.

4.2. The Kasteleyn model as an approach to traffic flow

The Kasteleyn model is a statistical model suggested by Kasteleyn [58] to describe close-
packed dimers on the hexagonal lattice. The configurations of this model are in one–to–
one correspondence with those of a specific five-vertex model with the allowed vertices
displayed in Fig. 4.1.

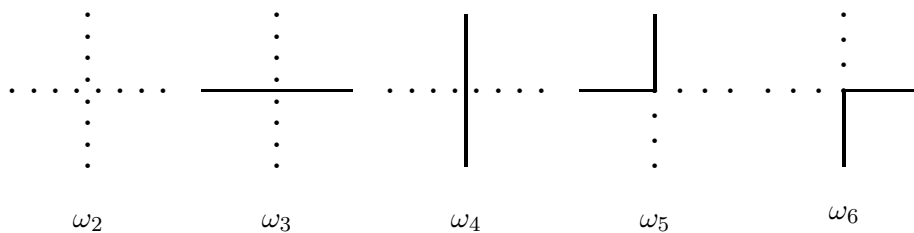$$\omega_2 \qquad \omega_3 \qquad \omega_4 \qquad \omega_5 \qquad \omega_6$$

Figure 4.1.: Allowed vertices of the five-vertex model.

The Boltzmann weights in the actual case are given through the parameterization

$$\{\omega_2, \omega_3, \omega_4, \omega_5, \omega_6\} = \{1, x, t, \sqrt{xt}, \sqrt{xt}\}, \qquad (4.1)$$

with x, and t being elements of $\mathbb{R}^+$.
A typical allowed configuration of this model is shown as Fig. 4.1. The trajectories of the

heavy lines are obviously very similar to those of cars on a one-dimensional highway with periodic boundary conditions.
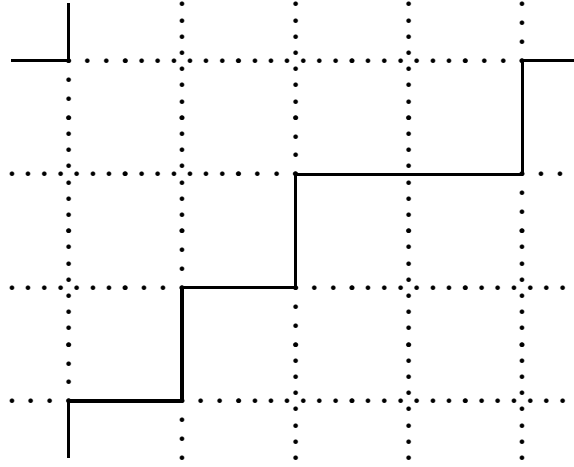

Figure 4.2.: A typical allowed configuration for a 4×5 lattice. The contribution of this configuration to Z reads $x^5 t^4$.

The partition function of this model is given by

$$Z = \sum_{\{\mathcal{C}\}} \prod_{\text{Vertices } v} \omega_{k(v)} = \sum_{\{\mathcal{C}\}} x^{N_x(\mathcal{C})} t^{N_t(\mathcal{C})}. \tag{4.2}$$

The symbol $\mathcal{C}$ denotes an allowed configuration of vertices and the function $k(v)$ gives the number of the Boltzmann weight occurring at vertex v in the configuration $\mathcal{C}$. The variables N_x and N_t denote the number of horizontal and vertical thick lines respectively. The statistical quantity which allows for the calculation of physical expectation values is the free energy per site defined as

$$f(x,t) = \lim_{M,N \to \infty} \frac{1}{MN} \ln Z \tag{4.3}$$

for a quadratic lattice with N columns and M rows and periodic boundary conditions.
It turns out that this model represents the free fermion case of the integrable five-vertex model studied in [60]. The solution will not be reproduced here, instead the results will be summarized.
The phase diagram of the model consists of four regions in the (x,t)-plane denoted by J, E, I, and D.
The phase J is given by

$$J = \{x, t \in \mathbb{R}^+ : t > 1 + x\}. \tag{4.4}$$

In this phase the whole lattice is covered by vertices of type ω_4. In traffic language it describes the trajectories of close-packed and standing or completely jammed cars, as can be seen from Fig. 4.3 (a). Therefore this phase is called the jammed phase (J).
In Region E,

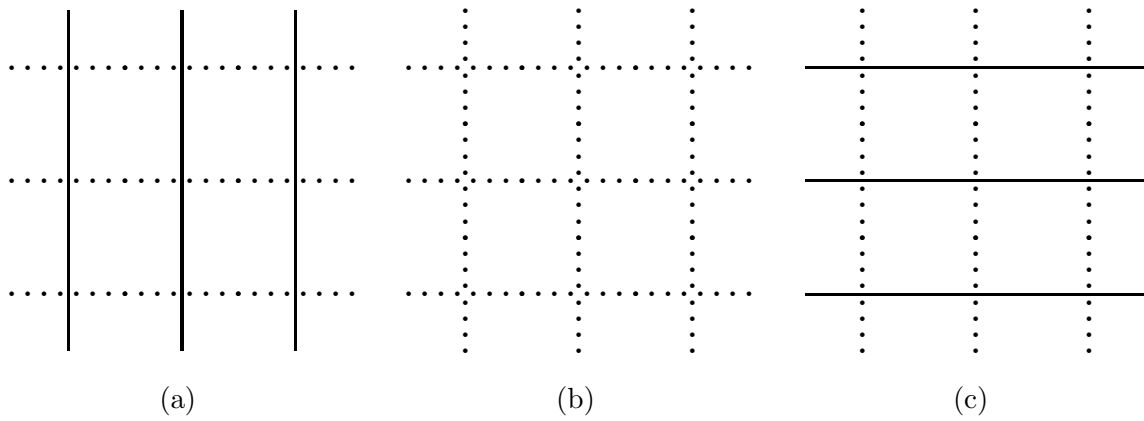$$E = \{x, t \in \mathbb{R}^+ : x < 1, t < |1 - x|\}, \tag{4.5}$$

Figure 4.3.: The three ordered phases. (a) The completely jammed phase J. (b) The empty phase E. (c) The phase with infinite speed I.

the lattice is completely covered by vertices of type ω_2. Thus, this phase describes an empty street and will be called the empty phase E (Fig. 4.3 (b)). The phase

$$C = \{x, t \in \mathbb{R}^+ : x > 1, t < |1 - x|\} \tag{4.6}$$

corresponds to the zero-density limit of cars moving with infinite speed (Fig. 4.3 (c)) . Normal trajectories of cars at all intermediate densities exist in the region

$$D = \{x, t \in \mathbb{R}^+ : |1 - x| < t < |1 + x|\}. \tag{4.7}$$

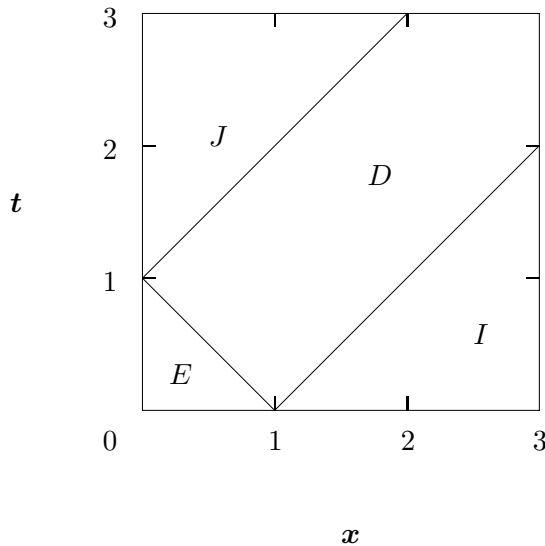The whole phase diagram is shown in Fig. 4.4.

Figure 4.4.: Phase diagram of the five-vertex model in the free fermion case.

From now on the behaviour of the vertex model in phase D will be examined exclusively, since only in this phase the density of cars ρ can assume all values between 0 and 1. The

density is the average number of steps in temporal (t) direction and is thus given by

$$\rho(x,t) = \frac{1}{NM}\langle N_t \rangle = t\frac{\partial}{\partial t}f(x,t). \tag{4.8}$$

Whereas the calculation of the density is straightforward, obtaining the average velocity is much more complicated, since the quantity $\langle N_x/N_t \rangle$ can not be computed by taking derivatives of the partition function. Therefore, as an approximation it is assumed that

$$v = \frac{\langle N_x \rangle}{\langle N_t \rangle}, \tag{4.9}$$

where the quantity $\langle N_x \rangle$ can be computed from

$$\frac{1}{NM}\langle N_x \rangle = x\frac{\partial}{\partial x}f(x,t). \tag{4.10}$$

The fundamental diagram displays the current j versus ρ. The current is given by the product

$$j = v\rho = \frac{\langle N_x \rangle}{NM}, \tag{4.11}$$

where Eq. (4.8) has been used.
Using the results of [60] one finds

$$\begin{aligned}
x\frac{\partial}{\partial x}f &= \frac{x}{2\pi}\int_{-\alpha_0\pi}^{\alpha_0\pi}\frac{\partial}{\partial x}\ln\left(1 + xe^{i\theta}\right)d\theta \\
&= \frac{1}{2\pi i}\int_{-\alpha_0\pi}^{\alpha_0\pi}\frac{\partial}{\partial\theta}\ln\left(1 + xe^{i\theta}\right)d\theta \\
&= \alpha_0 + \frac{1}{\pi}\arctan\left(\cot(\alpha_0\pi) + \frac{x}{\sin(\alpha_0\pi)}\right) - \frac{1}{2},
\end{aligned} \tag{4.12}$$

with $\alpha_0 = 1 - \rho$.
The fundamental diagram for different values of x is displayed in Fig. 4.5. This diagram shows a remarkable feature, namely the existence of two qualitatively different traffic-flow regimes. For $x < 1$ the flow reaches its maximum value

$$j(x, \rho_{\max}) = \frac{1}{2} - \rho_{\max} \tag{4.13}$$

at the density

$$\rho_{\max} = \frac{1}{\pi}\arccos(x). \tag{4.14}$$

In addition one has $j(x,0) = j(x,1) = 0$.
In the other regime, where $x > 1$, the traffic flow decreases monotonically with the increase of ρ from $j(x,0) = 1$ to $j(x,1) = 1$.
Since the idea of describing traffic flow by the global, i.e., Gibbsian statistics of a classical statistical model was totally new, the authors in [59] compared their results with the properties of a similar cellular automaton.
This cellular automaton describes the stochastic process according to the following rules. The sites of a chain can be occupied by at most one car where all cars move exclusively in one direction, say to the right. In each discrete time step all cars are updated in parallel.
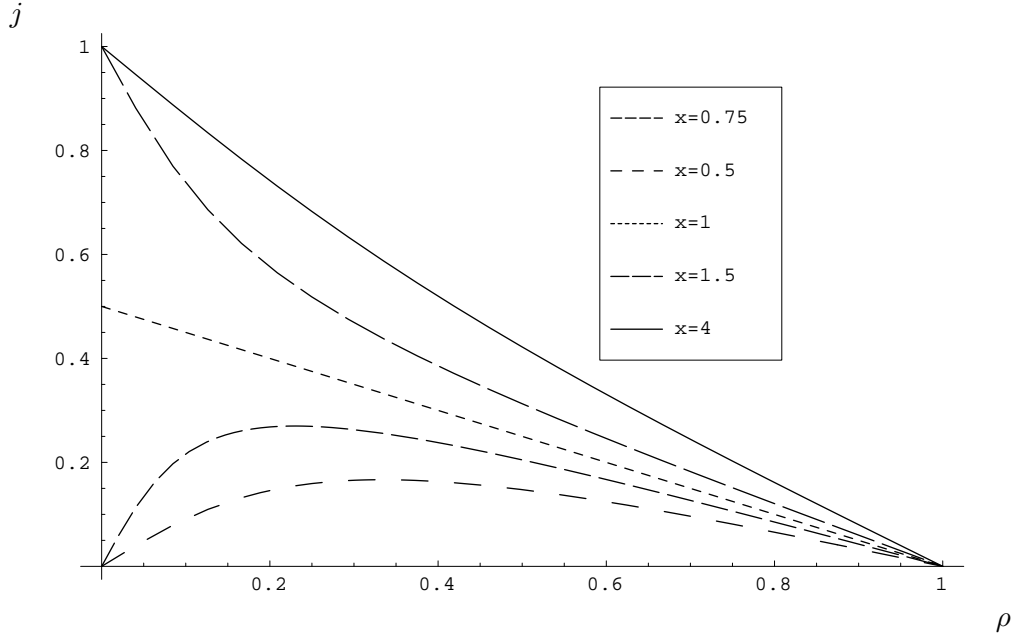
Figure 4.5.: Flow j for different values of x.

The maximum distance a car can travel during one update is restricted by the distance to the car in front of it. How far a car actually travels is decided in the following way. If the distance to the next car comprises n sites, one picks m random numbers until either this chosen random number is larger than the hopping probability p, or m is equal to n. Finally, the car moves m sites.

For this process the stationary probability measure is given by the mean-field measure. This can be seen by characterizing the state of the system at time t by the number d_i ($i = 1, \ldots, N$) of empty sites between car i and car $i + 1$. Thus, the master equation has the following form

$$P_{t+1}(\{d_i\}) = \sum_{s_1=0}^{d_N} \cdots \sum_{s_N=0}^{d_{N-1}} \prod_{i=0}^{N} [p^{s_i}(\delta_{d_i,s_{i+1}} + (1 - \delta_{d_i,s_{i+1}})q)] \\ \cdot P_t(\{d_i - s_i + s_{i+1}\}). \tag{4.15}$$

The variable s_i denotes the distance car i moves in the time step $t \to t + 1$ and $q = 1 - p$. The solution of (4.15) is simply given by $P(\{d_i\}) = 1/\binom{N}{n}$. This can be seen from

$$1 = \sum_{s_1=0}^{d_N} \cdots \sum_{s_N=0}^{d_{N-1}} \prod_{i=0}^{N} [p^{s_i}(\delta_{d_i,s_{i+1}} + (1 - \delta_{d_i,s_{i+1}})q)], \tag{4.16}$$

which follows from

$$1 = \sum_{s_i}^{d_{i-1}} p^{s_i}(\delta_{d_{i-1},s_i} + (1 - \delta_{d_{i-1},s_i})q) \tag{4.17}$$

after an interchange of the product and the sums. The probability f_n that a car moves exactly n sites (in the thermodynamic limit $N \to \infty$) reads

$$f_n = (1 - \rho)^n p^n [(1 - \rho)q + \rho]. \tag{4.18}$$

Thus, for the cellular automaton one has

$$j_{\mathrm{CA}} = \frac{\rho(1-\rho)p}{1-(1-\rho)p}. \tag{4.19}$$

In order to compare the CA result with the one for the vertex model, one has to rescale the flow of the vertex model with a factor of 2. Then the maxima of both flows lie on the line $1 - 2\rho$ and a relation between x and p, identifying curves with the same maximum, can be given by
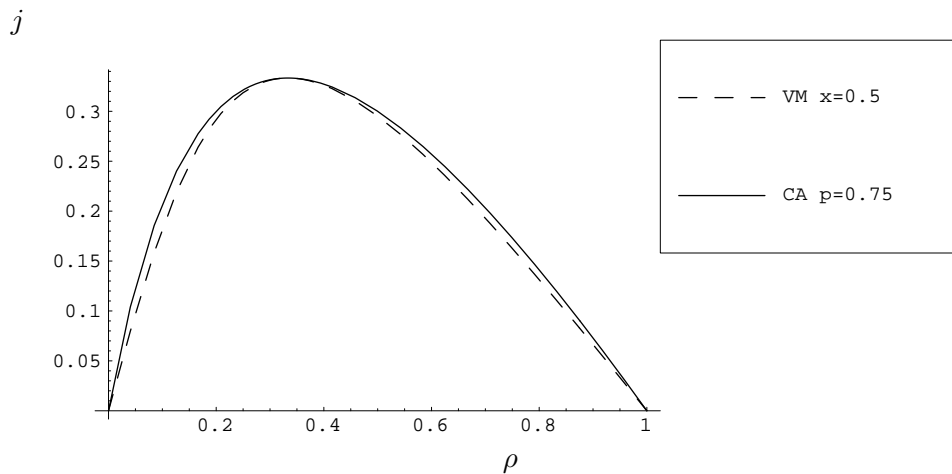

Figure 4.6.: Comparison of $2 \cdot j$ and j_{CA} for $p = \frac{3}{4}$ and $x = \frac{1}{2}$.

$$p = \frac{1 - (2/\pi)\arccos(x)}{(1 - (1/\pi)\arccos(x))^2}. \tag{4.20}$$

As Fig. 4.6 shows, the overall agreement of both curves is very good.

4.3. Generalization of the Kasteleyn approach

Above, it has been shown that the Kasteleyn model can be used for the description of traffic flow. Nevertheless, it has one shortcoming, which is the fact that in principle cars are able to move with infinite speed. Therefore, some of the allowed configurations can not be interpreted as trajectories of a massive particle moving in one dimension. In order to overcome this problem, a three-parameter generalization of the Kasteleyn model will be proposed, whose extremal limit describes a traffic model with maximal velocity normalized to one.

In order to give a less dominant weight to trajectories which contain many vertices of type ω_3, one can choose the following parameterization for the vertex weights instead of the one given by Eq. (4.1)

$$\{\omega_2, \omega_3, \omega_4, \omega_5, \omega_6\} = \{1, y, t, \sqrt{xt}, \sqrt{xt}\}, \tag{4.21}$$

with x, y and t being elements of $\mathbb{R}^+$. The configuration displayed in Fig. 4.2, e.g., has the total weight x^4yt^4. In the limit $y \to 0$ a car that has moved at one time step must stand still in the next time step.

The partition function takes the form

$$Z = \sum_{\{\mathcal{C}\}} x^{N_x(\mathcal{C})} y^{N_y(\mathcal{C})} t^{N_t(\mathcal{C})}. \tag{4.22}$$

This model is again located on a submanifold of the integrable five-vertex model of [60]. Unfortunately, this submanifold is described by a free fermion model only for $x = y$, which is the case treated in [59]. Away from the free fermion line, the contour integrations needed for the computation of the free energy can not be performed, so that no explicit solution for the free energy is available. Nevertheless, the phase diagram of the model is known. Interestingly, for y small and x large enough , i.e.

$$y < x - 4, \tag{4.23}$$

a new phase emerges. This phase describes a lattice half-filled with cars. All cars have velocity one. As displayed in Fig. 4.7, the whole lattice is completely covered alternatingly by vertices of type ω_5 and ω_6. Note that in this phase the discrete symmetry of the underlying square lattice is spontaneously broken.
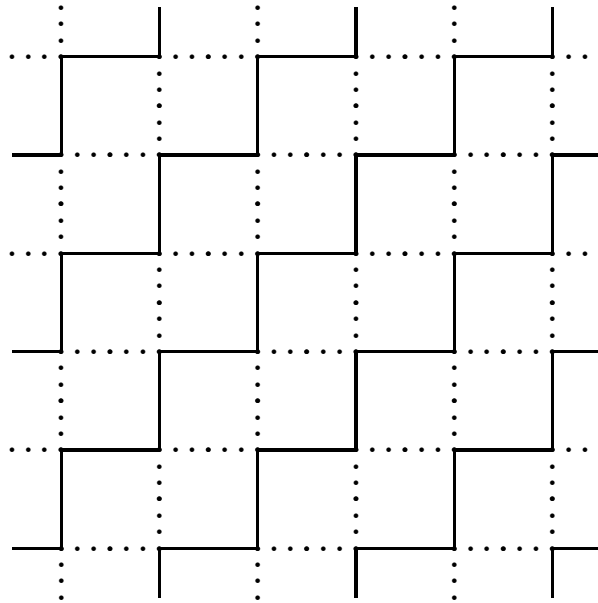

Figure 4.7.: Optimal flow phase O for $y < x - 4$.

In the region $y < x$ a variable $\mu \in [0, 1)$ such that

$$y = \mu x \tag{4.24}$$

can be defined.

Using the results of [60] and substituting the present parameterization for the vertices, the following phase boundaries are found.

The line separating the intermediate phase D and the jammed phase J is still given by

$$t = 1 + x, \tag{4.25}$$

irrespective of the value of μ. The curve separating phase D from the empty phase E begins at $t = 1$ for $x = 0$ end terminates at $x = \mu^{-1}$ for $y = 0$. One parameterization of

this curve is given by

$$t = \frac{1 - \mu x}{x(1 - \mu) + 1}, \quad x \in [0, \mu^{-1}]. \tag{4.26}$$

The end of this line at $x = \mu^{-1}$ marks the beginning of the curve separating D and the infinite speed phase I with

$$t = \mu(\mu x - 1), \quad x > \mu^{-1}. \tag{4.27}$$

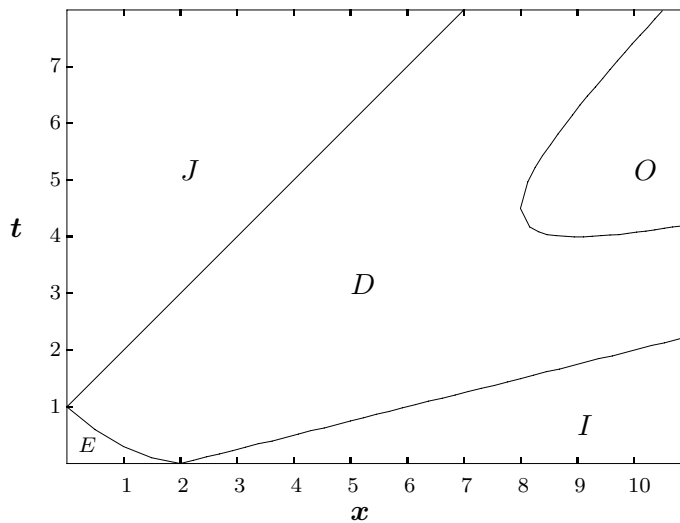The phase boundary between D and the new phase O can not be given by one equation

Figure 4.8.: Phase diagram for $\mu = 1/2$.

relating t to x and μ, since to one value of $x > 4/(1 - \mu)$ correspond two values on the t-axis. Introducing

$$R_\pm = \frac{1}{2} \left(1 \pm \sqrt{1 - \frac{4}{x(1 - \mu)}} \right), \tag{4.28}$$

this curve has the parameterization

$$t = \frac{1}{x} \left(x - \frac{1}{R_\pm} \right)^2, \quad x > \frac{4}{1 - \mu}. \tag{4.29}$$

Like above, exclusively region D will be examined further. The next step is the calculation of a fundamental diagram. In a way similar to the one used in [59] the average velocity is approximated by

$$v = \frac{\langle N_x \rangle + \langle N_y \rangle}{\langle N_t \rangle} \tag{4.30}$$

with

$$\langle N_y \rangle = NM \cdot y \partial_y f. \tag{4.31}$$

As the free energy of the model under consideration can not be calculated, this program can not be carried through. Fortunately, expansions of f for ρ in the neighbourhood of

zero and one have been derived in [60]. These results can be used to derive the asymptotics of the fundamental diagram for small and large ρ.

In the neighbourhood of one the asymptotics of j_{5V} is described by

$$j_{5V}(\rho, x) = (1 - \rho)\frac{x}{1 + x} + \mathcal{O}\left((1 - \rho)^3\right). \tag{4.32}$$

For small values of ρ one finds two different regimes. If $y > 1$, this gives

$$j_{5V}(\rho, y) = 1 - \rho\left(1 + \frac{y}{y - 1}\right) + \mathcal{O}\left(\rho^3\right), \tag{4.33}$$

whereas for $y < 1$ one has

$$j_{5V}(\rho, x, y) = \frac{\rho}{1 + x - y}(x - y) + \frac{\rho y}{1 - y} + \mathcal{O}\left(\rho^3\right). \tag{4.34}$$

These expansions already yield some very interesting information. In the limit of y going to zero, the only allowed trajectories will be such that a car moves at most one step into the x-direction per time step. This is obvious, since in this limit the only allowed vertices are the ones shown in Fig. 4.9, turning the five- into a four-vertex model.
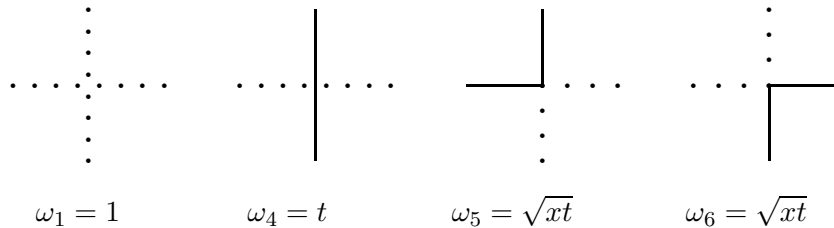

$$\omega_1 = 1 \qquad\qquad \omega_4 = t \qquad\qquad \omega_5 = \sqrt{xt} \qquad\qquad \omega_6 = \sqrt{xt}$$

Figure 4.9.: Allowed vertices of the four-vertex model derived in the limit $y \to 0$.

A microscopic model with similar properties is the Nagel-Schreckenberg (NaSch) model with $v_{\max} = 1$. The flow of this model in the stationary state is known exactly and is given by

$$j_{\mathrm{NaSch}} = \frac{1}{2}\left(1 - \sqrt{1 - 4q(1 - \rho)\rho}\right). \tag{4.35}$$

As can be seen directly the flow is a symmetric function with respect to $\rho = 1/2$. The same holds for the flow of the five-vertex model in the limit $y \to 0$. Expanding the NaSch flow (4.35) as above, one sees that both j_{NaSch} and j_{4V} have the same asymptotics for ρ near zero and one if $q = \frac{x}{x+1}$ to lowest order. Whereas the next term in the expansion of j_{NaSch} is proportional to ρ^2, the second term in the expansion of j_{4V} is proportional to ρ^3. For values of y with $0 < y < 1$, one finds that the slope of the fundamental diagram near $\rho = 0$ becomes steeper with increasing y.

For $y > 1$ the behaviour changes drastically, just as in the free fermion case. Now the fundamental diagram starts with a value of $j_{5V} = 1$ at $\rho = 0$.

Interestingly, at $\rho = 1$ the slope of the fundamental diagram depends only on x.

The question is now, whether one can find a microscopic cellular automaton (CA) model, which shows similar features such as the expansions of j_{5V}?

Therefore on can reconsider the stochastic process from above and permit a a car to be in one of two states, i.e., either moving or standing still. At the beginning of an update all

cars are in state 1, corresponding to standstill. If the distance to the next car comprises d empty cells, then d random numbers are picked. If the first random number picked is smaller than the starting probability p, the car changes its state from 1 to 2, i.e., from standing still to moving, and moves one step ahead. If the random number is larger than p, the car stays in state 1 and will not move at all during this update. As long as the consecutive random numbers picked are smaller than the driving probability q, the car remains in state 2 and moves forward one cell. If one either arrives at a random number larger than q or one runs out of random numbers, which means that the car has traveled already d cells, the car changes to state 1 and remains immobile during this update. For $p = q$ this process is exactly the one described above. The limit $q = 0$ corresponds to the Nagel-Schreckenberg model with $v_{\text{max}} = 1$.

Already here it should be mentioned that the stationary state for $p = q$ is of the mean-field type, whereas it is known that for $q = 0$ one has the so-called two-cluster measure (see App. B).

As indicated by extensive Monte-Carlo simulations the fundamental diagram (in the thermodynamic limit) does not seem to be affected by the use of the forward sequential version of the update as described above. The reason is that differences can only be due to boundary effects, since in the bulk there is no difference between both updating schemes. Of course, for nonequilibrium systems such differences can be crucial, but here they do not seem to matter. On account of that, in the following, the CA will be solved in case of forward sequential update using the MPA and for parallel update using COMF.

Introducing the probability vector $|P\rangle \in \left(\mathbb{C}^3\right)^{\otimes L}$ describing the probability measure of a chain of length L, the master equation reads

$$|P\rangle(t+1) = T_{\rightarrow} \cdot |P\rangle(t) \tag{4.36}$$

with

$$T_{\rightarrow} = \tau_L \cdot \tau_{L-1} \cdot \cdots \cdot \tau_1. \tag{4.37}$$

The operators τ_i act non-trivially at the sites i and $i+1$ and are given by

$$\tau_i = \begin{pmatrix} 1 & 0 & 0 & 0 & 0 & 0 & 0 & 0 & 0 \\ 0 & 1 & 0 & 0 & 0 & 0 & 0 & 0 & 0 \\ 0 & 0 & 0 & p & 0 & 0 & q & 0 & 0 \\ 0 & 0 & 0 & 1-p & 0 & 0 & 1-q & 0 & 0 \\ 0 & 0 & 0 & 0 & 1 & 0 & 0 & 1 & 0 \\ 0 & 0 & 0 & 0 & 0 & 0 & 0 & 0 & 0 \\ 0 & 0 & 0 & 0 & 0 & 0 & 0 & 0 & 0 \\ 0 & 0 & 0 & 0 & 0 & 0 & 0 & 0 & 0 \\ 0 & 0 & 0 & 0 & 0 & 0 & 0 & 0 & 0 \end{pmatrix}_{i,i+1}. \tag{4.38}$$

The ordered local basis is given by $\{0, 1, 2\}$.

A possible ansatz for the invariant measure is

$$|P\rangle = \frac{1}{Z_L} \text{Tr} \left[\bar{\mathcal{D}} \otimes \mathcal{D}^{\otimes L-1} \right], \tag{4.39}$$

where the components of the vectors

$$\bar{\mathcal{D}} = \begin{pmatrix} \bar{E} \\ \bar{D} \\ \bar{F} \end{pmatrix}, \quad \mathcal{D} = \begin{pmatrix} E \\ D \\ 0 \end{pmatrix} \tag{4.40}$$

are operators acting on some auxiliary vector-space A.

This ansatz yields the stationary state, if $\bar{\mathcal{D}}$ and $\mathcal{D}$ are such that the following identity holds:

$$\tau \cdot \bar{\mathcal{D}} \otimes \mathcal{D} = \mathcal{D} \otimes \bar{\mathcal{D}}. \tag{4.41}$$

This identity is true, if the components of the vectors $\bar{\mathcal{D}}$ and $\mathcal{D}$ satisfy the following algebra:

$$
\begin{aligned}
\bar{E}E &= E\bar{E}, \\
\bar{E}D &= E\bar{D}, \\
p\bar{D}E + q\bar{F}E &= E\bar{F}, \\
(1-p)\bar{D}E + (1-q)\bar{F}E &= D\bar{E}, \\
\bar{D}D + \bar{F}D &= D\bar{D}, \\
0 &= D\bar{F}.
\end{aligned}
\tag{4.42}
$$

As indicated above, on the $q = 0$ submanifold of the parameter space the model under consideration reduces to the NaSch model. On this submanifold the stationary probility measure is given by the two-cluster measure. Thus, it makes sense to investigate whether this measure is still invariant away from the NaSch manifold. As in the matrix-product ansatz, the following choice for E and D acting on $A = \mathbb{C}^2$ suffices (see Appendix B)

$$E = \begin{pmatrix} e & 1 \\ 0 & 0 \end{pmatrix}, \quad D = \begin{pmatrix} d & 0 \\ \tilde{d} & 0 \end{pmatrix}. \tag{4.43}$$

The algebra of E and D is such that all its words[1] can be reduced to one of the following: E, D, ED and DE. Therefore the following ansatz for the remaining matrices has been chosen:

$$
\begin{aligned}
\bar{E} &= a_1\mathbb{1} + b_1 E + c_1 D + d_1 ED + e_1 DE, \\
\bar{D} &= a_2\mathbb{1} + b_2 E + c_2 D + d_2 ED + e_2 DE, \\
\bar{F} &= a_3\mathbb{1} + b_3 E + c_3 D + d_3 ED + e_3 DE.
\end{aligned}
\tag{4.44}
$$

Inserting this in (4.42), the algebra reduces to a set of equations for the real parameters occurring in the matrices, which can be solved quite easily to give

$$\bar{E} = E = \begin{pmatrix} 1 & 1 \\ 0 & 0 \end{pmatrix}, \tag{4.45}$$

$$D = \mu \begin{pmatrix} 1-p & 0 \\ p-q & 0 \end{pmatrix}, \tag{4.46}$$

$$\bar{D} = \mu \begin{pmatrix} 1 & 0 \\ -q & 0 \end{pmatrix}, \tag{4.47}$$

$$\bar{F} = \mu \begin{pmatrix} 0 & 0 \\ p & p \end{pmatrix}. \tag{4.48}$$

---

[1]Words are products of operators.

The real parameter μ controls the average density of particles and can be thought of as a generalized fugacity.

With this representation of the algebra (4.42) it is straightforward to compute the fundamental diagram in the thermodynamic limit. The density ρ is given by

$$\rho = \lim_{L \to \infty} \frac{\text{Tr}\left[\bar{D}C^{L-1}\right]}{\text{Tr}\left[\bar{C}C^{L-1}\right]}, \tag{4.49}$$

with $C = E + D$ and $\bar{C} = \bar{E} + \bar{D} + \bar{F}$. Diagonalizing C and keeping only the contributions
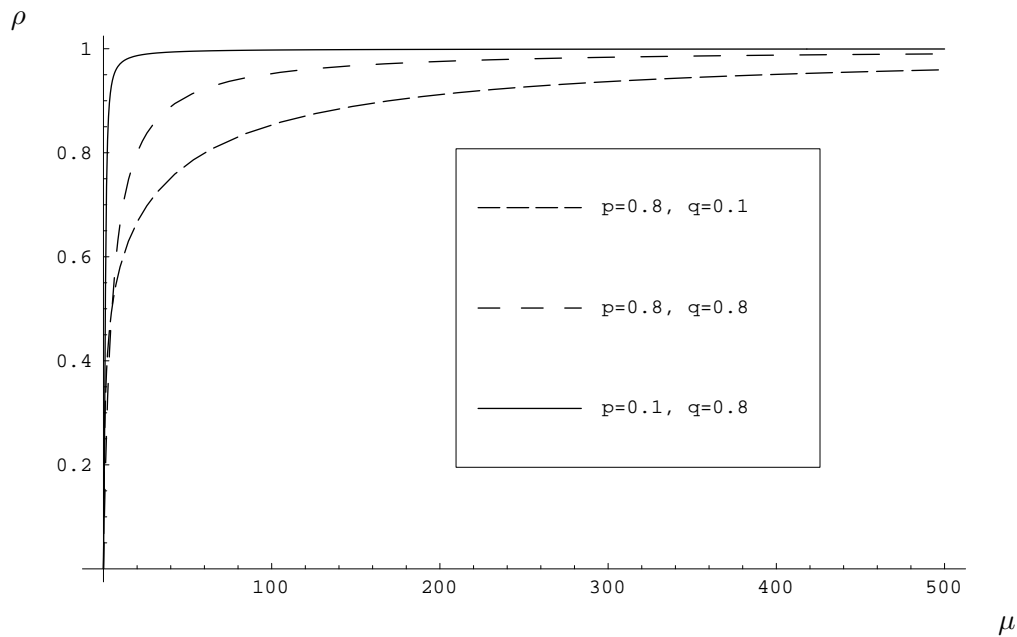

Figure 4.10.: Density ρ as function of μ for different values of p and q.

coming from the largest eigenvalue

$$\lambda = \frac{1}{2}\left(1 + \mu(1-p) + \sqrt{(1 + \mu(1-p))^2 + 4\mu(p-q)}\right), \tag{4.50}$$

one has

$$\rho(\mu) = \frac{\mu\lambda(\lambda - q)}{(2\lambda + \mu p)\mu(p-q) + \lambda^2(1-\mu)}. \tag{4.51}$$

As μ varies from zero to infinity, $\rho(\mu)$ increases monotonically from zero to one, i.e., all possible values of ρ can be reached, if μ is suitably tuned (see Fig. 4.10).

The definition of the flow is somewhat more involved. It is necessary to introduce the quantities

$$P_d(d = k) := \lim_{L \to \infty} \frac{\text{Tr}\left[\bar{D}E^k DC^{L-3}\right]}{\text{Tr}\left[\bar{C}C^{L-1}\right]}, \tag{4.52}$$

which is the probability to have *exactly* k empty cells in front of a car that has come to rest at site one during the last update step, and

$$P_d(d > k) := \lim_{L \to \infty} \frac{\text{Tr}\left[\bar{D}E^{k+1}C^{L-3}\right]}{\text{Tr}\left[\bar{C}C^{L-1}\right]}, \tag{4.53}$$

which gives the probability of having *more* than k empty cells in front of a car standing at site one. With these probabilities the flow j_{CAII} is

$$j_{\text{CAII}} := \sum_{n=1}^{\infty} npq^{n-1} P_d(d = n) + np(1-q)q^{n-1} P_d(d > n). \tag{4.54}$$

With $E^2 = E$ one easily derives

$$P_d(d \geqq k+1) = \frac{1}{\lambda} P_d(d \geqq k). \tag{4.55}$$

Thus

$$j_{\text{CAII}} = \frac{\partial}{\partial x} \sum_{n=0}^{\infty} x^n \Big|_{x=q/\lambda} \cdot [pP_d(d+1) + p(1-q)P_d(d > 1)]$$

$$= \frac{1}{(\lambda - q)^2} \frac{p\mu(1-q)(\lambda - q)(\lambda(1+\mu) + \mu(p-q))}{(2\lambda + \mu p)\mu(p-q) + \lambda^2(1-\mu)}. \tag{4.56}$$
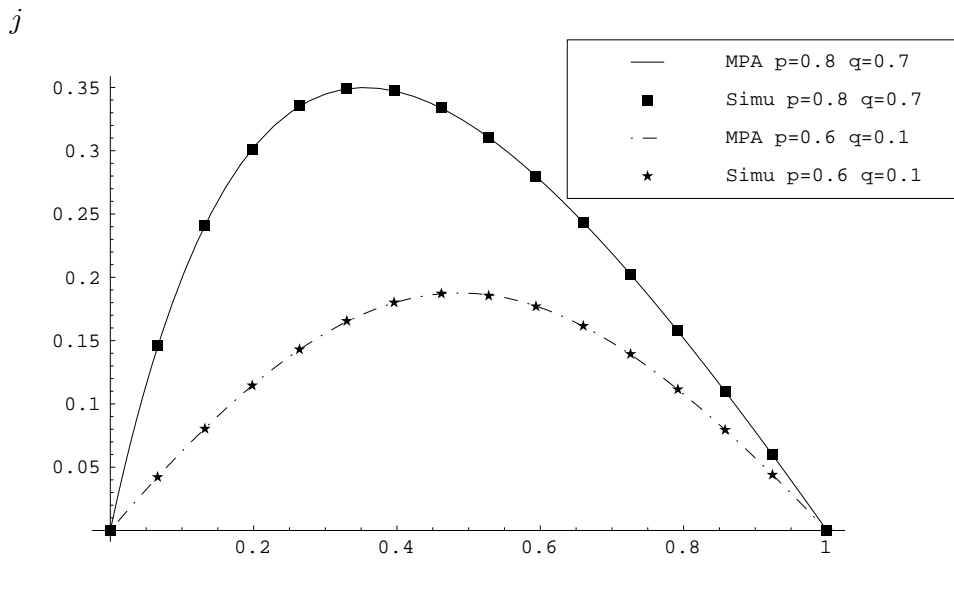

Figure 4.11.: Exact solution versus Monte-Carlo data for different values of the hopping probabilities.

At this point it would be desirable not only to have the graph of the fundamental diagram parameterized by μ, but to eliminate μ and to obtain $j_{\text{CAII}}(\rho)$. This reparameterization turned out to be very difficult and has not been performed. The stationary state derived from the MPA has been compared with Monte-Carlo simulations (see Fig. 4.11), showing perfect agreement, which indicates the uniqueness of the stationary state.

From now on the solution of the parallel update will be presented. As the interaction range of the stochastic process studied in this case is, in principle, the whole line, the so-called car-oriented mean-field theory (COMF) [38] seemed to be more appropriate than the matrix-product ansatz. In this method only the gaps between consecutive cars are studied rather than their actual positions. Therefore one introduces quantities P_n, which are the probabilities to find exactly n empty cells in front of a car. In addition, it proves

useful to define g_n to be the probability that a randomly picked car moves exactly n steps in the next time step. One has, e.g.,

$$g_0 = P_0 + (1-p)\sum_{n\geq 1} P_n = P_0 + (1-p)[1-P_0], \tag{4.57}$$

where the normalization

$$\sum_{n\geq 0} P_n(t) = 1 \tag{4.58}$$

has been used. Furthermore one introduces $P_{\text{Step}}(m, d; t)$, which is the probability that a car which has d empty cells in front of it moves m cells in the time step from t to $t+1$. Hence, one finds the following set of evolution equations for the probability distribution

$$P_i(t+1) = \sum_{d=0}^{\infty} \sum_{m=d-i}^{d} P_{\text{Step}}(m, d; t) g_{i+m-d}(t), \quad i = 0, 1 \ldots \tag{4.59}$$

Although the first impression might be that this system of equations is fairly simple, the solution is not obvious. Analyzing (4.59) one has to write out $P_{\text{Step}}(m, d; t)$ explicitly, which uncovers the fact that (4.59) is a set of coupled nonlinear evolution equations.
As mentioned before, Monte-Carlo simulations indicate that the stationary state is unaffected by the use of fully parallel or forward sequential update. Assuming that both stationary states are equal, the special properties of the algebra describing the two-cluster measure immediately imply

$$P_n = \lambda P_{n+1}, \quad n = 1, 2 \ldots, \tag{4.60}$$

for some real parameter λ. Thus, the following ansatz for the probabilities should be made:

$$P_i = \begin{cases} P_0 & \text{for } i = 0, \\ c\lambda^i & \text{for } i \geq 1. \end{cases} \tag{4.61}$$

Now one is left with three real parameters only and the use of three convenient equations should be enough to determine these parameters. The first two equations are (4.58) and (4.59) with $i = 0$. As third equation one chooses the obvious relation between the car density ρ and the P_i given by[2]

$$\sum_{i\geq 0} (i+1)P_i = \frac{1}{\rho}. \tag{4.62}$$

With this equation the determination of P_0, c and λ is straightforward. Collecting all the results one can, after some algebra, compute the flow

$$\begin{aligned} j &= \rho \left(p \sum_{k=1}^{\infty} kq^{k-1} \left[P_k + (1-q)(1 - \sum_{j=0}^{k} P_k) \right] \right) \\ &= \frac{p(1-\rho)(1-q-W(p,q,\rho))}{2p(1-q)(1-\rho) - q(1-q-2\rho+2q\rho+W(p,q,\rho))} \end{aligned} \tag{4.63}$$

---

[2] A unit consisting of a car with m empty cells in front occupies $m+1$ cells.

with

$$W(p, q, \rho) := \sqrt{(1-q)\left(1 - q(1-2\rho)^2 - 4p\,(1-\rho)\,\rho\right)}. \qquad (4.64)$$

In the limit of $q \to 0$ this flow reduces to the NaSch flow. The two-cluster measure for the forward sequential update and the COMF result for the fully parallel update show perfect agreement. It can thus be concluded that in the thermodynamic limit both updates are indeed equivalent.
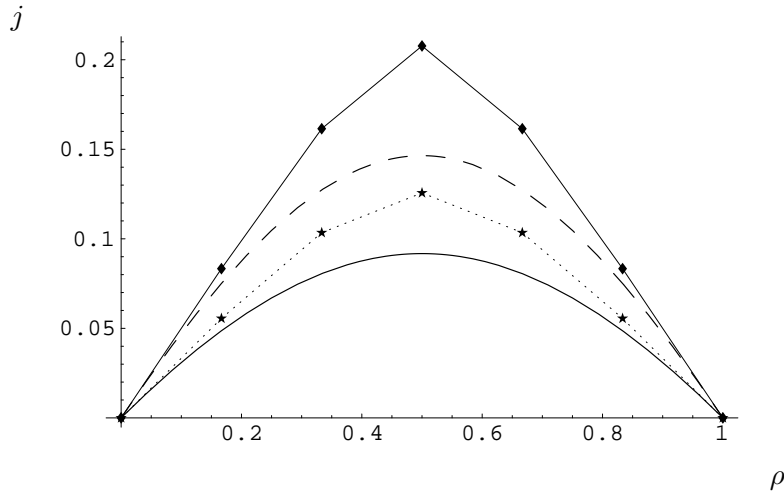

Figure 4.12.: Comparison between the fundamental diagrams of the four-vertex model on a 6×9-lattice and the NaSch model. $\blacklozenge$ and $\star$ correspond to the four-vertex results with $x = 1$ and $x = 1/2$ respectively. The dashed and the solid line represent the NaSch result for $p = 1/2$ and $p = 1/3$ respectively.

Finally, the fundamental diagrams derived from the vertex model approach on the one hand, and the cellular automaton approach on the other hand will be compared in the limit of $v_{\max} = 1$. This corresponds to the limits $y \to 0$ and $q \to 0$, respectively. Since no explicit solution of the free energy of the vertex model is available, the canonical partition function for a small system has been computed analytically. In [59] the fundamental diagrams of the dimer model and the associated cellular automaton have been compared by rescaling the first one in such a way that the maxima of both models resided on the same line. Here a different approach will be chosen. In the limit of $\rho \to 0$ the slope of the fundamental diagram is nothing but the average velocity of a single car moving on an empty highway. Setting

$$p = \frac{x}{x+1}, \qquad (4.65)$$

free moving cars in both models have the same average velocity, which allows for a reasonable comparison between the fundamental diagrams of both models.

As can be seen from Fig. 4.12, the flow in the NaSch model is smaller than the flow of the four-vertex model. It is known that the correlations in the NaSch model decay exponentially, whereas the correlations in the four-vertex model decay algebraically with $1/r^2$, since this model is critical in the disordered phase D. This result is very interesting, since such phenomena have been observed in real traffic. On the hand one finds *metastable states* [43] and on the other hand Kerner [61] has recognized the so-called *synchronized flow*;

both situations are characterized by very strong correlations, which lead to an unusually
high flow.

5. Dynamics of the asymmetric simple exclusion process with parallel update and open boundaries

5.1. Introduction

The dynamics of the asymmetric simple exclusion process (ASEP) with parallel update and open boundaries is examined. The space and time dependent generalization of the $(2,1)$-cluster approximation will be used to derive evolution equations for the two-site probabilities. The predictions of these equations are compared with Monte-Carlo data. It will turn out that this approximation gives fairly accurate results concerning time dependent values of the local densities for all portions of the phase space – with one exception: The so-called coexistence line or shock profile line.
For this line and some special initial conditions a different (macroscopic) approach to the dynamics will be proposed, which completes the description of the dynamics of this model.

5.2. The ASEP in discrete time

The ASEP in discrete time is a simple probabilistic cellular automaton for the description of flow of particles through a one-dimensional system. In this model particles occupy the sites of a chain of length L, where the occupation number per site is at most one. At every discrete time step $t \to t+1$ these particles evolve according to the following rules:

(i) A particle on a site labeled by $i \in \{1, \dots, L-1\}$ moves to site $i+1$ with probability p, if this site is not occupied by another particle.

(ii) A particle on site L leaves the system with probability β.

(iii) If the first site is not occupied, a particle enters the system with probability α.

The stationary state of this model has been calculated recently using the matrix product ansatz [62, 63]. Note that for periodic boundary conditions the ASEP with parallel update is equivalent to the NaSch model with $v_{\max} = 1$, which has been treated already in Chap. 4. The phase diagram consists of three phases. A maximum current phase C, a low density phase A, and a high density phase B, where the last two phases can be split further into AI, AII, BI, and BII (see Fig. 5.1).

Maximum current phase C
This phase is given by $\alpha, \beta > 1 - \sqrt{1-p}$. The current is independent of the input and the removal probability and one finds

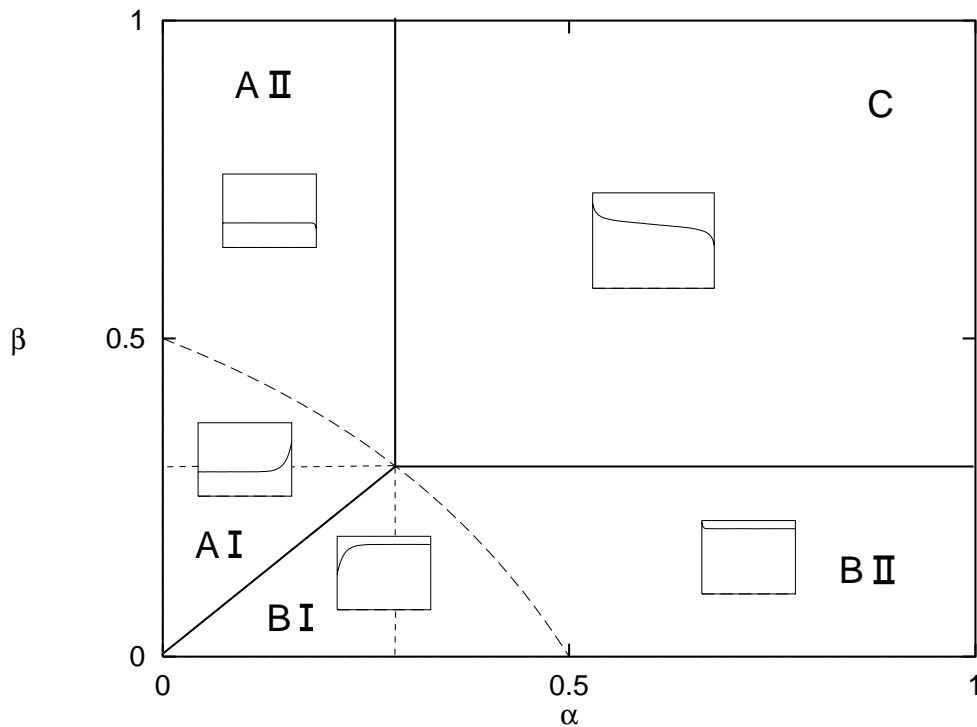$$j_C = \frac{1}{2}\left(1 - \sqrt{1-p}\right). \tag{5.1}$$

Figure 5.1.: Phase diagram for the ASEP for $p = 0.5$. C is the maximum current phase,
A and B are the low and the high density phase, respectively. The straight
dashed lines are the boundaries between phase $A\,I$ and $A\,II$ ($B\,I$ and $B\,II$).
The curved dashed line is the line given by (5.6) and intersects the line $\alpha = \beta$
at $\alpha = \beta = 1 - \sqrt{1-p} = q$. The inserts show typical density profiles in the
various phases; note that the profile is qualitatively the same in region $A\,I$
($B\,I$) and in the portion of region $A\,II$ ($B\,II$) below the curved dashed line.
(This figure is taken from [64].)

The density profile decays (increases) algebraically from the boundaries to its bulk value
$\rho = 1/2$ (see Fig. 5.1).

High density phase B
This phase is characterized by $\beta < \alpha$ and $\beta < 1 - \sqrt{1-p}$. The stationary current computes
to

$$j_B = \frac{\beta(p - \beta)}{p - \beta^2}. \tag{5.2}$$

Moving from the rightmost site into the bulk, one finds a flat density profile with density

$$\rho_B = \frac{p - \beta}{p - \beta^2}. \tag{5.3}$$

If $\alpha < 1 - \sqrt{1-p}$, this bulk value of the density is reached exponentially from below. This
subregion of the parameter space is called BI.
For values of $\alpha > 1 - \sqrt{1-p}$ the bulk value is reached exponentially from above with a
different correlation length. Now one is in subregion BII.

Low density phase A
The low density phase is described by $\alpha < \beta$ and $\alpha < 1 - \sqrt{1-p}$ with current

$$j_A = \frac{\alpha(p-\alpha)}{p-\alpha^2}. \tag{5.4}$$

In contrast to phase B, the density profile is flat in the left part of the system with

$$\rho_A = \frac{\alpha(1-\alpha)}{p-\alpha^2}. \tag{5.5}$$

Again one finds two subregions AI for $\beta < 1 - \sqrt{1-p}$ and AII for $\beta > 1 - \sqrt{1-p}$ in both of which the bulk density is reached exponentially from above and below, respectively, if one moves from the rightmost site into the bulk of the chain.

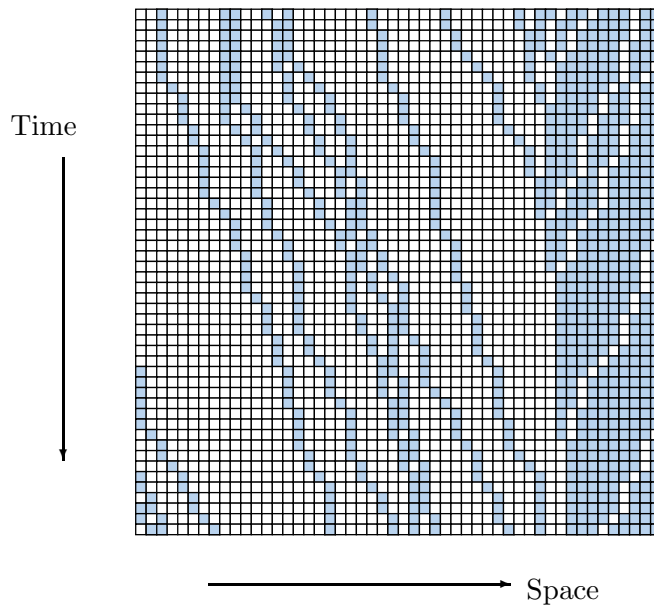In addition, one finds two special lines in the phase diagram.

Figure 5.2.: Typical space time diagram for $p = 0.45$, $\alpha = \beta = 0.1$ in the stationary state. One clearly sees a shock front performing a random walk.

Coexistence or shock profile line
On the line $\alpha = \beta < 1 - \sqrt{1-p}$ the system decomposes into two parts: a low density regime in the left part and a high density regime in the right part with a very small transition region (see Fig. 5.2).
On a coarse grained level, the density profile shows a kink. The kink performs an unbiased random walk with reflective boundaries. Thus, after long times, the probability to find the kink at a given position becomes equal for all positions. Therefore, the averaged density profile has a linear shape and simply interpolates between the density of the low density regime and the high density regime.

Two cluster line [65]
Along the line

$$(1 - \alpha)(1 - \beta) = 1 - p \tag{5.6}$$

the $(2, 1)$-cluster approximation becomes exact, or, seen from a different point of view, the algebra connected with the matrix product approach has a finite dimensional representation (see App. B). The density profiles along this line are flat and the correlations decay exponentially.

5.3. Time and space dependent (2,1)-cluster approximation

From the exact evolution equations of the two-cluster probabilities (see App. C) one sees that, generically, two-cluster probabilities at time $t + 1$ depend on four-cluster probabilities at time t. Using conditional probabilities[1], the four-cluster probabilities can be approximated by

$$p_i(\alpha, \beta, \gamma, \delta) \approx p_i(\alpha, \underline{\beta}) p_{i+1}(\beta, \gamma) p_{i+2}(\underline{\gamma}, \delta). \tag{5.7}$$

This is the essence of the $(2, 1)$-cluster approximation.
With the help of this approximation, (C.2), (C.3) and (C.4) turn into temporal evolution equations without proliferation, i.e., going backward in time, two-cluster probabilities couple only to two-cluster probabilities.
Thus, starting from a given initial state, the equations can be iterated numerically to give the (approximated) probability distribution at any desired time t. Of course, the same information could be gained from Monte Carlo simulations – with one serious drawback: Studying dynamical quantities the ergodicity of a system can not be used any longer to increase the speed of the simulations tremendously. Instead, one has to consider a large number of samples, which drastically increases the amount of time needed to perform the Monte Carlo simulations. As a rule of thumb one can say that the amount of time that is needed for the t-fold iteration of the two-cluster equations is of the order that is needed to perform the Monte-Carlo simulation of one sample only! The reason is that the two-cluster approximation already contains the sample-average. On account of that, the two-cluster approximation allows for the examination of the ASEP on much larger time and length scales. Due to this property, the two-cluster approximation could play an important rôle in the forecasting of traffic flow in cities, where the restriction to a maximal velocity of one is often a reasonable assumption.
Next, it will be clarified for which portion of the parameter space the two cluster approximation gives acceptable results, comparing the two cluster results with Monte-Carlo (MC) data. In all cases $p = 1/2$ was chosen. The system length has been fixed to $L = 50$. At $t = 0$ all systems are empty of particles. Since the different phases of the ASEP can be distinguished by the form of their density profiles, the temporal evolution of the density profile has been chosen as a testing ground for the quality of the two-cluster approximation.

Low density phase A
 In the low density regime one finds a good qualitative and quantitative agreement between the MC and two-cluster data (see Fig. 5.3 and Fig. 5.4).

---

[1]A symbol like $p_i(\alpha, \underline{\beta})$ denotes the probability to find the cluster α, β at sites $i, i + 1$ given that at site $i + 1$ one is sure to find β.
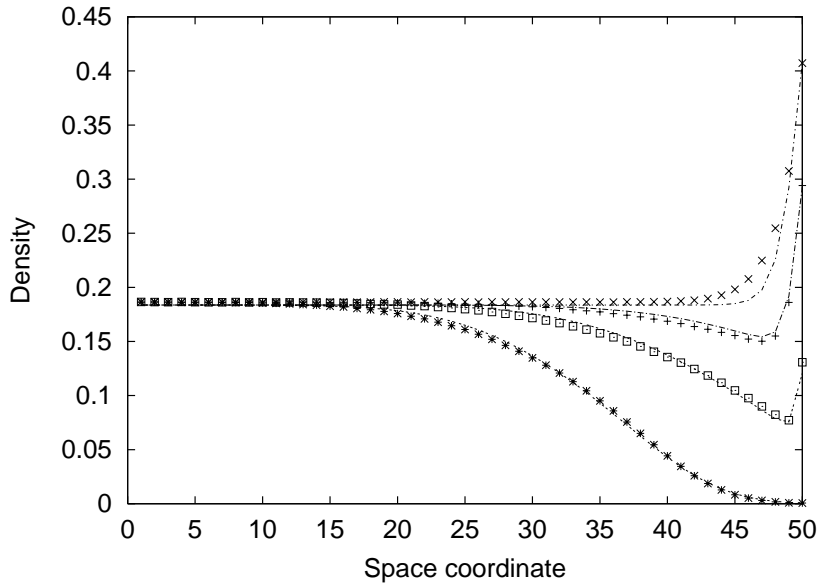
Figure 5.3.: Density profiles in phase AI for $\alpha = 0.1$ and $\beta = 0.2$. $*$, $\square$, $+$ and $\times$ correspond to MC data at times 75, 100, 125 and 250 respectively. The different lines correspond to the two-cluster data at the same times.
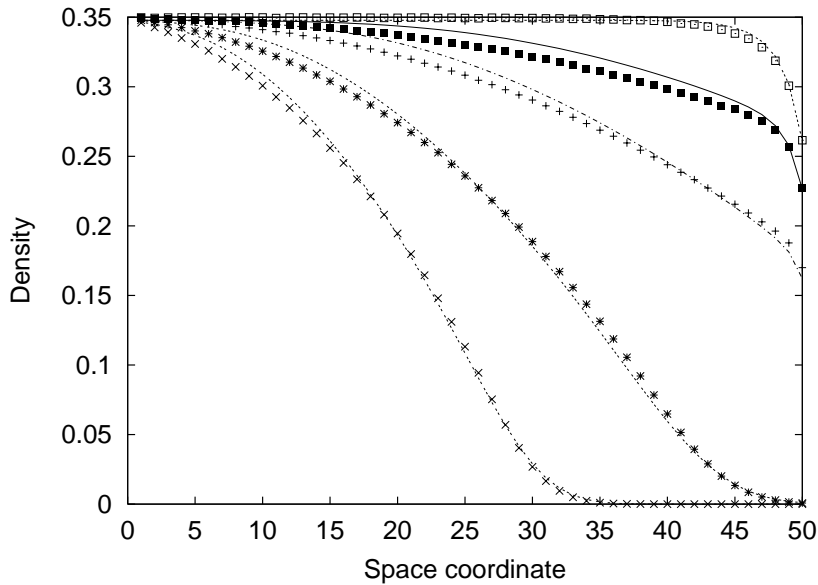
Figure 5.4.: Density profiles in phase AII for $\alpha = 0.2$ and $\beta = 0.5$. $\times$, $*$, $+$,solid square and $\square$ correspond to MC data at times 50, 75, 125, 175 and 750 respectively. The different lines correspond to the two-cluster data at the same times.

High density phase B

In this phase three different regimes can be distinguished (see Fig. 5.5 and Fig. 5.6). As long as the system has not "felt" its right boundary yet, the two-cluster approximation shows a good quantitative agreement with the MC data. At intermediate times, when one
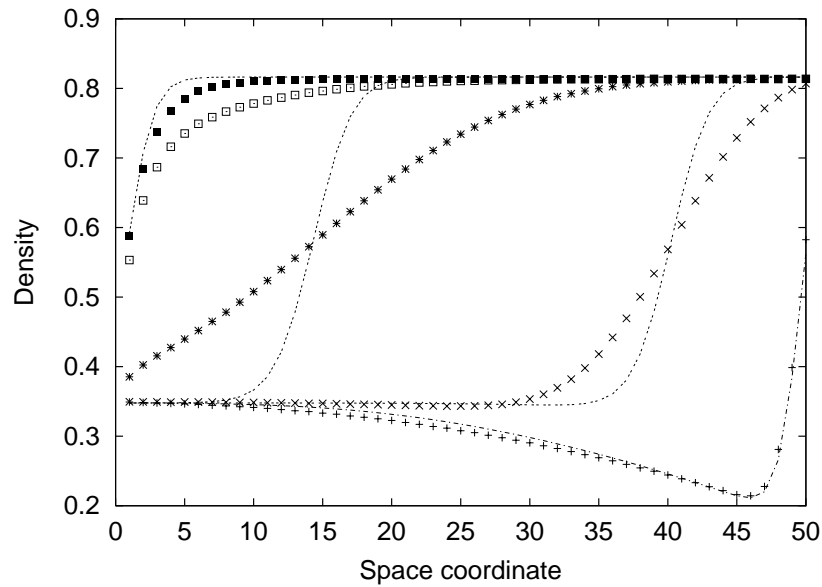
Figure 5.5.: Density profiles in phase *BI* for $\alpha = 0.2$ and $\beta = 0.1$. $+$, $\times$, $*$, $\square$ and solid square correspond to MC data at times 125, 250, 500, 750 and 1000 respectively. The lines correspond to the two-cluster data at times 125, 250, 500 and 750 (higher curves correspond to later times).

Figure 5.6.: Density profiles in phase *BII* for $\alpha = 0.5$ and $\beta = 0.2$. $+$, $\times$, $*$ and $\square$ correspond to MC data at times 125, 250, 500 and 750 respectively. The lines correspond to the two-cluster data at the same times.

sees some kind of a shock front moving back from the right boundary to the left end, the quantitative agreement becomes much worse. Finally, at large times, the accuracy found for phase *A* is recovered. Nevertheless, it would be wrong to draw the conclusion that

the two-cluster approximation becomes worse in phase B, since this phase is connected to phase A via a particle-hole (and left-right) transformation. The observed discrepancies have a very simple explanation. Performing the particle-hole transformation on the initial state, i.e. the empty chain, one obtains the fully occupied chain. Thus, starting with the fully occupied state in phase A would lead to the same differences between the two-cluster prediction and the MC data as found in Phase B.

Maximum current phase C

In phase C the two-cluster approximation shows the best agreement with the MC data
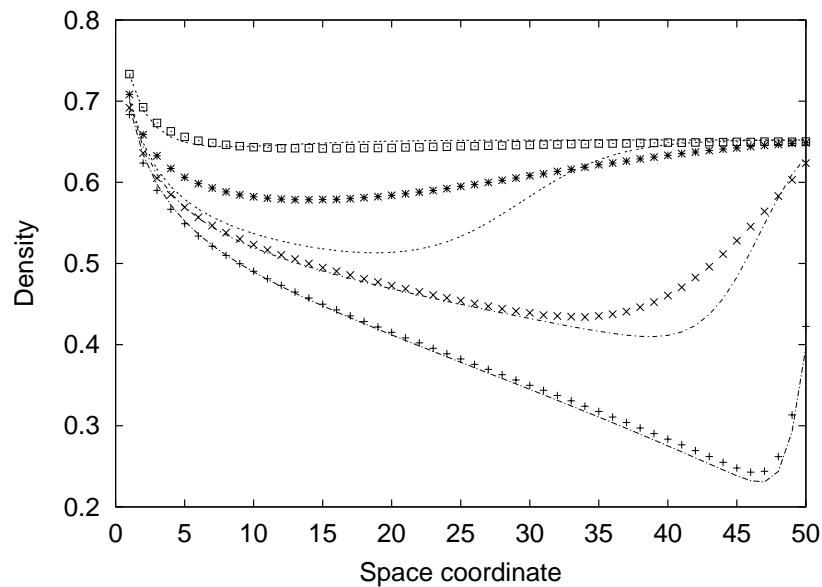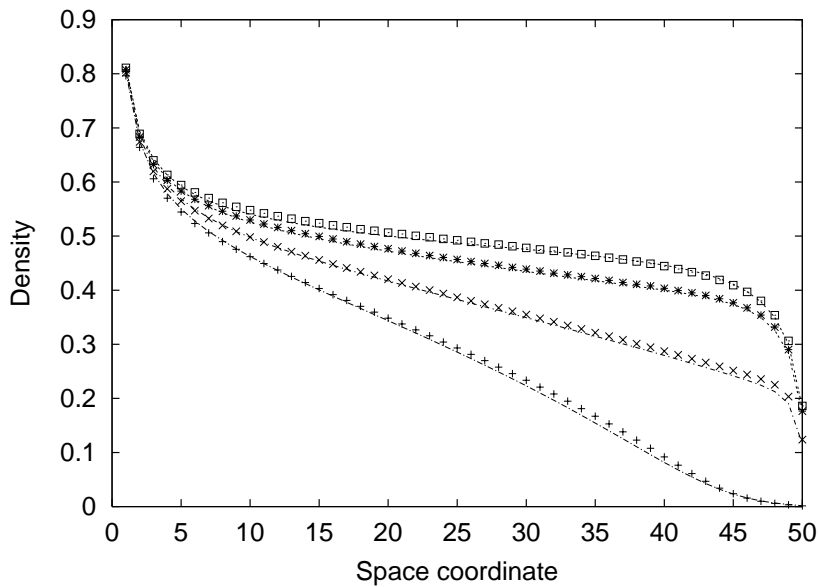

Figure 5.7.: Density profiles in phase C for $\alpha = 0.2$ and $\beta = 0.1$. $+$, $\times$, $*$, and $\square$ correspond to MC data at times 75, 125, 250 and 500 respectively. The lines correspond to two-cluster data at the same times.

(see Fig. 5.7). Since in this phase the system is governed by the properties of the bulk, it seems plausible that the cluster approximation works well for the periodic system, too. On this account exhaustive investigations of the ASEP with periodic boundaries have been performed. The expected agreement of the two-cluster approximation and the MC data could be confirmed.

Shock profile line

On the shock profile line $\alpha = \beta < 1 - \sqrt{1-p}$ the two-cluster approximation fails (see Fig. 5.8). Instead of converging towards a linear profile at large times, the two-cluster equations evolve towards a frozen in kink with a continuous transition between the low density and the high density part (see Fig. 5.9). The same behaviour is known from simple mean-field calculations for the ASEP with random sequential update [1]. Nevertheless, a description of the dynamics on the shock profile line is still possible using a domain wall picture. This will be the content of the next section.
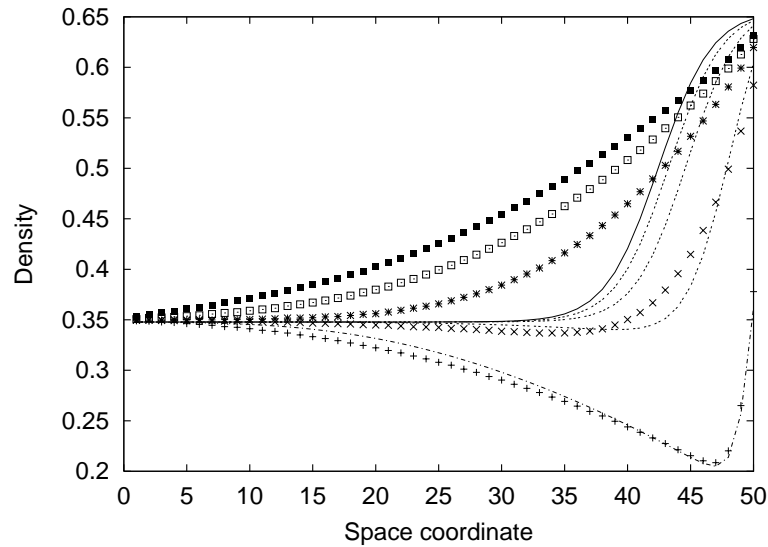
Figure 5.8.: Density profiles on the shock profile line for $\alpha = 0.2$ and $\beta = 0.2$. $+$, $\times$, $*$, $\square$ and solid square correspond to MC data at times 125, 250, 500, 725 and 1000 respectively. The lines correspond to two-cluster data at the same times (higher curves correspond to later times).
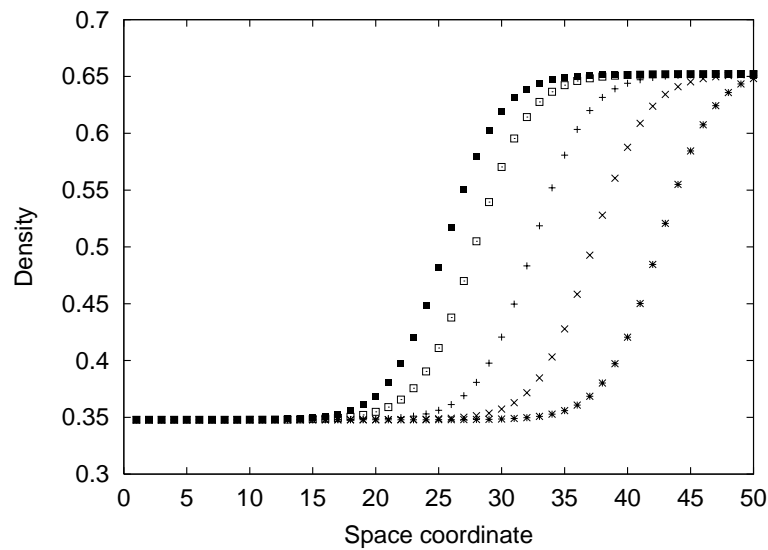
Figure 5.9.: Density profiles on the shock profile line for $\alpha = 0.2$ and $\beta = 0.2$ using the two-cluster approximation. $*$, $\times$, $+$, $\square$ and solid square correspond to times 10^3, 10^4, 10^5, 10^6 and 10^7 respectively. The profile does not change, if one increases the time from $t = 10^7$ to $t = 10^8$.

5.4. Dynamics of the ASEP using a domain wall picture

In [41] a domain wall picture for the large time dynamics of driven lattice gases with open boundaries was proposed. As will be seen, this picture allows even for the description of the short time dynamics, if one starts from an initial configuration that can be expressed

Figure 5.10.: Initial shock profile ρ_0 propagating to the right with velocity V.

as a special shock front. The empty lattice is an extremal example for such an initial configuration.

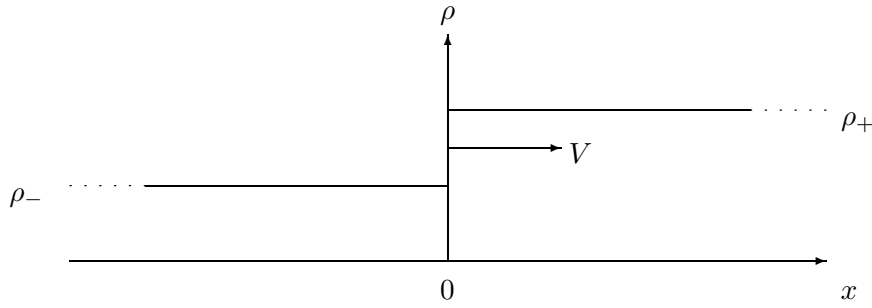In the following the domain wall approach to the dynamics of the ASEP will be explained. The local particle density $\rho(x,t) = \langle \tau_x(t) \rangle$ satisfies a lattice continuity equation[2]

$$\triangle_t \rho(x,t) = -\triangle_x j_x(t), \tag{5.8}$$

where $j_x(t)$ denotes the local particle current along the bond connecting site x with site $x+1$. On a coarser scale in space and time this turns into the usual continuity equation

$$\partial \rho / \partial t + \partial j / \partial x = 0. \tag{5.9}$$

Suppose that at $t = 0$ the following density profile is given (see also Fig. 5.4) in an infinitely large system

$$\rho_0(x) = \begin{cases} \rho_- & \text{for } x < 0, \\ \rho_+ & \text{for } x \geq 0. \end{cases} \tag{5.10}$$

A solution of (5.9) (in the weak sense) is given by

$$\rho(x,t) = \rho_0(x - Vt). \tag{5.11}$$

Inserting (5.11) in (5.9) and integrating from minus to plus infinity yields

$$V = \frac{j_+ - j_-}{\rho_+ - \rho_-}. \tag{5.12}$$

Regarding a finite system with injection and removal of particles at the ends, it is not clear a priori if a prepared shock front will propagate through the system and keep its shape for all times. However, Monte-Carlo simulations on the shock profile line indicate that, at late stages of the dynamics, the density profiles consists of mainly two regions (see Fig. 5.2): a low density region in the left and a high density region in the right part of the system. This finding is due to the fact [41] that each of the boundaries tries to enforce its own stationary state in the bulk (see Fig. 5.11). The crucial step in the domain wall approach is to identify candidates for these bulk stationary states. In the present case the states on the two-cluster line have been chosen. These states lead to flat density profiles and

---

[2] The forward difference operator is defined by $\triangle : f(x) \mapsto f(x+1) - f(x)$.
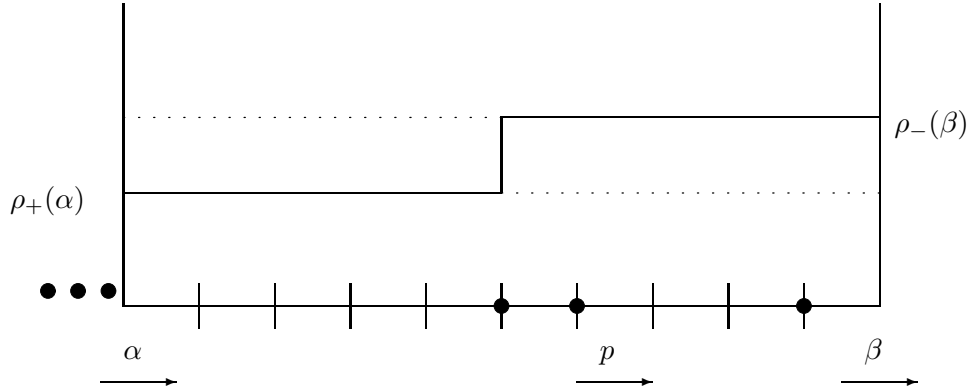
Figure 5.11.: The injection and the removal rates fix the densities in the low and high density part of the system.

produce the correct values of the densities and the currents in the stationary state, which can be both evaluated as functions of α and β. One finds

$$\rho_-(\alpha) = \frac{(1-\alpha)\alpha}{p - \alpha^2}, \qquad j_- = \frac{\alpha(p-\alpha)}{p - \alpha^2}, \qquad (5.13)$$

$$\rho_+(\beta) = \frac{p - \beta}{p - \beta^2}, \qquad j_+ = \frac{\beta(p-\beta)}{p - \beta^2}. \qquad (5.14)$$

A candidate for a microscopic probability measure of a shock front at position i can be given by

$$|\psi(x)\rangle = \begin{pmatrix} 1 - \rho_-(\alpha) \\ \rho_-(\alpha) \end{pmatrix}^{\otimes i} \otimes \begin{pmatrix} 1 - \rho_+(\beta) \\ \rho_+(\beta) \end{pmatrix}^{\otimes L + 1 - i}. \qquad (5.15)$$

Of course, this measure neglects the particle-hole attraction in the bulk of the system, which is known to be present on very small length scales. But, since the domain wall description is a macroscopic one, the fine structure of correlations should be irrelevant. Another weak point in assigning this special measure to the shock front comes from the fact that it assumes the shock to be sharp. For $p = 1$ it has been shown in [63] that the low and high density region are separated by a narrow transition region with mean density $1/2$. As there is no simple argument for the width of this transition region for general p, for the sake of simplicity, it will be taken to be zero. Since the shock front moves with velocity $V = \frac{j_+ - j_-}{\rho_+ - \rho_-}$, the simplest assumption for the dynamics of this front is to assume that it performs a random walk with right and left hopping probabilities given by

$$D_{R/L} = \frac{j_{+/-}}{\rho_+ - \rho_-}. \qquad (5.16)$$

This argument has to be modified for early stages of the dynamics when the system fills with particles. As ρ_+ and j_+ are both zero in this case, it is useful to set

$$D_L^0 = 0 \quad \text{and} \quad D_R^0 = \frac{j_-}{\rho_-}. \qquad (5.17)$$

Hence, the dynamics can be described by a random walker (i.e. the shock front position) starting at the left end of the system. This random walker has two internal degrees of

freedom. As long as it has not reached the right end of the system it remains in state one. In this state the walker moves with hopping probability D_R^0 and represents a shock front with densities $(\rho_-(\alpha)|0)$. Once it has reached the right end it bounces off and switches to state two in which it will remain forever. In the second state it moves with hopping probabilities $D_{R/L}$ in the bulk. If it has reached the far left or far right site of the chain, it only moves with probability D_R or D_L, respectively (reflecting boundaries). The random walker in state two represents a shock front with densities $(\rho_-(\alpha)|\rho_+(\beta))$.

The knowledge of the probability $p(k, x, t)$ to find the random walker in state k at site x at time t suffices to calculate the local density for every site of the chain by adding up the density contributions of the different shock fronts. The $p(k, x, t)$ fulfill a set of recursion relations (see App. D) and can thus be computed.
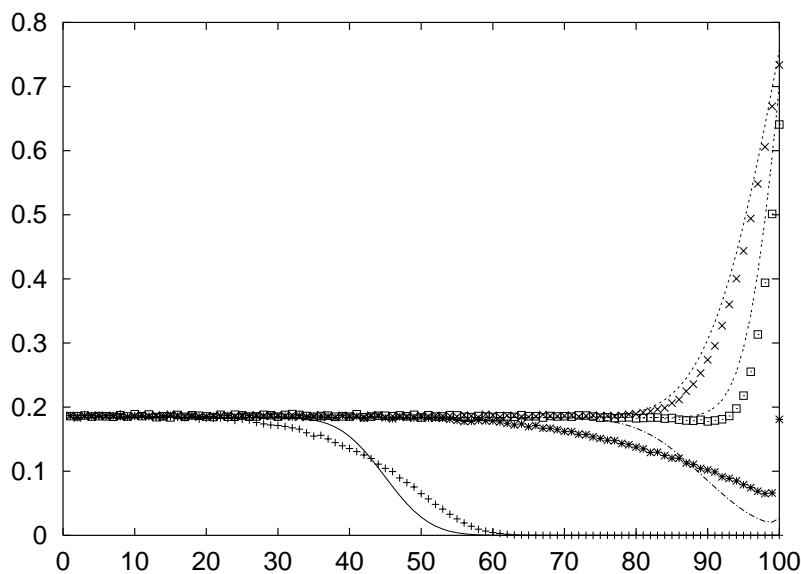

Figure 5.12.: Density profiles for $\alpha = \beta = 0.1$. The symbols $+$, $\times$, $*$, and $\square$ correspond to MC data at times 100, 500, 200, and 300. The lines correspond to analytical data from the domain wall approach at the same times.

In this work the recursion relations have been solved numerically and so the dynamics of the density profile has been extracted (see Figs. 5.12 and 5.13). One finds that the predictions of the domain wall picture become better, if either

    a) α goes to zero (compare Figs. 5.12 and 5.13)

or

    b) t goes to infinity (see Fig. 5.14).

An explanation for case a) can be given by the fact that with $\alpha \cdot p \cdot L = \epsilon$ going to zero the domain wall picture becomes exact [41]: Suppose that in this limit, one finds a configuration of the type: $0 \ldots 0 1 \ldots 1$. The position of the interface between the zero density part and the jammed part may be anywhere between the ends of the chain. Then, at each time step, if a process occurs at all, either a particle enters or leaves the system, because the probability that both processes occur simultaneously is of the order of ϵ^2. A particle that has entered, will move to the interface position, where it sticks. Thus,
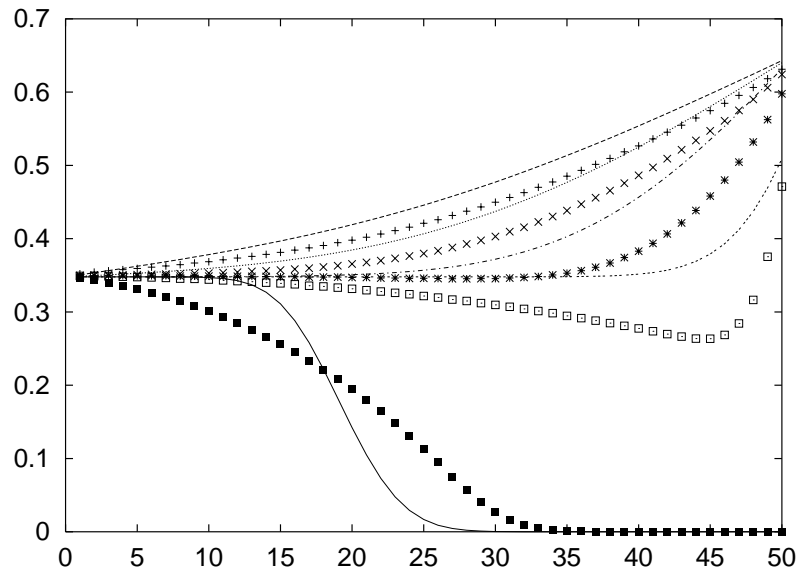
Figure 5.13.: Density profiles for $\alpha = \beta = 0.2$. The symbols $+$, $\times$, $*$, $\square$, and solid square correspond to MC data at times 950, 600, 300, 150 and 50. The lines correspond to analytical data from the domain wall approach at the same times.
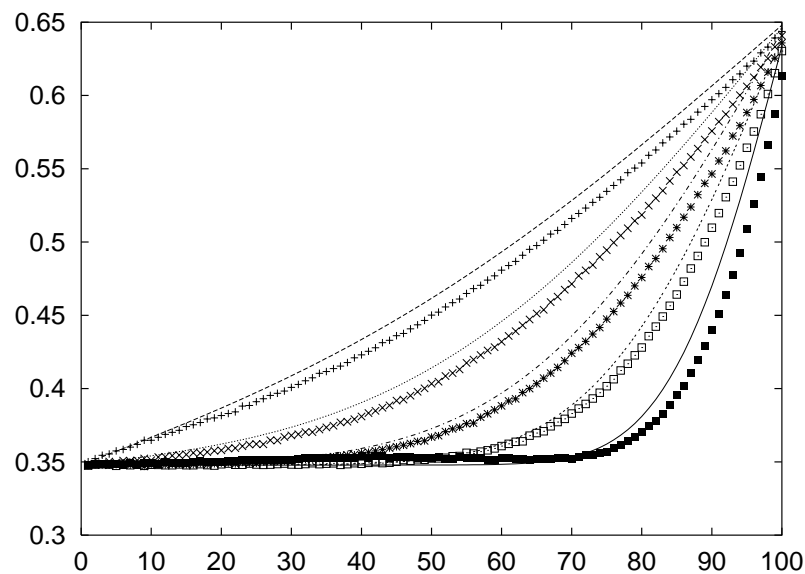
Figure 5.14.: Density profiles for $\alpha = \beta = 0.2$. The symbols $+$, $\times$, $*$, $\square$, and solid square correspond to MC data at times 4000, 2000, 1000, 500 and 200. The lines correspond to analytical data from the domain wall approach at the same times. Note that at $t = 0$ the profile was flat with the density chosen by the left boundary.

the domain wall moves one step to the left. A hole that has been created by removing a particle at the right end propagates leftwards to the interface, where it comes to rest.

Now, the interface moves one step to the right. During this motion of the particle/hole, no other process will take place almost for sure, owing to the limit that has been taken. Therefore, a shock front of the type $(0|1)$ will always be present, and only the position of the interface will perform a random walk.

In case b) one has to distinguish between very early stages of the dynamics and intermediate times. At early stages errors might occur because of the fact that one neglects microscopic correlations. For particles that leave a mega-jam it is known that they arrange in such a way that the current is maximized. In this model this can only be the case, if one has some kind of particle-hole attraction. If the total current into the system is predicted correctly by the shock front dynamics, the space covered by the particles must be underestimated. This is clearly seen in all MC data.

For intermediate times, it is hard to judge, what the reason for the discrepancies might be. Note that the qualitative picture changes when the shock front reaches the right boundary. At early stages of the dynamics one always sees that at the beginning of the chain the density profile predicted by the domain wall picture lies above the MC profile. At some point in the bulk both profiles cross and to the right of the crossing the domain wall prediction understimates the MC curve. At intermediate stages of the dynamics, when the first particles reach the right boundary, the agreement between the domain wall picture and the MC data is worst. Finally, at late stages of the dynamics, one finds that the domain wall density profile lies completely above the MC curve and anticipates the evolution of the MC data.

The reason is most presumably that some sort of boundary effects come into play, when the first particles reach the right boundary. I.e., the system's state can not be described by a superposition of kinks. In order to clarify this point, a different initial condition was tested. At $t = 0$ a flat profile with density $\rho_+(\alpha)$ has been chosen. The results are displayed in Fig. 5.14. As one can see, the discrepancy between the MC data and the shock front prediction is always of the same type and the overall agreement with the MC data is clearly improved. The reason for this finding is most probably the fact that, due to the new initial condition, in the course of the dynamics no states are created that largely deviate from the shock front picture.

In addition, it should be mentioned that the shock front velocity V has been derived for an infinite system. It is no saying what exactly at the boundaries happens. A slowing of the domain wall near the boundaries is one possible scenario. Moreover, the values $\rho_\pm$ have to be regarded as those densities that one finds if one follows the density profile from the ends into the bulk until one sees a uniform density but has not reached a point deep in the bulk . The profile exactly at the boundaries is allowed to largely deviate from this bulk stationary profiles.

Recently, Dudzinski and Schütz [66] have studied the relaxation spectrum of the ASEP with random sequential update. They have found that in the phases AI, BI, and on the shock profile line, for values of α and β not too large, the lower part of the relaxation spectrum of the associated stochastic Hamiltonian is well described by the relaxation spectrum of the random walk performed by the associated domain wall. There are two reasons to believe that this property carries through to the ASEP with parallel update. Firstly, in the limit of the parameters α, β, and p going to zero the transfer matrix of the ASEP with parallel update becomes the stochastic Hamiltonian of the ASEP with random sequential update. Secondly, the results from above indicate so. Therefore, at the end of this chapter the relaxation spectrum of a random walker with hopping probabilities D_R and D_L and reflective boundaries will be computed.

The master equation which governs the dynamics of the random walker with hopping

probabilities D_R and D_L can be solved by the introduction of so-called ghost coordinates [1]. The eigenfunctions are plane waves of the form

$$|\psi(k,x)\rangle = e^{ikx} + c(k)q^x e^{-ikx} \tag{5.18}$$

where

$$q = \frac{D_R}{D_L}, \tag{5.19}$$

and

$$c(k) = \frac{q - e^{ik}}{q(e^{-ik} - 1)}. \tag{5.20}$$

The possible momenta are

$$k = \frac{n\pi}{L+1} - \frac{i}{2}\ln q \qquad \text{with} \qquad n \in \{1, 2, \dots, L\}. \tag{5.21}$$

Hence, the spectrum is real and the eigenvalues of excited states are

$$\lambda(k) = 1 + D_R + D_L - 2\sqrt{D_R D_L}\cos\left(\frac{\pi n}{L+1}\right). \tag{5.22}$$

On the shock profile line this formula reduces to

$$\lambda_S(k) = 1 + 2\frac{\alpha(p-\alpha)}{p - 2\alpha + \alpha^2}\left(1 - \cos\left(\frac{\pi n}{L+1}\right)\right). \tag{5.23}$$

It would now be very interesting to compare this spectrum with the spectrum of the ASEP gained from exact diagonalizations or DMRG calculations. On account of the results from above a good agreement can be expected.

6. Exactly solvable two-leg ladder models for traffic flow

6.1. Introduction

Analytic investigations of spin systems (quantum and classical) on quasi one-dimensional lattices have become by now quite popular [67]. Results are available for the ground state properties [28, 30] on the one hand and for the spectral properties of exactly solvable systems [68, 69] on the other hand.

The relevance of stochastic hopping models defined on an n-leg ladder for the modeling of traffic flow on highways is obvious, but, unlike in spin systems, only a few analytic investigations exist [70, 71, 72].

6.2. Periodic boundaries and stationary state from a maximum-flow principle

The vertices of a two-leg ladder with L rungs can be occupied by N particles with hard-core exclusion. These particle move along the ladder according to the following stochastic rules which are applied in parallel to all particles at each discrete time step:

$$\begin{matrix} \cdots 10 \cdots \\ \cdots * * \cdots \end{matrix} \rightarrow \begin{matrix} \cdots 01 \cdots \\ \cdots * * \cdots \end{matrix} \qquad \text{with prob. } p_1 = 1, \qquad (6.1)$$

$$\begin{matrix} \cdots * * \cdots \\ \cdots 10 \cdots \end{matrix} \rightarrow \begin{matrix} \cdots * * \cdots \\ \cdots 01 \cdots \end{matrix} \qquad \text{with prob. } p_2, \qquad (6.2)$$

$$\begin{matrix} \cdots 11 \cdots \\ \cdots 00 \cdots \end{matrix} \rightarrow \begin{matrix} \cdots 0 * \cdots \\ \cdots * 1 \cdots \end{matrix} \qquad \text{with prob. } p_3, \qquad (6.3)$$

$$\begin{matrix} \cdots 00 \cdots \\ \cdots 11 \cdots \end{matrix} \rightarrow \begin{matrix} \cdots * 1 \cdots \\ \cdots 0 * \cdots \end{matrix} \qquad \text{with prob. } p_4. \qquad (6.4)$$

The symbol $*$ is a place-holder and can be a 1 or a 0. As one can see, particles in the upper leg hop deterministically one site to the right, if this site is empty (see (6.1)). If a particle at site i in the upper leg has a right neighbour at site $i+1$, this jammed particle takes a look into the lower leg. If the sites i and $i+1$ in the lower leg are both empty, the jammed particle at site i in the upper leg moves to site $i+1$ in the lower leg with probability p_2 (see (6.3)). Free particles in the lower leg, i.e. particles with no right neighbour, move one step to the right with probability p_2 (see (6.2)). Jammed particles in the lower leg can move into the upper leg with probability p_4 in the same way jammed particles in the upper leg can move into the lower leg (see (6.4)).

In the context of traffic flow this model can be seen as a minimal model for a European highway with speed-limit and a small fraction of trucks present. The trucks will most of

the time occupy the right lane (lower leg) and act as disturbances for cars in this lane, leading to an effective speed reduction. If the density of trucks is not large, neglecting them should only cause minor errors. The effective speed reduction is thus put in by hand, introducing a hopping probability p_2 for the lower leg.

The totally deterministic version of this model has been studied recently by Belitsky *et al.* [70] with a different focus. This special case will be discussed in the next section, where a generalization to open boundaries will be investigated.

Monte-Carlo simulations indicate that in the long time limit the inter-leg currents vanish, which is not obvious. In order to understand why this has to happen, it is instructive to consider the behaviour of the two legs without coupling, i.e., in the limit $p_3 = p_4 = 0$.

The process on the upper leg is known as cellular automaton 184, following the classification of Wolfram [22]. Since the process has a particle-hole symmetry, it is sufficient to examine densities $\rho < 1/2$. The particles arrange such that in front of every particle one finds at least one hole. The action of the dynamics on a configuration $\tau_1, \tau_2, \ldots, \tau_{L-1}, \tau_L$ is such that every occupation number is shifted one site to the right, yielding $\tau_L, \tau_1, \ldots, \tau_{L-2}, \tau_{L-1}$. Thus, after a certain number of steps, which is at most L, the starting configuration reproduces. The current j_{184} as a function of density becomes

$$j_{184} = \begin{cases} \rho & \text{for } \rho \leq \frac{1}{2}, \\ 1 - \rho & \text{for } \rho > \frac{1}{2}. \end{cases} \tag{6.5}$$

In the lower leg one has the Nagel-Schreckenberg model with $v_{\max} = 1$ (ASEP with parallel update) and hopping probability p_2. Thus, the current density relation reads

$$j_{\text{NaSch}}(\rho, p_2) = \frac{1 - \sqrt{1 - 4p_2\rho(1-\rho)}}{2}. \tag{6.6}$$

From now on p_3 and p_4 are taken to be greater than zero. One finds that the fundamental diagram of the two-leg ladder decomposes in three parts. For each of the three parts the stationary state can be constructed[1].

The first part is given by values of $\rho = (N_1 + N_2)/2L < 1/4$, where N_i is the particle number in leg i at $t = 0$. The state with all particles in the upper leg and at least one hole in front each particle is a stationary state, simply because it is a stationary state of CA184. Such an arrangement is possible, since the total density does not exceed $\rho = 1/4$. No jamming will ever occur, and so particles will never change into the lower leg. The probability distribution decomposes into the direct product of CA184 with density ρ and the Nagel-Schreckenberg model with density 0. Hence, for $\rho < 1/4$ the total current is given by ρ alone.

Exactly at $\rho = 1/4$ a new situation arises. The particles in the upper leg arrange as $\tau, 1-\tau, \tau, \ldots, \tau, 1-\tau$ with $\tau \in \{0, 1\}$. Thus, adding further particles into the lower leg, although jams will occur, no particle will be able to move into the upper leg, since no configuration 00 can be found. As a consequence of that, the current in the region of $1/4 < \rho < 3/4$ will be the sum of the maximal current in the upper leg and the NaSch current in the lower leg.

If one exceeds a density of 3/4, because no space is left in the lower leg, particles have to be put into the upper leg. The total current is carried by the upper leg alone and is given by the corresponding CA184 current.

---

[1]The stationary state is not unique here. Nevertheless, in the thermodynamic limit the differences between degenerate stationary states vanish.

Altogether one has

$$j(\rho) = \begin{cases} \rho & \text{for } \rho \le \frac{1}{4}, \\ \frac{1}{4} + \frac{j_{\text{NaSch}}(2\rho - 1/2, p_2)}{2} & \text{for } \frac{1}{4} < \rho \le \frac{3}{4}, \\ 1 - \rho & \text{for } \rho > \frac{3}{4}. \end{cases} \tag{6.7}$$

It has been checked that this flow-density relation shows excellent agreement with Monte-
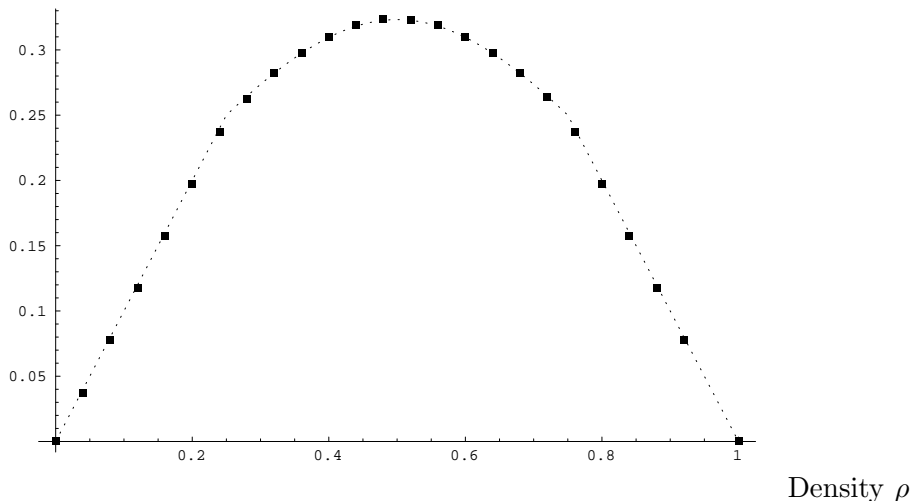

Figure 6.1.: Fundamental diagram for $L = 100$ and $p_2 = p_3 = p_4 = 0.5$. The boxes represent Monte-Carlo data, the dashed line displays the analytical result of (6.7).

Carlo data (see fig. 6.1).

As can be seen by direct calculation, the cars are always distributed on both legs in such a way that the total flow is maximized. This is insofar interesting as it displays the microscopic behaviour of the particles: A jammed particle tries to perform a lane change, in order to maximize the flow it carries.

Therefore, future studies should pose the question whether this maximization principle is generic for two-leg ladder models or if it is special for the case of deterministic motion in one leg.

6.3. Exact solution of a two-leg ladder model at a bottleneck

In [70] the deterministic version of the two-leg ladder model of Sec. 6.1 has been studied. In this case any asymmetry between both legs vanishes. This fact can be used to introduce a simplified description in the following way: In order to compute quantities like the current j or the local density per rung, the dynamics of the two-leg ladder model is equivalent to the dynamics of a three state model on a chain of length L. Each site i of the three state model can be in one of the states $\{0, 1, 2\}$, which corresponds to the occupation number of rung i of the two-leg ladder model (see Fig. 6.2).

Of course, any information on the occupation number of the distinct legs is lost. The complete table for the dynamical rules of the three state model is displayed in Tab. 6.1.

In the following, this three state model will be examined with open boundaries instead of periodic ones. Therefore, the dynamics is slightly altered for the first site and the last site
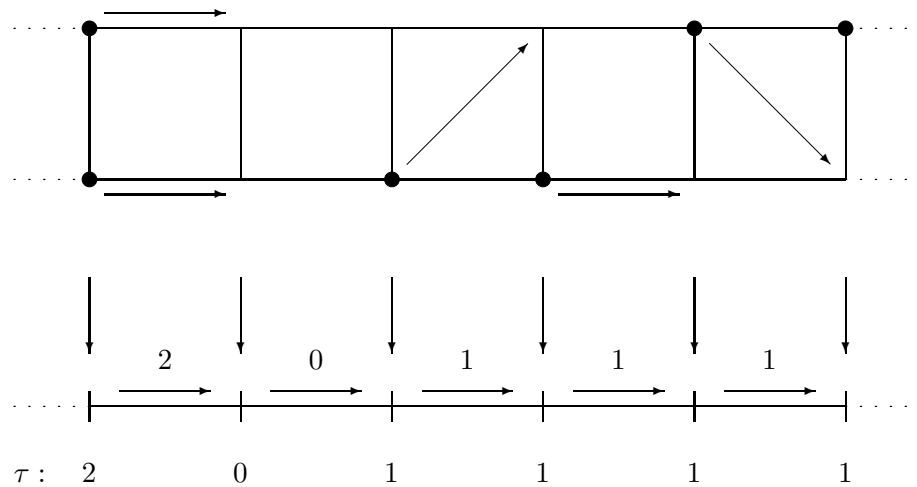
Figure 6.2.: Connection between two-leg ladder model and three state model on a chain. The numbers on top of the horizontal arrows denote the number of particles that hop along the associated bond.

t	$t+1$	t	$t+1$	t	$t+1$
(000)	0	(100)	1	(200)	2
(001)	0	(101)	1	(201)	2
(002)	0	(102)	1	(202)	2
(010)	0	(110)	1	(210)	1
(011)	0	(111)	1	(211)	1
(012)	1	(112)	2	(212)	2
(020)	0	(120)	0	(220)	0
(021)	1	(121)	1	(221)	1
(022)	2	(122)	2	(222)	2

Table 6.1.: Complete rule table for three state model. The image of the central site under the parallel dynamics is displayed.

of the chain. If the occupation number of the first site is smaller than two, a particle may enter the system with probability α. If the occupation number of the last site is larger than one, a particle may leave the system with probability β.

With the arguments of [73] it can be shown that each allowed configuration in the stationary state can be divided into three parts: a free flow part, a jammed flow part, and an interface of varying width (see Fig. 6.3).

The free flow part is defined to be the part of the configuration up to the rightmost zero. It consists of ones and zeros only. The jammed flow part starts with the leftmost two, and consists of ones and twos only. These parts can never overlap, but may be separated by an interface consisting of ones only. If the position of the last zero is given by f and that
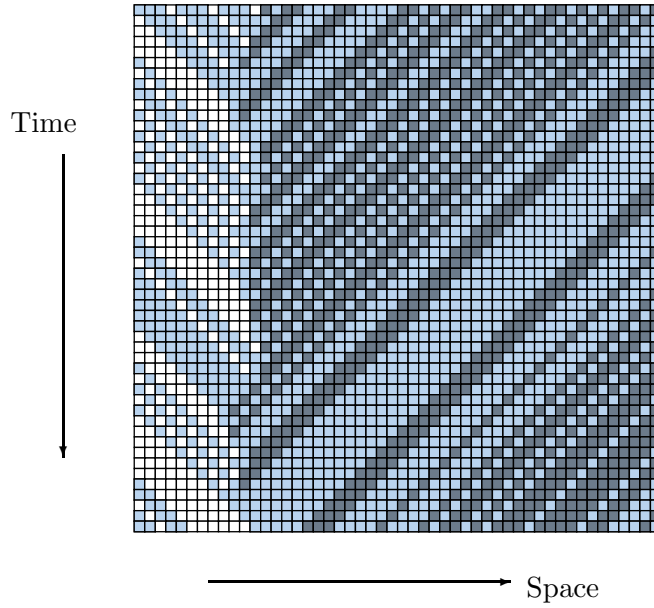
Time

Space

Figure 6.3.: Typical space time diagram for $\alpha = \beta = 0.5$ and $L = 50$. Light grey squares correspond to cells with one car and dark grey squares to doubly occupied cells. One can clearly see the free flow part, the jammed flow part and the interface.

of the first two by j, then the bulk dynamics follows the rules

$$
\begin{aligned}
\tau_i(t+1) &= \tau_{i-1}(t) && (i = 2, \dots, f+1), \\
\tau_i(t+1) &= \tau_{i+1}(t) && (i = j-1, \dots, L-1), \\
\tau_i(t+1) &= \tau_i(t) = 1 && (i = f+2, \dots, j-2).
\end{aligned}
\tag{6.8}
$$

This induces for a configuration in the stationary state the master equation

$$
\begin{aligned}
P(\tau_1, \dots, \tau_f, 1^n, \tau_j, \dots, \tau_L) = {} & F(\tau_1, \tau_2) J(\tau_{L-1}, \tau_L) \times \\
& \times \Big[P(\tau_2, \dots, \tau_f, 1^{n+2}, \tau_j, \dots, \tau_{L-1}) + \\
& + \sum_{k=0}^{n} \big(P(\tau_2, \dots, \tau_{f-1}, 1^k, 0, 2, 1^{n-k}, \tau_j + 1, \dots, \tau_{L-1}) + \\
& + P(\tau_2, \dots, \tau_{f-1}, 1^k, 0, 1, 2, 1^{n-k-1}, \tau_j + 1, \dots, \tau_{L-1}) \big) \Big].
\end{aligned}
\tag{6.9}
$$

Here F and J are given by

$$
F = \begin{pmatrix} 1-\alpha & 1-\alpha & 0 \\ \alpha & \alpha & 0 \\ 0 & 0 & 0 \end{pmatrix},
\tag{6.10}
$$

and

$$
J = \begin{pmatrix} 0 & 0 & 0 \\ 0 & \beta & 1-\beta \\ 0 & \beta & 1-\beta \end{pmatrix}.
\tag{6.11}
$$

Iteration of (6.9) suggests the following ansatz for the probabilities P:

$$P(\tau_1,\dots,\tau_f,1^n,\tau_j,\dots,\tau_L) = \frac{1}{Z_L} P_f(\tau_1,\dots,\tau_f) P_i(n) P_j(\tau_j,\dots,\tau_L), \tag{6.12}$$

$$P_f(\tau_1,\dots,\tau_f) = c_f x^f \prod_{i=1}^{f-1} F(\tau_i,\tau_{i+1}), \tag{6.13}$$

$$P_j(\tau_j,\dots,\tau_L) = c_j y^{L-j-1} \prod_{i=j}^{L-1} J(\tau_i,\tau_{i+1}). \tag{6.14}$$

The quantities c_f, x, c_j, y and $P_i(n)$ have to be determined and Z_L is a normalization. From the exact solutions of small systems these quantities have been guessed to be given by

$$x = \frac{\beta^2}{\alpha^2(1-\beta)}, \tag{6.15}$$

$$c_f = 1 - \alpha, \tag{6.16}$$

$$y = c_j = \frac{1}{1-\beta}. \tag{6.17}$$

The probability for the interface reads

$$P_i(n) = \begin{cases} 1 & \text{for } n = 0, \\ \frac{\beta}{\alpha(1-\beta)} & \text{for } n = 1, \\ \frac{\beta^n}{\alpha^n(1-\beta)^n}\left[(1-\beta)\sum_{i=1}^{n-1}\alpha^i\beta^{n-i-1} + \beta^{n-1}\right] & \text{for } n > 1. \end{cases} \tag{6.18}$$

It can be shown that these quantities satisfy the master equation (6.9).
In the following the current and the density profile in the stationary state will be computed, thus clarifying the phase diagram of the model. In a first step the partition function Z_L has to be computed. After some algebra one finds

$$Z_L = \frac{1}{(1-\beta)^{L-1}}\left[\sum_{i=1}^{2L}\left(\frac{\beta}{\alpha}\right)^{i-1} + \left(\frac{\beta}{\alpha}\right)^{2L}(1-\beta)^{-1}\right]. \tag{6.19}$$

The current j in the stationary state is simply given by the current into the system

$$j = \alpha(1 - \rho_2(1)). \tag{6.20}$$

$\rho_2(1)$ denotes the probability to find a two at site one and is given by

$$\rho_2(1) = \frac{1}{Z_L}(1-\beta)^{1-L}. \tag{6.21}$$

Thus, one has

$$j = \alpha\left(1 - \left[\sum_{i=1}^{2L}\left(\frac{\beta}{\alpha}\right)^{i-1} + \left(\frac{\beta}{\alpha}\right)^{2L}(1-\beta)^{-1}\right]^{-1}\right). \tag{6.22}$$

In the limit of L going to infinity this formula simplifies drastically

$$j = \max(\alpha, \beta). \tag{6.23}$$

From this finding one infers a phase transition along the line $\alpha = \beta$. The nature of this phase transition will be clarified in the rest of this chapter. Therefore, the form of the density profiles in the stationary state will be studied.

If $\rho_j(k)$ denotes the probability to find the variable $j \in \{0, 1, 2\}$ at site k, then the total density at site k, denoted $\rho(k)$, can be derived from

$$\rho(k) = \rho_2(k) + 1 - \rho_0(k). \tag{6.24}$$

Introducing

$$c = \frac{(1-\alpha)(1-\beta)(\alpha+\beta)}{\beta(1-\beta)^L} \tag{6.25}$$

one finds that

$$\rho_2(k+1) - \rho_2(k) = \frac{c}{Z_L} \left(\frac{\beta}{\alpha} \right)^{2k}, \tag{6.26}$$

and

$$\rho_0(k) - \rho_0(k+1) = \frac{c}{Z_L} \left(\frac{\beta}{\alpha} \right)^{2k+1}. \tag{6.27}$$

Note that for $\alpha = \beta$ the local density $\rho_2(k)$ ($\rho_0(k)$) increases (decreases) linearly if k runs from 1 to L. Thus, the density profile on this line has to decrease linearly as well.

Adding up all contributions gives

$$\rho_2(k) = \rho_2(1) + \frac{c}{Z_L} \frac{\left(\frac{\beta}{\alpha} \right)^2 \left(1 - \left(\frac{\beta}{\alpha} \right)^{2(k-1)} \right)}{1 - \left(\frac{\beta}{\alpha} \right)^2} \tag{6.28}$$

as well as

$$\rho_0(L-r) = \rho_0(L) + \frac{c}{Z_L} \left(\frac{\beta}{\alpha} \right)^{2L+1} \frac{\left(\frac{\alpha}{\beta} \right)^2 \left(1 - \left(\frac{\alpha}{\beta} \right)^{2r} \right)}{1 - \left(\frac{\alpha}{\beta} \right)^2}. \tag{6.29}$$

$\rho_2(1)$ has been given already in (6.21). Finally, this yields

$$\rho_0(L) = \frac{1-\alpha}{Z_L} \left(\frac{\beta^2}{\alpha^2(1-\beta)^2} \right)^L. \tag{6.30}$$

With the help of these equations the exact density profiles for systems of arbitrary length can be computed. One finds three distinct cases: a high density phase (B) for $\beta < \alpha$, a coexistence line for $\alpha = \beta$, and a low density phase (A) for $\beta > \alpha$.

Typical density profiles for all three cases can be seen in Figs. 6.4–6.6. In phase A (B) one finds profiles which are flat in the left (right) part of the system, where the flat part is reached exponentially from above (below) if one follows the density profile from the right (left) into the bulk. Hence, the phase transition from the low density into the high density phase is of first order, since the density changes discontinuously while crossing the coexistence line. The same scenario has been found for the ASEP with sublattice-parallel update and deterministic hopping in the bulk [74].

Figure 6.4.: Density profile in the high density phase for $L = 30$, $\alpha = 3/6$ and $\beta = 2/5$.
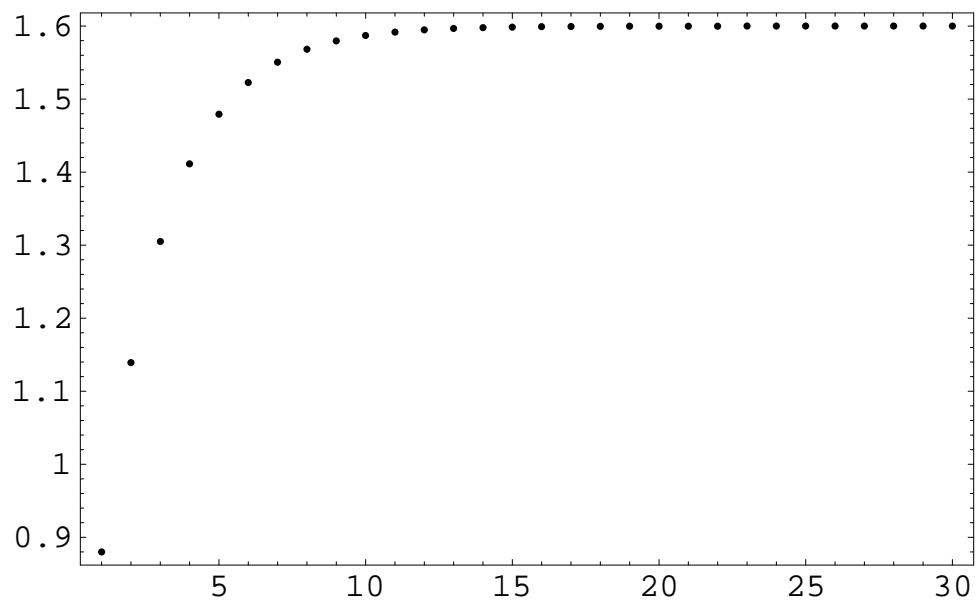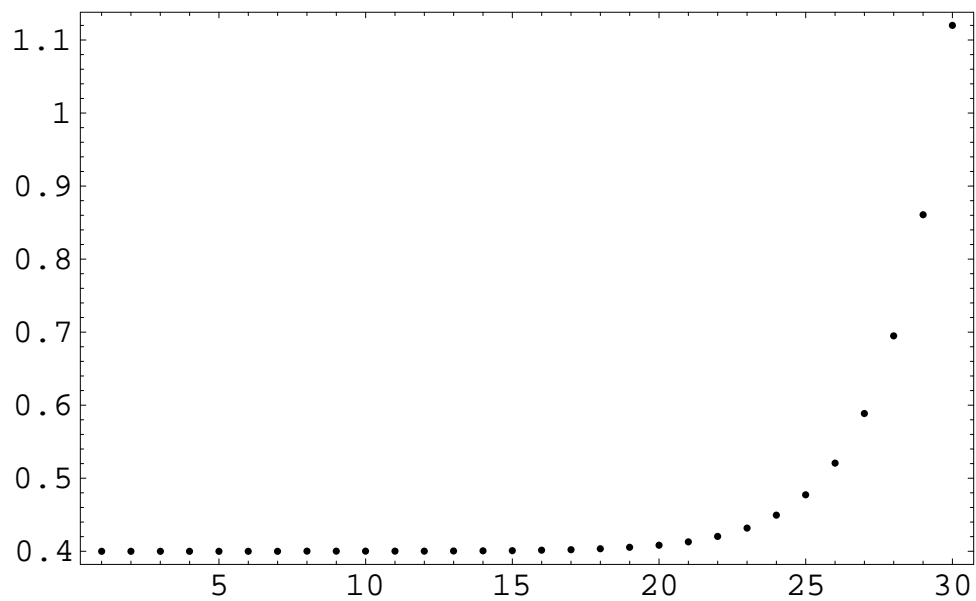

Figure 6.5.: Density profile in the low density phase for $L = 30$, $\alpha = 2/5$ and $\beta = 3/6$.
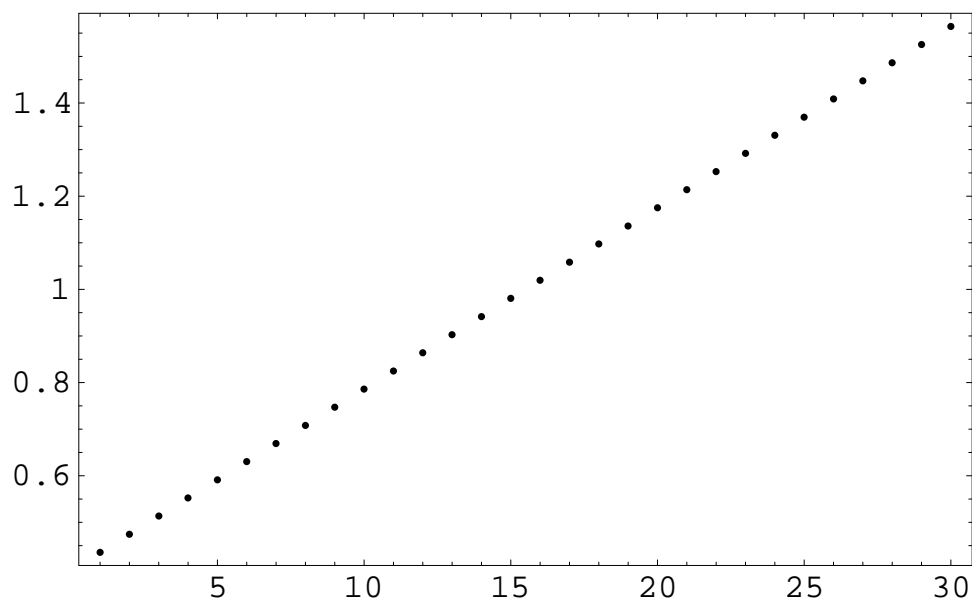
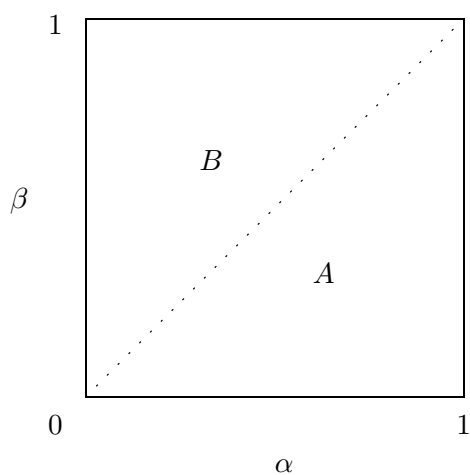Figure 6.6.: Density profile on the coexistence line for $L = 30$, $\alpha = 2/5$ and $\beta = 2/5$.

Figure 6.7.: Phase diagram for the two-leg ladder model with open boundaries in the $\alpha - \beta$ plane. Region A is the low density phase and region B is the high density phase.

7. Summary and outlook

The present work studies low-dimensional stochastic models far from equilibrium. Such models can be applied for the description of various physical phenomena and for many problems beyond physics, such as the modeling of traffic flow, biological processes, spreading of diseases, opinion formation in human groups, and financial markets.

Most of the existing results in the field of nonequilibrium stochastic processes have been derived for the stationary properties of homogeneous one-dimensional systems with nearest neighbour interaction. In this work the question has been raised, if one can still find exact solutions or good approximate descriptions, if the generic settings (nearest neighbour interactions, stationarity, etc.) are relaxed, e.g. regarding interactions with a wider range, or quasi one-dimensional systems.

The main conclusion of this thesis is that such extensions are possible! The methods developed for a small set of paradigmatic models like the ASEP or the Nagel-Schreckenberg model for traffic flow turn out to be very robust and universal. This is insofar interesting as one is still lacking a well developed theory for the description of models far away from equilibrium.

In the first chapter of this thesis an introduction to the field of low-dimensional stochastic models for the description of systems far from equilibrium has been given and the concepts of matrix product ansatz and optimum ground states have been introduced.

In the second chapter the generalization of a proposition by Krebs and Sandow [34] to stochastic processes with interaction range $r \geq 2$ has been given. By construction it could be shown that the stationary state of such processes in continuous time can always be written as a matrix product state. The proof of this proposition has led to the most general cancelling-mechanism for such systems, which is one of the main results of this chapter.

The cancelling-mechanism reduces the determination of the stationary state to a local problem. This allows for a systematic search for exact solutions, e.g. by using finite-dimensional matrices, which usually yields restrictions on the boundary rates. In principle, it is also possible to determine all processes which are solved by a $n-$dimensional representations of a given algebra.

Another important application of the results of this chapter is of a more theoretical nature. Since the mathematical structure of the stationary state is known, it is possible to derive rather general results. An example for nearest-neighbour processes can be found in [35], where a relation between expectation values in ordered-sequential dynamics and sublattice-parallel dynamics could be established. The cancelling-mechanism is an important ingredient in the proof of this result.

Furthermore it has been shown that the DMRG approach asymptotically yields a MPS [75]. Together with the results of Chap. 2 this indicates that the DMRG might yield excellent results for the stationary states of stochastic systems. First results are very promising [76, 77, 78, 79].

As an application, two models with three-site interactions have been investigated. These models are interesting by themselves, since they might be of relevance for the description

of traffic flow or granular matter. It was possible to find the stationary state of the periodic system, which in both cases is given by a finite-dimensional representation of the algebra obtained from the MPA. For the open system with boundary interactions the solutions of the periodic systems could be extended for special values of the input and output rates. For general values of the boundary rates one most presumably needs infinite-dimensional representations. However, both models have a fundamental diagram with only one maximum. Using the argumentation of [41], one can expect that the phase diagrams of model A and B with boundary interactions essentially look like the well known phase diagram of the ASEP [31, 32].

A generalization of the KS-proposition to other update schemes [64] has been presented in [35]. A similar generalization is also possible in our case and will be presented elsewhere [44].

For stochastic processes with an interaction range $r = 2$ in [80, 81] the dynamical version of the MPA, the so-called *dynamic matrix product ansatz* (DMPA), was introduced. In the future one should try to generalize the DMPA to processes with arbitrary (but finite) interaction range.

One of the most tantalizing unsolved problems connected with the KS proposition is to decide whether matrix product states are generic for stochastic processes with periodic boundary conditions. In [82] Krebs claims that a similar proposition does not hold for p.b.c. He proposes a counter-example, the zero-energy eigenstate of which can not be written as a trace over a product of matrices. Unfortunately, the proposed Hamiltonian is not a stochastic one. Hence, the problem of the ubiquity of MPS for stochastic processes with p.b.c. remains unsolved.

In the third chapter the stationary state of a staggered hopping model with reflective boundaries has been calculated exactly, extending ideas from the solution of a $U_q[SU(2)]$-symmetric hopping model. This stationary state turned out to be an optimum ground state. It has been shown that optimum ground states for stochastic Hamiltonians with reflective boundaries come into play quite naturally. They are connected with the occurrence of a trivial representation of the quadratic algebra derived from the matrix product ansatz. However, using a counterexample, it has been pointed out that optimum ground states are not enforced by reflective boundaries. All attempts to derive the stationary state of the staggered hopping model for periodic or open boundaries have failed. Nevertheless, the solution of this problem is still very tempting to derive, since it will lead to a much deeper understanding of the underlying mathematical structures. In addition to that, the following two questions should be answered: Firstly, is it possible to calculate dynamical properties of the staggered hopping model? Secondly, can one generalize the results to arbitrary quenched bond disorder?

In the fourth chapter the statistical properties of a classical vertex model have been used for the description of traffic flow. The distinct phases of the vertex model represent different situations that can be found in real highway traffic. For comparison, a cellular automaton model with properties similar to the vertex model has been proposed. This model could be solved exactly, using the so-called two cluster measure or the car-oriented mean-field theory. The fundamental diagrams of both models were compared, which has shown that the vertex model produces a higher flow. This finding can be explained by the strong correlations of the vertex model, since this model is critical with an algebraic decay of two-point correlation functions. In [23] Rujàn has proposed a construction, which allows to transform the transfer matrix of a two-dimensional classical model into the stochastic transfer matrix of a cellular automaton. This program hinges on the knowledge of the largest eigenvalue and the associated eigenvector of the transfer matrix. Since the vertex

model studied in Chap. 4 is integrable, the whole spectrum of the transfer matrix can be derived by the use of the Bethe ansatz – at least in principle. Realizing the construction of Rujàn would be very interesting, since then a more realistic comparison between the vertex model and the proposed cellular automaton can be expected.

Chapter five offers a description of the dynamical properties of the ASEP with parallel update, which can be seen as a minimal model for traffic flow at bottlenecks. Using the time and space dependent version of the $(2, 1)$-cluster approximation, a set of recursion relations in time for the temporal evolution of the probability distribution has been derived. As long as one is not on the shock-profile line, these recursion relation allow for a very efficient numerical prediction of the dynamics of any observable quantity. Due to the failure of the $(2, 1)$-cluster approximation on the shock-profile line, in this special case a different approach has been chosen. A domain wall picture, proposed for the late time behaviour of driven lattice gases with random sequential update by Kolomeisky *et al.* [41], has been transformed into the setting of the parallel update. Surprisingly, this picture gave fairly accurate results – even for early stages of the dynamics! The spectrum of this domain wall has been computed exactly. Most tentatively this spectrum coincides with the low energy spectrum of the Markov generator of the ASEP for some values of the parameters. This point should be elucidated in the future performing suitable MC simulations or using the DMRG. On the other hand one should try to generalize the DMPA [80, 81] to stochastic processes in discrete time, since this might lead to an improved description of the dynamics of the ASEP.

Finally, stochastic models on two-leg ladders have been studied. These models allow an interpretation in the context of two-lane highways. In the first part of the chapter a stochastic version of a model of Belitsky *et al.* [70] has been examined. Surprisingly the stochasticity leads to a simplification, since both legs decouple in the limit of large times. Thus, the system decomposes into the direct product of CA184 and the Nagel-Schreckenberg model with $v_{\max} = 1$. The cars are distributed on both legs in such a way that the total current is maximized. Whether this maximization of the current is a generic feature of such models or if it is just found accidentally, is a very interesting question to be answered in the future, because such a maximization principle would be an invaluable tool for analytical descriptions such as mean-field theory or cluster-approximations.

In the second part, the model proposed by Belitsky *et al.* has been studied with open boundaries, i.e., injection of particles at the left end and removal of particles at the right end. In the stationary state the system decomposes into three coexisting phases. The total probability distribution is the direct product of the probabilities of the phases. The phase diagram of this model is clarified. One finds two phases separated by a first order transition line.

Two possible extensions are systems with non-deterministic bulk behaviour on the one hand and exactly solvable stochastic n-leg ladder models on the other hand. The latter systems are very likely to exist and the formal analogy with the quantum Hamiltonian formalism should be exploited here.

A. Proofs of the generalized Krebs-Sandow propositions

In this appendix the proofs of the propositions of Chap. 2 are presented. Once the correct cancelling-mechanism is identified, the proofs are a rather straightforward generalization of that of KS [34].

Proof. Proposition A

(i)

$$H_L^{(p)}(r)|P_L\rangle_0 = \text{Tr}[H_L^{(p)}(r)\mathcal{D}^{\otimes L}] = \text{Tr}\left[\sum_{k=1}^{L} h_{k,k+1,\dots,k+r-1}\mathcal{D}^{\otimes L}\right]$$

$$\stackrel{(2.5)}{=} \text{Tr}\left[\sum_{k=1}^{L} \mathcal{D}^{\otimes(k-1)} \otimes \mathcal{X}(r) \otimes \mathcal{D} \otimes \mathcal{D}^{\otimes(L-k-r+1)}\right] -$$

$$- \text{Tr}\left[\sum_{k=1}^{L} \mathcal{D}^{\otimes(k-1)} \otimes \mathcal{D} \otimes \mathcal{X}(r) \otimes \mathcal{D}^{\otimes(L-k-r+1)}\right]$$

$$= 0.$$

Here it has been used that due to the periodic boundary conditions the sites $L + 1, L + 2, \dots$ can be identified with sites $1, 2, \dots$. For convenience, $Z_L = 1$ has been assumed, which can be achieved by e.g. rescaling $\mathcal{D}$.

(ii)

$$H_L(r)|P_L\rangle_0 = \langle W|H_L(r)\mathcal{D}^{\otimes L}|V\rangle$$

$$= \langle W|\left[h_{\text{left}}(r) + \sum_{k=1}^{L-r+1} h_{k,k+1,\dots,k+r-1} + h_{\text{right}}(r)\right]\mathcal{D}^{\otimes L}|V\rangle$$

$$\stackrel{(2.5)-(2.7)}{=} - \langle W|\mathcal{X}(r) \otimes \mathcal{D}^{\otimes(L-r+1)} + \mathcal{D}^{\otimes(L-r+1)} \otimes \mathcal{X}(r)|V\rangle$$

$$+ \sum_{k=1}^{L-r+1} \langle W|\mathcal{D}^{\otimes(k-1)} \otimes \mathcal{X}(r) \otimes \mathcal{D} \otimes \mathcal{D}^{\otimes(L-k-r+1)}|V\rangle -$$

$$- \sum_{k=1}^{L-r+1} \langle W|\mathcal{D}^{\otimes(k-1)} \otimes \mathcal{D} \otimes \mathcal{X}(r) \otimes \mathcal{D}^{\otimes(L-k-r+1)}|V\rangle$$

$$= 0.$$

□

Now we come to the proof of Proposition B.

Proof. Proposition B

As a first step one defines the vector space A.

Definition 4 (Vector space A). *Let, for $L = 1, 2, \ldots,$ A_L be an m^L-dimensional vector space with orthogonal basis vectors $|s_1, s_2, \ldots, s_L\rangle$ ($s_i = 1, 2, \ldots, m$). In addition one has the one-dimensional space A_0 with basis vector $|vac\rangle$. The vector space A is defined in analogy to the Fock space as follows:*

$$A = \bigoplus_{L=0}^{\infty} \mathcal{H}_L. \tag{A.1}$$

Note that the basis vectors of the A_L are in one-to-one correspondance with the states of the stochastic process on a chain of length L. The set of all the basis vectors of all A_L (embedded in A) will now be taken as a basis for A.

As a next step m matrices D_i are defined through their action on all the basis-vectors of A.

Definition 5. *The matrices D_i are linear mappings between the subspaces A_L and A_{L+1}. More explicitly:*

$$\forall_{s_i \in 1, \ldots, m} : \qquad D_{s_i} : A_L \to A_{L+1}$$
$$D_{s_i} |s_1, s_2, \ldots, s_L\rangle \mapsto |s_i, s_1, s_2, \ldots, s_L\rangle \tag{A.2}$$

At this stage it is useful to define the vectors $|V\rangle \in A$ and $\langle W| \in A^*$. $|V\rangle$ is nothing but the vacuum vector $|vac\rangle$. For the $\langle W|$ one sets

$$\langle W| := \sum_{L=1}^{\infty} \sum_{s_1, s_2, \ldots, s_L} P_L(s_1, s_2, \ldots, s_L) \, \langle s_1, s_2, \ldots, s_L|$$

With this definitions it is obvious that

$$P(s_1, \ldots, s_L) = \langle W| D_{s_1} D_{s_2} \cdots D_{s_L} |V\rangle \tag{A.3}$$

and therefore $|P_L\rangle_0 = \langle W| \mathcal{D}^{\otimes L} |V\rangle$.

The last definition which has to be made, is that of the matrices stored in the vector $\mathcal{X}(r)$.

Definition 6. *Like the D_i, the $X_{i_1, i_2, \ldots, i_{r-1}}$ are defined through their action on basis vectors*

$$\mathcal{X}(r) \otimes \begin{pmatrix} \overbrace{|1, 1, \ldots, 1\rangle}^{L - r + 1 \ places} \\ |1, 1, \ldots, 2\rangle \\ \vdots \\ |m, m, \ldots, m-1\rangle \\ |m, m, \ldots, m\rangle \end{pmatrix} = \mathcal{X}(r) \otimes \mathcal{D}^{\otimes(L-r+1)} |V\rangle$$

$$:= \left[\sum_{k=1}^{L-r+1} h_{k, k+1, \ldots, k+r-1} + h_r(r) \right] \mathcal{D}^{\otimes L} |V\rangle \tag{A.4}$$

for all $L \geq r - 1$. The action on the basis vectors which are not included in this definition is irrelevant, as the physical interactions given above are not well-defined for systems of length $L < r - 1$ and so the action on these basis states can be chosen totally arbitrary.

What remains to be shown is that the objects that have been defined so far fulfil the algebraic relations (2.5)-(2.7).

The relation (2.7) is met trivially, as it is just the case $L = r - 1$ of (A.4).

To understand why the other two relations are valid, one directly convinces oneself that for all $n = 0, 1, 2, \ldots$

$$\mathcal{D}^{\otimes n} \otimes \mathcal{X}(r) \otimes \mathcal{D}^{L-r+1-n} |V\rangle = \left[\sum_{k=n+1}^{L-r+1} h_{k,k+1,\ldots,k+r-1} + h_r(r) \right] \mathcal{D}^{\otimes L} |V\rangle. \tag{A.5}$$

As a consequence, for all $L = r, r+1, \ldots$

$$\left[\mathcal{X}(r) \otimes \mathcal{D} - \mathcal{D} \otimes \mathcal{X}(r) - h_{1,2\ldots,r} \mathcal{D}^{\otimes r} \right] \otimes \mathcal{D}^{\otimes(L-r)} |V\rangle = 0, \tag{A.6}$$

which proves (2.5).

For the last equation one needs that $|P_L\rangle_0$ is a zero-energy eigenstate of $H_L(r)$. Using (A.5), one derives

$$\langle W | \mathcal{X}(r) \otimes \mathcal{D}^{\otimes(L-r+1)} |V\rangle = [H_L(r) - h_{\text{left}}] |P_L\rangle_0, \tag{A.7}$$

but, as $H_L(r)|P_L\rangle_0 = 0$, this means

$$\langle W | \mathcal{X}(r) \otimes \mathcal{D}^{\otimes(L-r+1)} |V\rangle = -h_{\text{left}} |P_L\rangle_0, \tag{A.8}$$

which can be cast into the form

$$\langle W | \left[h_{\text{left}} + \mathcal{X}(r) \right] \otimes \mathcal{D}^{(L-r+1)} |V\rangle = 0, \tag{A.9}$$

showing the validity of (2.6). $\qquad\qquad\qquad\qquad\qquad\qquad\qquad\qquad\qquad\qquad\qquad$ $\square$

B. The connection between two-cluster measures and matrix product ansatz

The stationary state of a stochastic process on a chain of length L, where the local occupation number at site i is denoted τ_i, is of the $(2,1)$-cluster type, if the probabilitiy distribution factorizes in the following way:

$$P(\tau_1, \tau_2, \ldots, \tau_L) = \prod_{i=1}^{L} p(\tau_i, \tau_{i+1}). \tag{B.1}$$

Under this circumstances, the probabiltiy distribution can also be written as a matrix product state

$$P(\tau_1, \tau_2, \ldots, \tau_L) = \text{Tr}\left[\prod_{i=1}^{L} \left((1 - \tau_i)E + \tau_i D\right)\right], \tag{B.2}$$

where E and D are matrices defined by

$$E = \begin{pmatrix} p(0,0) & 1 \\ 0 & 0 \end{pmatrix}, \qquad D = \begin{pmatrix} p(1,1) & 0 \\ p(1,0)^2 - p(1,1)\,p(0,0) & 0 \end{pmatrix}. \tag{B.3}$$

C. Evolution equations for the two-cluster probabilities of the ASEP

Using the forward difference operator defined by

$$\triangle : f(x) \mapsto f(x+1) - f(x) \tag{C.1}$$

one can write down the evolution equations of the two cluster probabilities in the following way:

Left boundary:

$$
\begin{aligned}
\triangle_t p_1(00) &= \bar{\alpha} p_1(010) - \alpha p_1(00), \\
\triangle_t p_1(01) &= pp_1(10) - \alpha p_1(01) - \bar{\alpha} pp_1(010), \\
\triangle_t p_1(10) &= pp_1(110) + \alpha \left(p_1(00) + pp_1(010) \right) - pp_1(10), \\
\triangle_t p_1(11) &= \alpha \left(p_1(011) + \bar{p} \cdot p_1(010) \right) - pp_1(110).
\end{aligned}
\tag{C.2}
$$

Bulk: $(i \in \{2, 3, \dots, L-2\})$

$$
\begin{aligned}
\triangle_t p_i(00) &= p\bar{p} p_{i-1}(1010) + pp_{i-1}(0010) - pp_{i-1}(100), \\
\triangle_t p_i(01) &= pp_i(10) - pp_{i-1}(0010) - (2p - p^2)p_{i-1}(1010) - pp_{i-1}(10111), \\
\triangle_t p_i(10) &= pp_{i-1}(100) + p^2 p_{i-1}(1010) + pp_i(110) - pp_i(10), \\
\triangle_t p_i(11) &= pp_{i-1}(1011) + p\bar{p} p_{i-1}(1010) - pp_i(110).
\end{aligned}
\tag{C.3}
$$

Right boundary:

$$
\begin{aligned}
\triangle_t p_{L-1}(00) &= \beta p_{L-2}(001) + \bar{p}\beta p_{L-1}(101) - pp_{L-2}(100), \\
\triangle t p_{L-1}(01) &= pp_{L-1}(10) - \beta p_{L-1}(01) - p\bar{\beta} p_{L-2}(101), \\
\triangle_t p_{L-1}(10) &= pp_{L-2}(100) + p\beta p_{L-2}(101) + \beta p_{L-1}(11) - pp_{L-1}(10), \\
\triangle_t p_{L-1}(11) &= p\bar{\beta} p_{L-2}(101) - \beta p_{L-1}(11).
\end{aligned}
\tag{C.4}
$$

In order to shorten the notation, the abreviation $\bar{*} = 1 - *$ was introduced.

D. Recursion relations for $p(k, x, t)$

As a straightforward generalization of the usual approach to the simple random walk problem [83] one can derive the following recursion relations for the two-state random walker with reflective boundaries:

Left boundary:

$$
\begin{aligned}
p(1, 1, t+1) &= (1 - D_R^0)\, p(1, 1, t), \\
p(2, 1, t+1) &= (1 - D_R)\, p(2, 1, t) + D_L\, p(2, 2, t).
\end{aligned}
\tag{D.1}
$$

Bulk: $(j = 2, 3, \ldots, L)$

$$
\begin{aligned}
p(1, j, t+1) &= (1 - D_R^0)\, p(1, j, t) + D_R^0\, p(1, j-1, t), \\
p(2, j, t+1) &= D_R\, p(2, j-1, t) + (1 - D_R - D_L)\, p(2, j, t) + D_L\, p(2, j+1, t).
\end{aligned}
\tag{D.2}
$$

Right boundary:

$$
p(2, L+1, t+1) = D_R^0\, p(1, L, t) + D_R\, p(2, L, t) + (1 - D_L)\, p(2, L+1, t).
\tag{D.3}
$$

Bibliography

[1] G. M. Schütz. *Phase Transitions and Critical Phenomena*. Number 19. Academic Press, London, 2000.

[2] F. C. Alcaraz, M. Droz, M. Henkel, and V. Rittenberg. Reaction-diffusion processes, critical dynamics and quantum chains. *Ann. Phys.* **230**, page 250, 1994.

[3] V. Privman (ed.). *Nonequilibrium Statistical Mechanics in One Diemnsion*. Cambridge University Press, Cambridge, 1997.

[4] J. Marro and R. Dickman. *Nonequilibrium Phase Transitions in Lattice Models*. Cambridge University Press, Cambridge, 1999.

[5] T. Liggett. *Interacting Particle Systems*. Springer, Berlin, 1985.

[6] H. Spohn. *Large Scale Dynamics of Interacting Particles*. Springer, Berlin, 1991.

[7] B. Schmittmann and R. K. P. Zia. *Phase Transitions and Critical Phenomena*, volume 17. Academic Press, London, 1995.

[8] D. Chowdhury, L. Santen, and A. Schadschneider. Statistical physics of vehicular traffic and some related systems. *Phys. Rep.* **329**, page 199, 2000.

[9] D. Helbing. *Verkehrdynamik*. Springer, Berlin, 1997.

[10] J. T. MacDonald, J. H. Gibbs, and A. C. Pipkin. *Biopolymers* **6**, page 1, 1968.

[11] J. T. MacDonald and J. H. Gibbs. *Biopolymers* **7**, page 707, 1969.

[12] V. Méndez and J. Fort. Dynamical evolution of discrete epidemic models. *Physica* **A 284**, page 309, 2000.

[13] M. Henkel, E. Orlandini, and J. E. Santos. Reaction-diffusion processes from equivalent integrable quantum chains. *Ann. Phys.* **259**, page 163, 1997.

[14] J. P. Bouchaud and M. Potters. *Théorie des risque financier*. Aléa-Saclay, 1997.

[15] D. Chowdhury and D. Stauffer. A generalized spin model of financial markets. *Eur. Phys. J.* **B8**, page 477, 1999.

[16] R. N. Mantegna and H. E. Stanley. *An Introduction to Econophysics*. Cambridge University Press, 2000.

[17] R. Baxter. *Exactly Solved Models in Statistical Mechanics*. Academic Press, New York, 1982.

[18] Yu. A. Izyumov and Yu. N. Skryabin. *Statistical Mechanics of Magnetically Ordered Systems*. Consultants Bureau, New York, 1988.

[19] M. Gaudin. *La Fonction d'Onde de Bethe pour les Modèles Exacts de la Méchanique Statistique.* Commisariat à l'Énergie Atomique, Paris, 1983.

[20] I. Oppenheim, K. E. Shuler, and G. H. Weiss. *Stochastic processes in chemical physics: The master equation.* MIT Press, Cambridge, 1977.

[21] N. G. van Kampen. *Stochastic processes in physics and chemistry.* Elsevier, Amsterdam, 1992.

[22] S. Wolfram. *Theory and Applications of Cellular Automata.* World Scientific, 1986.

[23] Pàl Rujàn. Cellular automata and statistical mechanical models. *J. Stat. Phys.* **49**, page 139, 1987.

[24] J. de Boer and A. Schadschneider. Exact ground states of generalized Hubbard models. *Phys. Rev. Lett.* **75**, page 2489, 1995.

[25] A. Klümper, A. Schadschneider, and J. Zittartz. Equivalence and solution of anisotropic spin-1 models and generalized $t-j$ fermion models in one dimension. *J. Phys. A: Math. Gen.* **24**, page L955, 1991.

[26] A. Klümper, A. Schadschneider, and J. Zittartz. Groundstate properties of a generalized VBS-model. *Z. Phys.* **B87**, page 281, 1992.

[27] A. Klümper, A. Schadschneider, and J. Zittartz. Matrix product ground states for one-dimensional spin-1 quantum antiferromagnets. *Europhys. Lett.* **24**, page 293, 1993.

[28] H. Niggemann and J. Zittartz. Optimum ground states for spin-$\frac{3}{2}$ ladders with two legs. *J. Phys. A: Math. Gen.* **31**, page 9819, 1998.

[29] H. Niggemann. *Exact ground states of one- and two-dimensional quantum spin systems.* Dissertation Thesis, University of Cologne, 1998.

[30] H. J. Mikeska and A. K. Kolezhuk. Finitely correlated generalized spin ladders. *Int. J. Mod. Phys.* **B12**, page 2325, 1998.

[31] B. Derrida, M. R. Evans, V. Hakim, and V. Pasquier. Exact solution of a 1-d asymmetric exclusion model using a matrix formulation. *J. Phys. A: Math. Gen.* **26**, page 1493, 1993.

[32] G. M. Schütz and E. Domany. Phase transitions in an exactly soluble one-dimensional exclusion process. *J. Stat. Phys.* **72**, page 277, 1993.

[33] H. Hinrichsen, S. Sandow, and I. Peschel. On matrix product ground states for reaction-diffusion models. *J. Phys. A: Math. Gen.* **29**, page 2643, 1996.

[34] K. Krebs and S. Sandow. Matrix product eigenstates for one-dimensional stochastic models and quantum spin chains. *J. Phys. A: Math. Gen.* **30**, page 3165, 1997.

[35] N. Rajewsky and M. Schreckenberg. Exact results for one-dimensional cellular automata with different types of updates. *Physica* **A245**, page 139, 1997.

[36] F. H. L. Eßler and V. Rittenberg. Representations of the quadratic algebra and partially asymmetric diffusion with open boundaries. *J. Phys. A: Math. Gen.* **29**, page 3375, 1996.

[37] M. Schreckenberg, A. Schadschneider, K. Nagel K, and N. Ito. Discrete stochastic models for traffic flow. *Phys. Rev.* **E51**, page 2939, 1995.

[38] A Schadschneider and M Schreckenberg. Car-oriented mean-field theory for traffic flow models. *J. Phys. A: Math. Gen.* **30**, page L69, 1997.

[39] P. Meakin, P. Ramanlal, L. M. Sander, and R. C. Ball. Theory of growth of ballistic aggregates. *Phs. Rev.* **A34**, page 5091, 1986.

[40] G. Schütz, R. Ramaswamy, and M. Barma. Pairwise balance and invariant measures for generalized exclusion processes. *J. Phys. A: Math. Gen.* **29**, page 837, 1996.

[41] A. B. Kolomeisky, G. M. Schütz, E. B. Kolomeisky, and J. P. Straley. Phase diagram of one-dimensional driven lattice gases with open boundaries. *J. Phys. A: Math. Gen.* **31**, page 6911, 1998.

[42] T.Antal and G. M. Schütz. Asymmetric exclusion process with next-nearest-neighbor interaction: Some comments on traffic flow and a nonequilibrium reentrance transition. *Phys. Rev.* **E62**, page 83, 2000.

[43] R. Barlovic, L. Santen, A. Schadschneider, and M. Schreckenberg. Metastable states in cellular automata for traffic flow. *Eur. Phys. J.* **B5**, page 793, 1998.

[44] K. Klauck and A. Schadschneider. To be published.

[45] H. Hayakawa and K. Nakanishi. Universal behavior in granular flows and traffic flows. *Prog. Theor. Phys. Suppl.* **130**, page 57, 1998.

[46] F. Spitzer. Interaction of markov processes. *Adv. Math.* **5**, page 246, 1970.

[47] J. M. Carlson, E. R. Grannan, and G. H. Swindle. Self-organizing systems at finite driving rates. *Phys. Rev.* **E47**, page 93, 1993.

[48] S. Sandow and G. M. Schütz. On $U_q[SU(2)]$-Symmetric Diffusion. *Europhys. Lett.* **26**, page 7, 1994.

[49] V. Pasquier and H. Saleur. Common structures between finite systems and conformal field theories through quantum groups. *Nucl. Phys.* **B330**, page 523, 1990.

[50] J. Fuchs. *Affine Lie-Algebras and Quantum Groups.* Cambridge University Press, Cambridge, 1992.

[51] A. B. Kolomeisky and B. Widom. A simplified "ratchet" model of molecular motors. *J. Stat. Phys.* **93**, page 633, 1998.

[52] J. Prost, J. F. Chauwin, L. Peliti, and A. Ajdari. Asymmetric pumping of particles. *Phys. Rev. Lett.* **72**, page 2652, 1994.

[53] J. Rousselet, L. Salome, A. Ajdari, and J. Prost. Directional motion of brownian particles induced by a periodic asymmetric potential. *Nature* **370**, page 446, 1994.

[54] S. Leibler. Moving forward noisily. *Nature* **370**, page 412, 1994.

[55] M. O. Magnasco. Forced thermal ratchets. *Phys. Rev. Lett.* **71**, page 1477, 1993.

[56] R. D. Astumian and M. Bier. Fluctuation driven ratchets: Molecular motors. *Phys. Rev. Lett.* **72**, page 1766, 1994.

[57] C. R. Doering, W. Horsthemke, and J. Riordan. Nonequilibrium fluctuation-induced transport. *Phys. Rev. Lett.* **72**, page 2984, 1994.

[58] P W Kasteleyn. Dimer statistics and phase transitions. *J. Math. Phys.* **4**, page 287, 1963.

[59] J G Brankov, V B Priezzhev, A Schadschneider, and M Schreckenberg. The Kasteleyn model and a cellular automaton approach to traffic flow. *J. Phys. A: Math. Gen.* **29**, page L229, 1996.

[60] H Y Huang, F Y Wu, H Kunz, and D Kim. Interacting dimers on the honeycomb lattice: an exact solution of the five-vertex model. *Physica* **A228**, page 1, 1996.

[61] B. S. Kerner. The physics of traffic. *Physiscs World* **12**, page 25, 1999.

[62] M. R. Evans, N. Rajewsky, and E. R. Speer. Exact solution of a cellular automaton for traffic. *J. Stat. Phys.* **95**, page 45, 1999.

[63] J. deGier and B. Nienuis. Exact stationary state for an asymmetric exclusion process with fully parallel update. *Phys. Rev.* **E59**, page 4899, 1999.

[64] N. Rajewsky, L. Santen, A. Schadschneider, and M. Schreckenberg. The asymmetric exclusion process: Comparison of update procedures. *J. Stat. Phys.* **92**, page 151, 1998.

[65] N. Rajewsky. *Exact results for one-dimensional stochastic processes.* Dissertation Thesis, University of Cologne, 1997.

[66] M. Dudzinski and G. M. Schütz. Relaxation spectrum of the asymmetric exclusion process with open boundaries. Preprint.

[67] E. Dagotto and T. M. Rice. Surprises on the way from one- to two-dimensional quantum magnets: The ladder materials. *Science* **271**, page 618, 1996.

[68] H. Frahm and A. Kundu. The phase diagram of an exactly solvable t-j ladder model. *J. Phys.: Condens. Matter* **11**, page L557, 1999.

[69] M. T. Batchelor and M. Maslen. Ground state energy and mass gap of a generalized quantum spin ladder. *J. Phys. A: Math. Gen.* **33**, page 443, 2000.

[70] V. Belitsky, J. Krug, E. Jordão Neves, and G. M. Schütz. A cellular automaton for two-lane traffic. Preprint.

[71] T. Nagatani. Self-organaization and phase transition in a traffic-flow model of a two-lane roadway. *J. Phys. A: Math. Gen.* **26**, page L781, 1993.

[72] M. E. Fouladvand. Reaction-diffusion models describing a two-lane traffic flow. *cond-mat/0004030*, 2000.

[73] L. G. Tilstra and M. H. Ernst. Synchronous asymmetric exclusion processes. *J. Phys. A: Math. Gen.* **31**, page 5033, 1998.

[74] G. M. Schütz. Time-dependent correlation functions in a one-dimensional asymmetric exclusion process. *Phys. Rev.* **E47**, page 4265, 1993.

[75] S. Rommer and S. Östlund. Class of ansatz wave functions for one-dimensional spin systems and their relation to the density matrix renormalization group. *Phys. Rev.* **B55**, page 2164, 1997.

[76] Y. Hieida. Application of the density matrix renormalization group method to a non-equilibrium problem. *J. Phys. Soc. Jpn.* **67**, page 36, 1998.

[77] M. Kaulke and I. Peschel. A DMRG study of the q-symmetric Heisenberg chain. *Eur. Phys. J.* **B5**, page 727, 1998.

[78] E. Carlon, M. Henkel, and U. Schollwöck. Density matrix renormalization group and reaction-diffusion processes. *Eur. Phys. J.* **B12**, page 99, 1999.

[79] A. Kemper. *Transfermatrix-DMRG für zweidimensionale klassische Modelle.* Diploma Thesis, University of Cologne, 2000.

[80] R. B. Stinchcombe and G. Schütz. Operator algebra for stochastic dynamics and the Heisenberg chain. *Europhys. Lett.* **29**, page 663, 1995.

[81] R. B. Stinchcombe and G. Schütz. Application of operator algebras to stochastic dynamics and the Heisenberg chain. *Phys. Rev. Lett.* **75**, page 140, 1995.

[82] K. Krebs. On matrix product states for periodic boundary conditions. *J. Phys. A: Math. Gen.* **33**, page L149, 2000.

[83] F. Spitzer. *Principles of Random Walk.* Springer Verlag, Heidelberg, 1976.

Acknowledgements

Zusammenfassung

Eine Vielzahl von interessanten physikalischen Phänomenen wird realisiert durch Systeme fernab vom thermodynamischen Gleichgewicht. Die wohl wichtigsten Beispiele sind getriebene Gittergase, Reaktions-Diffusions Systeme sowie die kritische Dynamik von klassischen Spin-Systemen. Die dabei auftretenden Modelle zeigen ein sehr breites Anwendungsspektrum, das oft weit über die Grenzen der Physik hinausgeht. Beispiele sind die Beschreibung von Straßenverkehr, biologische Mechanismen des Wachstums und der Proteinsynthese, die Ausbreitung von Epidemien, die Meinungsbildung in Gruppen von Menschen und die Modellierung von Finanzmärkten.

Die Physik des Nichtgleichgewichts ist jedoch bei weitem noch nicht so gut verstanden wie die Physik des Gleichgewichts. Gerade deswegen sind die großen Fortschritte, die in jüngerer Zeit auf dem Gebiet gemacht wurden, umso bemerkenswerter. Diese Fortschritte beruhen in starkem Maße auf der Beobachtung, daß Syteme des Nichtgleichgewichts phänomenologisch durch spezielle stochastische Prozesse beschrieben werden können. Bei diesen Prozessen handelt es sich um sogenannte Markov Prozesse. Für diese wiederum gilt, daß die zeitliche Entwicklung der Wahrscheinlichkeitsverteilung durch die Wirkung eines linearen Operators, des sogenannten Markov Erzeugers, gegeben ist. Wie dieser lineare Operator die Dynamik der Wahrscheinlichkeitsverteilung generiert, darüber gibt die Master Gleichung Auskunft. Sie hat dieselbe mathematische Form wie eine Schrödinger Gleichung in imaginärer Zeit. Diese Beobachtung allein eröffnet die Möglichkeit, Methoden aus der Gleichgewichts-Physik zu benutzen. Aus diesem Grunde war es möglich die stationären Zustände und teilweise auch die dynamischen Eigenschaften von einigen niedrigdimensionalen stochastischen Prozessen auf dem Gitter zu berechnen. In aller Regel war die Wechselwirkung (WW) bei diesen Prozessen räumlich homogen und spielte sich nur zwischen nächsten Nachbarn ab. Aus diesem Grunde war es naheliegend die benutzten Verfahren auf Prozesse zu übertragen, bei denen die Wechselwirkung komplizierter ist.

Eine der fruchtbarsten Methoden bei der analytischen Berechnung von stationären Zuständen stellt der sogenannte Matrix-Produkt-Ansatz dar. Bei diesem Ansatz wird versucht, die Wahrscheinlichkeit einer Konfiguration im stationären Zustand als Produkt von Matrizen zu schreiben. Die Wahrscheinlichkeit für eine spezielle Konfiguration auf einer Kette der Länge L wird dabei zum Produkt von L Matrizen, d.h. jedem Platz der Kette wird eine Matrix zugeordnet. Welche Matrix einem Platz zugeordnet wird, richtet sich nach dem Zustand dieses Platzes in der betrachteten Konfiguration. Der Vorteil dieses Ansatzes besteht darin, daß die Forderung an den Matrix-Produkt-Zustand ein stationärer Zustand zu sein, sich allein auf Grund eines lokalen Kriteriums, des sogenannten Cancelling-Mechanismus, überprüfen läßt. Krebs und Sandow [34] konnten zeigen, daß sich der stationäre Zustand von eindimensionalen stochastischen Prozessen mit Nächster-Nachbar-WW im Inneren des Systems und Randfeldern auf dem ersten und letzten Platz der Kette *immer* als Matrix-Produkt-Zustand schreiben läßt. Im zweiten Kapitel der vorliegenden Arbeit konnte gezeigt werden, daß sich das Ergebnis von Krebs und Sandow stark erweitern läßt. Es wurde bewiesen, daß der stationäre Zustand eines stochastischen Prozesses mit Wechselwirkungsreichweite r im Inneren und $r-1$ an den Rändern sich

ebenfalls *immer* als Matrix-Produkt-Zustand schreiben läßt. Dieses Ergebnis wurde angewendet auf zwei Hüpfmodelle mit Relevanz für die Beschreibung von Verkehrsfluß.

Als nächstes wurde in Kapitel 3 der stationäre Zustand eines stochastischen Prozesses mit räumlich alternierender WW und reflektierenden Rändern exakt berechnet. Der stationäre Zustand hat die besondere Eigenschaft, daß er ein sogenannter Optimum-Grundzustand ist. Darüber hinaus wurde gezeigt, daß Optimum-Grundzuständen bei stochastischen Prozessen mit reflektierenden Rändern eine besondere Bedeutung zukommt. Untersucht man solche Prozesse mit Hilfe des Matrix-Produkt-Ansatzes, so findet man genau dann Optimum-Grundzustände, wenn der Cancelling-Mechanismus, der durch die WW am Rande generiert wird, seine einfachste Form annimmt. Darüber hinaus konnte durch Angabe eines Gegenbeispiels gezeigt werden, daß Optimum-Grundzustände jedoch nicht durch reflektierende Ränder bedingt werden. Bei der Lösung des Modells mit alternierender WW wurde Gebrauch von der Tatsache gemacht, daß sich dieses Modell im Falle von verschwindender Alternierung auf ein Modell mit der Symmetrie der Quantengruppe $U_q[SU(2)]$ reduziert. In diesem Fall lassen sich die stationären Zustände im Sektor zur Teilchenzahl N durch N-fache Anwendung der Absteiger von $U_q[SU(2)]$ auf das Vakuum erzeugen. In Analogie dazu wurden in der vorliegenden Arbeit verallgemeinerte Absteiger für das alternierende Modell hergeleitet. Aufgrund dieser Konstruktion war es möglich Rekursionsbeziehungen für beliebige Korrelationsfunktionen anzugeben. Die verallgemeinerten Absteiger repräsentieren jedoch nicht mehr eine globale Symmetrie des stochastischen Hamiltonians. Aus diesem Grund ist es zu erwarten, daß das alternierende Modell nicht mehr integrabel ist.

Im vierten Kapitel wurden die statistischen Eigenschaften eines klassischen 5-Vertex-Modells zur Beschreibung von Verkehrsfluß, d.h. eines Problems aus der Physik des Nichtgleichgewichts, benutzt. Die Grundidee beruht auf der Beobachtung, daß die erlaubten Konfigurationen des Vertex-Modells auf dem Quadratgitter den Raum-Zeit Trajektorien von Autos stark ähneln. Diese Idee geht auf Schreckenberg *et al.* zurück [59]; diese Autoren beschränkten sich jedoch auf die Betrachtung einer speziellen Linie im Parameterraum, auf der sich das Modell durch freie Fermionen darstellen läßt. Bei der Behandlung der freien Energie mit Hilfe des Bethe-Ansatzes ist dies der Fall, in dem die Bethe-Ansatz Gleichungen entkoppeln. Damit ist es möglich die freie Energie relativ leicht zu berechnen und damit das Fundamentaldiagramm, d.h. die Beziehung zwischen Fluß und Dichte, anzugeben. Man bemerkt aber, daß dann für gewisse Parameter Fundamentaldiagramme auftreten, die für beliebig kleine Dichten Ströme in der Nähe von eins zeigen. Der Grund für diese (in diesem Zusammenhang unphysikalische) Beobachtung ist darin zu sehen, daß Trajektorien mit enorm hohen Geschwindigkeiten ein zu starkes Boltzmanngewicht bekommen. Aus diesem Grunde wurde die Arbeit [59] dahingehend verallgemeinert, daß das 5-Vertex-Modell auch für solche Paramter untersucht wurde, für die es sich nicht durch freie Fermionen ausdrücken läßt. Dies geschah durch Einführung eines weiteren Parameters, mit dem sich das Boltzmanngewicht von Trajektorien mit hohen Geschwindigkeiten steuern läßt. Das so gewonnene Modell ist immer noch integrabel, allerdings lassen sich die komplexen Wegintegrale, die zur Berechnung der freien Energie notwendig sind, nicht mehr explizit berechnen. Huang *et al.* [60] konnten jedoch durch geschickte Analyse der Bethe-Ansatz Gleichungen den Zusammenhang zwischen Phasenübergangspunkten und speziellen Verteilungen der Bethe-Ansatz-Wurzeln in der komplexen Zahlenebene finden. Mit Hilfe dieses Ergebnis konnte das Phasendiagramm des verallgemeinerten 5-Vertex-Modells geklärt werden. Im Gegensatz zum Fall Freier Fermionen zeigt sich in dem für die Beschreibung von Straßenverkehr interessanten Parameterbereich ein verändertes Phasendiagramm bestehend aus fünf Phasen. Vier Phasen sind dabei sogenannte eingefrorene

Phasen. In diesen Phasen ist die Dichte jeweils konstant und daher läßt sich dort kein Fundamentaldiagramm berechnen. In der fünften Phase, der sogenannten ungeordneten Phase, kommen jedoch alle Dichten vor. Hier wurde ausgehend von Entwicklungen der freien Energie in [60] die Asymptotik des Fundamentaldiagramms für kleine und große Dichten ermittelt. Um die restliche Information über das Fundamentaldiagramm zu erhalten, wurde ein Zellularautomat mit ähnlichen Eigenschaften vorgeschlagen. Der stationäre Zustand dieses Zellularautomaten wurde für den Forward-Sequential-Update mit Hilfe des Matrix-Produkt-Ansatzes und im Falle des voll parallelen Updates mit Hilfe der Car-Oriented Mean-Field Methode bestimmt. Die daraus erhaltenen Fundamentaldiagramme stimmen überein. Um zu überprüfen wie gut die genäherte Beschreibung durch den Zellularautomaten wirklich ist, wurde die freie Energie für ein kleines System analytisch berechnet. Das daraus erhaltene Fundamentaldiagramm zeigt erhöhte Werte für den Strom bei mittleren Dichten im Gegensatz zum Zellularautomaten. Der Grund liegt wohl darin, daß das Vertex-Modell in der ungeordneten Phase kritisch ist und Korrelationsfunktionen algebraisch zerfallen, wohingegen die Korrelationen des Zelluarautomaten exponentiell zerfallen. Die starken Korrelationen führen also hier zu einer Erhöhung des Flusses.

Im nächsten Kapitel wurde die Dynamik des asymmetrischen Exklusionsprozesses mit parallelem Update und offenen Rändern untersucht. Dabei konnte festgestellt werden, daß die zeit- und ortsabhängige Verallgemeinerung der $(2,1)$-Cluster Approximation in sehr guter Näherung zur Vorhersage der Dynamik benutzt werden kann. Dabei gibt es jedoch eine Ausnahme. Auf einer eindimensionalen Untermannigfaltigkeit des Parameterraumes, der sogenannten Schock-Profil- oder Koexistenzlinie, versagt die Cluster Approximation. Um auch auf dieser Linie Vorhersagen machen zu können, wurde ein kürzlich zur Beschreibung des zufällig sequentiellen Updates vorgeschlagenes Domänenwandbild an den parallelen Update angepaßt. Interessanterweise erlaubt es dieses Bild, obwohl es zur Beschreibung auf sehr großen Zeitskalen vorgeschlagen wurde, schon für kleine Zeiten eine akzeptable Beschreibung. Das Anregungsspektrum der Domänenwand wurde berechnet, denn es wird erwartet, daß dieses Spektrum in guter Näherung dem niedrigliegenden Anregungsspektrum des Exklusionsprozesses entspricht.

Zuletzt wurden stochastische Hüpfmodelle auf quasi-eindimensionalen Strukturen, sogenannten Leitern, untersucht. Im ersten Teil konnte ein Modell mit periodischen Randbedingungen und deterministischen Hüpfen in einem Bein der Leiter exakt gelöst werden. Diese Lösung ist möglich, da im stationären Zustand beide Beine der Leiter entkoppeln. Der stationäre Zustand ist das direkte Produkt der stationären Zustände des Zellularautomaten 184 im oberen Bein und dem Nagel-Schreckenberg Modell mit $v_{\max} = 1$ im unteren Bein. Die gesamte Dichte verteilt sich dabei so auf beide Beine, daß der Gesamtfluß maximiert wird.

Im zweiten Teil dieses Kapitels wurde ein Modell mit offenen stochastischen Rändern und deterministischem Hüpfen im Bulk betrachtet. Auch für dieses Modell konnte der stationäre Zustand exakt berechnet werden. Das Phasendiagramm besteht aus zwei Phasen, einer Phase hoher Dichte und einer Phase niedriger Dichte. Der Übergang zwischen beiden Phasen ist von erster Ordnung.

Kurze Zusammenfassung

Zusammenfassung

Verschiedene Verallgemeinerungen von bestehenden Zugängen zu niedrigdimensionalen stochastischen Modellen werden vorgestellt. Zu Beginn wird gezeigt, daß sich der stationäre Zustand einer großen Klasse von eindimensionalen stochastischen Prozessen immer als ein Matrix-Produkt-Zustand schreiben läßt. Danach wird die Lösung eines eindimensionalen stochastischen Prozesses mit räumlich alternierender Wechselwirkung und reflektierenden Rändern vorgestellt. Der mathematische Zusammenhang zwischen solchen Rändern und dem Auftreten von Optimum-Grundzuständen wird geklärt. Im vierten Kapitel wird die Gibbssche Wahrscheinlichkeitsverteilung eines klassischen Vertex-Modells zur Beschreibung von Straßenverkehr benutzt und das Phasendiagramm dieses Verkehrsmodells wird hergeleitet. Zum Vergleich wird ein Zellularautomat mit ähnlichen Eigenschaften betrachtet. Der stationäre Zustand des Zellularautomaten wird exakt berechnet. Anschließend wird die Dynamik des asymmetrischen Exklusionsprozesses mit offenen Rändern und parallelem Update untersucht. Es wird gezeigt, daß für große Bereiche des Phasendiagramms die orts- und zeitabhängige Verallgemeinerung der $(2,1)$-Cluster Approximation eine gute Übereinstimmung mit den Monte-Carlo Daten liefert. Zur Beschreibung der Dynamik im verbleibenden Bereich des Phasendiagramms wird ein Domänenwandbild herangezogen. Abschließend werden stochastische Prozesse auf Leitersystemen mit zwei Beinen betrachtet. Exakte Lösungen für periodische und offene Randbedingungen werden präsentiert.

Stichworte: Zellularautomaten; Markov Prozesse; Optimum-Grund-Zustände; Matrix-Produkt-Ansatz; Reaktions-Diffusions-Modelle; Verkehrsfluß; Vertex-Modelle

Erklärung

Ich versichere, daß ich die von mir vorgelegte Dissertation selbständig angefertigt, die benutzten Quellen und Hilfsmittel vollständig angegeben und die Stellen der Arbeit – einschließlich Tabellen, Karten und Abbildungen –, die anderen Werken im Wortlaut oder dem Sinn nach entnommen sind, in jedem Einzelfall als Entlehnung kenntlich gemacht habe; daß diese Dissertation noch keiner anderen Fakultät oder Universität zur Prüfung vorgelegen hat; daß sie – abgesehen von unten angegebenen Teilpublikationen – noch nicht veröffentlicht worden ist sowie, daß ich eine solche Veröffentlichung vor Abschluß des Promotionsverfahrens nicht vornehmen werde. Die Bestimmungen dieser Promotionsordnung sind mir bekannt. Die von mir vorgelegte Dissertation ist von Herrn Professor Dr. J. Zittartz betreut worden.

Köln, den 20. September 2000

Teilpublikationen:

K. Klauck, A. Schadschneider, *On the ubiquity of matrix-product states in one-dimensional stochastic processes with boundary interactions*, Physica **A 271**, Seite 102 (1999)

A. Schadschneider, D. Chowdhury, E. Brockfeld, K. Klauck, L. Santen und J. Zittartz, *A new cellular automata for city traffic*, erschienen in Traffic and Granular Flow '99: Social, Traffic, and Granular Dynamics, Herausgeber D. Helbing, H. J. Herrmann, M. Schreckenberg und D. E. Wolf (Springer, Berlin)

Lebenslauf

Persönliche Daten

Name:	Kai-Oliver Klauck
Geburtsdatum:	09.02.1971
Geburtsort:	Köln
Familienstand:	verheiratet
Staatsangehörigkeit:	deutsch

Schulbildung

1977 – 1981	GGS Nesselrodestr. in Köln-Niehl
1981 – 1990	Erich-Kästner-Gymnasium in Köln-Niehl
Mai 1990	Abitur
Juli 1990 – Juni 1991	Wehrdienst

Hochschulstudium

Okt. 1991	Immatrikulation an der Universität zu Köln, Studiengang Physik (Diplom)
Mai 1994	Vordiplom
Aug. 1997	Abschluß der Diplomarbeit bei Prof. Dr. H. Moraal
ab Sept. 1997	Anfertigung der vorliegenden Dissertation unter Anleitung von Prof. Dr. J. Zittartz

Arbeitsverhältnisse am Institut für
Theoretische Physik, Universität zu Köln

Sept. 1997 – Apr. 1999	Wissenschaftliche Hilfskraft
seit Mai 1999	Wissenschaftlicher Mitarbeiter